Cloning and characterization of EXC-1, an IRGP homologue that controls Intracellular Trafficking and the Maintenance of Shape in Small Biological Tubes

By

Kelly A. Grussendorf

Submitted to the Department of Molecular Biosciences and the Faculty of the Graduate School of the University of Kansas in partial fulfillment of the requirements for the degree of Doctor of Philosophy

Chairperson Dr. Matthew Buechner

Dr. Stuart Macdonald

Dr. Erik Lundquist

Dr. Yoshiaki Azuma

Dr. Deborah Smith

Date Defended: July 16, 2013

The Dissertation Committee for Kelly A. Grussendorf certifies that this is the approved version of the following dissertation:

Cloning and characterization of EXC-1, an IRGP homologue that controls Intracellular Trafficking and the Maintenance of Shape in Small Biological Tubes

Chairperson: Dr. Matthew Buechner

Date Approved: July 22, 2013

Abstract

Biological tubes are ubiquitous structures that carry out vital roles. The formation and maintenance of these tubule structures is a fundamental process in most organisms. The goal of this work is to get a better understanding of the molecules required for these processes. The *C. elegans* excretory canal provides an ideal model for these studies. The family of EXC proteins is required to maintain the tubule shape of the excretory canal. Mutations in the *exc* genes (EXcretory Canal abnormal) result in the formation of fluid-filled cysts in the lumen of the canal. *exc-1* mutants show cysts in the canals that are often located at the ends of the canals. These cysts vary in size and number; from cysts not much wider than normal lumen up to cysts expanded to the entire diameter of the worm. This dissertation describes the work that I carried out to map, clone, and characterize *exc-1*.

EXC-1 is homologous to the family of Immunity-Related GTPases (IRGP) and contains tandem Ras-homology domains. IRGPs make up a large family of proteins, with many of the members involved in the clearance of infectious pathogens, by assisting in autophagy. EXC-1 contains highest homology to the member of IRGPs, IRGC, of which very little is known. The family of IRGPs, and EXC-1's homology to this family and the Ras superfamily is described here.

exc-1 is expressed within the excretory canal and the amphid sheath cells, a glial structure that ensheaths the amphid neuron sensory endings. *exc-1* mutants exhibit occasional, abnormal formation of cyst-like structures along the process of the amphid sheath, but does not disrupt the formation of the amphid channel, the passageway for exposure of amphid dendrites to the outside environment.

exc-1 interacts genetically with *exc-5* (Faciogenital dysplasia protein 4 homologue) and *exc-9* (Cysteine Rich Intestinal Protein homologue) in a pathway of *exc-9* → *exc-1* → *exc-5*. Binding assays show that EXC-1 and EXC-9 bind when EXC-1 is in its wild-type or GTP-bound, active, form.

This work also describes the studies carried out to identify the subcellular role of EXC-1 within the canal. With a group of subcellular markers it has been identified that EXC-1 is required for proper trafficking of material from early endosomes to recycling endosome within the excretory canal, similar to EXC-5. This work indicates that EXC-1 and EXC-9 binding is required for downstream activation of EXC-5 for proper trafficking within the canal and maintenance of tubule shape.

Acknowledgements

Thank you to Dr. Matthew Buechner who has been a wonderful mentor throughout this whole process. I have learned many things from him, including how to think like a scientist and not to forget the importance of the basics. I also appreciate all of the help and editing of my first author manuscript, of which makes up a large part of this dissertation. Also, thank you to all the members of the Buechner lab, past and present, for making it an enjoyable place to work.

I would like to thank Shai Shaham and Barth Grant for the many constructs and tools that made these studies possible. I would also like to thank Brian Ackley for the many constructs and the use of his confocal microscope. I would also like to thank the members of my committee for their assistance and advice over the years, Dr. Stuart Macdonald, Dr. Erik Lundquist, Dr. Yoshiaki Azuma and Dr. Deborah Smith.

Many thanks to my family and friends for the support and encouragement over the years. A special thanks to my twin sister, my best friend, Shannon, who because of our unique relationship I was convinced we had a closer genetic tie than normal fraternal twins, which inspired me to study and enter the field of genetics.

Also, thank you to Dr. David McLeod, who saw in me the desire to teach and let me embrace it and explore different teaching styles. Thank you for allowing me to 'take over' your class, giving me the teaching experiences that I will take with me into my future career. I believe that I am where I am and where I am going in my career largely in part because of the amazing mentors I have had, Dr. Ellen Brisch, Dr. Matthew Buechner and Dr. David McLeod.

Table of Contents

Chapter 1: Introduction…….…..1

1.1 Focus of Research……...……...……2

1.2 Epithelial Structure…….……3

1.3 Biological Tubes……..5

1.4 *Caenorhabditis elegans*……...9

1.5 *Caenorhabditis elegans* excretory canal……...……12

1.6 *exc* mutants……17

Chapter 2: Mapping and Cloning of *exc-1*…….……19

2.1 Abstract…….…..20

2.2 Introduction……..…….20

2.3 *exc-1* phenotype……..……25

2.4 Mapping of *exc-1*……28

2.5 Rescue of *exc-1* with C46E1.3……...……34

2.6 *exc-1* mutation and cDNA analysis……...……37

2.7 *exc-1* acts cell autonomously……39

2.8 Alleles of *exc-1*……..…….41

2.9 Summary……...….43

2.10 Materials and Methods……43

2.11 Complications with mapping…….47

Chapter 3: EXC-1 in the Amphid Sheath…….……55

3.1 Abstract…….……..56

3.2 Introduction……56

3.3 Expression pattern of EXC-1……..…….60

3.4 Dye-filling assay…….....……62

3.5 Structure of amphid sheath in *exc-1*……...….63

3.6 Summary……...…….66

3.7 Materials and Methods…….……66

Chapter 4: EXC-1 is an IRGP homologue ……..……..69

4.1 Abstract……..……70

4.2 Introduction……70

4.3 IRGPs……..75

4.4 EXC-1 Ras domains……..……78

4.5 Different forms of EXC-1……..85

4.6 Summary……...……..88

4.7 Materials and Methods……..88

Chapter 5: Genetic Interactions between *exc-1* and other *exc* genes….90

5.1 Abstract……...…91

5.2 Introduction……91

5.3 *exc-1* does not interact with *exc-2, 3,4, 6* or *exc-7*…….……..95

5.4 *exc-1* interacts genetically with *exc-5* and *exc-9*……95

5.5 Summary…….……99

5.6 Material and Methods……...……99

Chapter 6: Binding Partners of EXC-1……100

6.1 Abstract……...…..101

6.2 Introduction……..102

6.3 Results of Yeast-two hybrid studies……..……110

6.6 Summary…….……..115

6.7 Materials and Methods……..……..115

Chapter 7: *exc-1* is necessary for trafficking……...……118

7.1 Abstract……..…119

7.2 Introduction……..……119

7.3 Subcellular localization of EXC-1……..……126

7.4 Subcellular Markers……...……128

7.5 Electron Micrograph Images……...…132

7.6 Summary ……..134

7.7 Materials and Methods……..….134

Chapter 8: FRAP assays……137

8.1 Abstract……138

8.2 Introduction……..138

8.3 FRAP results……139

8.4 Summary…….….144

8.5 Materials and Methods……144

Chapter 9: Discussion……...…146

References…….……..156

Chapter 1

Introduction

Chapter 1: Introduction

1.1 Focus of Research
1.2 Epithelial Structure
1.3 Biological Tubes
1.4 *Caenorhabditis elegans*
1.5 *Caenorhabditis elegans* excretory canal
1.6 *exc* mutants

1.1 Focus of Research

Biological tubes are ubiquitous and quite fascinating on both functional and structural levels. Most of our major organs are composed primarily of tubes, including the millions of nephrons within the kidney and the many intricate tubes of the vasculature system, varying extensively in shape and size. Tubes serve as a major transport system throughout our bodies, whether it be transporting blood to our toes, or assisting in sending a signal to our brain. Regardless of shape and size, all tubes need to properly carry out the complex molecular mechanisms required to develop and maintain this structure. Some tubes may be transient and short lived, while some tubes function for decades, throughout the organism's entire life. These persevering tubes often require constant remodeling and monitoring to remain functional on the structural and subcellular level.

To get a better understanding of the molecular mechanisms underlying development and maintenance of the shape of small biological tubes I have used the model organism, *Caenorhabditis elegans*. The *C. elegans* excretory canal provides an ideal system to examine tube formation and maintenance. Using this genetically tractable organism I have mapped, identified, and characterized the gene *exc-1;* an IRGP (Immunity-Related GTPase) homologue required to maintain the narrow lumen within this single-celled tube.

1.2 Epithelial Structure

Epithelial structures make up a large part of all biological tissues. These epithelial structures line the outside the body, the inside of the body, and can act as a barrier between two regions of the body. Epithelium can act as protection, such as our skin, or the lining of our lungs, both working to constantly fight off many of the world's pathogens and hazards. Epithelial structures also carry out the vital functions that include absorption of materials or excretion of chemicals and hormones, including the body's waste.

Epithelia perform a wide array of functions and adopt different structures and cellular arrangements to do this. An epithelium is often made of many cells that form a sheet-like structure. This sheet is held together and able to communicate through cellular junctions. These junctions include: anchoring junctions (ex. desmosomes and hemidesmosomes), occluding junctions (ex. tight junctions) and channel-forming junctions (ex. gap junctions).

Epithelial cells are polarized cells, having two (at least) distinct membrane domains and asymmetric organization of intracellular organelles and proteins. The apical domain is exposed to the external environment, or the lumen of the cavity. This apical surface is responsible for distinctive activities depending on cell type, such as excretion from kidney cells. The basal domain is attached to a basal lamina, which makes up part of the extracellular matrix. This attachment to the basal lamina and extracellular matrix, allows for epithelial cells to communicate with tissues around them, and absorb and secrete material into the surrounding area. See Figure 1.2a.

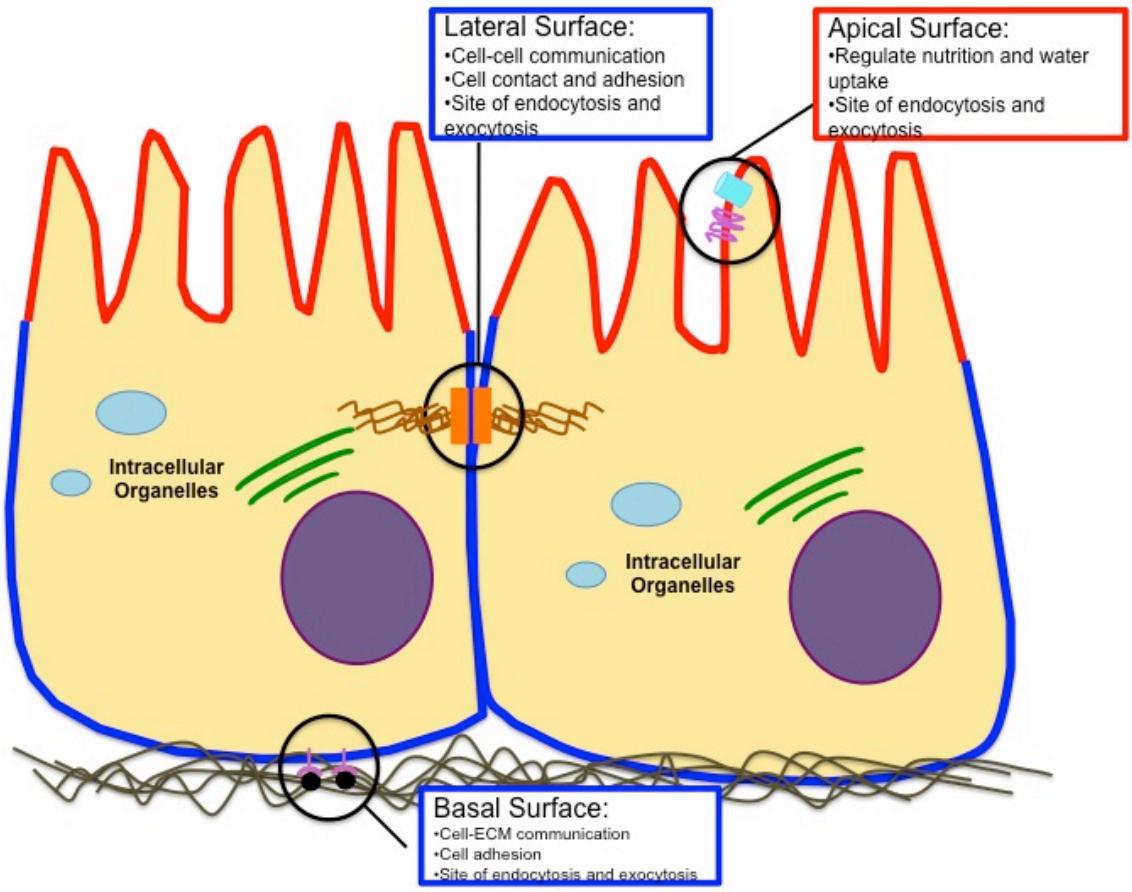

Figure 1.2a Simplified diagram of epithelial cells.
Apical surface indicated in red. Basal and lateral surfaces indicated in blue. A few of the many intracellular organelles within a cell are also diagrammed.

1.3 Biological Tubes

Epithelial structures can be found in a sheet-like structure, but also exist as tubular structures as well. As with epithelial sheets, it is imperative that biological tubes maintain proper apical and basal polarity as well, allowing them to carry out their integral role within the organism. Tubes can be found in many different sizes and levels of complexity. The diameter of biological tubes can vary from smaller than a micron to many centimeters wide. And their complexity can be very simple, such as the esophagus, made of a single tube, to the highly complex tubing found within the kidney. Tubes often act to transport material from one sight to another, whether it is modifying the material as it passes or acting as a passive conduit. To transport material, biological tubes are often born in one place and send out processes to their final destination (Lubarsky and Krasnow, 2003).

Tubes can be found as multicellular structures, being many cells thick across in diameter, or unicellular, composed of an individual cell, Figure 1.3a. The focus of this dissertation is on small, unicellular tubes. No matter the size and complexity of the tube, all require basic molecular functions, such as polarization and trafficking of material and organelles to specific locations. The apical surface faces towards the lumen, absorbing nutrients as they pass through, or secreting materials destined for transportation. The basal surface faces the outside of the tube to secrete and take up materials from the surrounding areas, Figure 1.3a.

Development of tubes occurs in many different ways. Multicellular tubes can form by different mechanisms including wrapping, budding, cavitation or cord hollowing, Figure 1.3b. Unicellular tubes, however, form by different techniques including cell

hollowing, self-fusion and cell fusion, Figure 1.3b (Baer et al., 2009). Cell hollowing occurs when vesicles form, coalesce, and fuse to form a lumen that will continue to grow and expand. Cell hollowing occurs in the *C. elegans* excretory canal, the focus of this dissertation (Buechner et al., 1999b; Nelson et al., 1983b). Cell fusion occurs when cells migrate to meet and only make cellular contacts at the dorsal and lateral regions, allowing for a lumen to form between these sites, as seen in the *Drosophila* heart tube (Santiago-Martinez et al., 2008). Self-fusion occurs when a cell wraps around and adheres to itself via an autocellular junction, a mechanism used by the *C. elegans* excretory duct (Lubarsky and Krasnow, 2003; Schottenfeld-Roames and Ghabrial, 2013; Stone et al., 2009).

Once the tube is formed, reaching its desired shape and size, maintenance of this structure is required for as long as the organism may need. The molecular mechanisms of this maintenance of tubular structure while the organism ages and grows are still relatively unknown; and will be the focus of this dissertation.

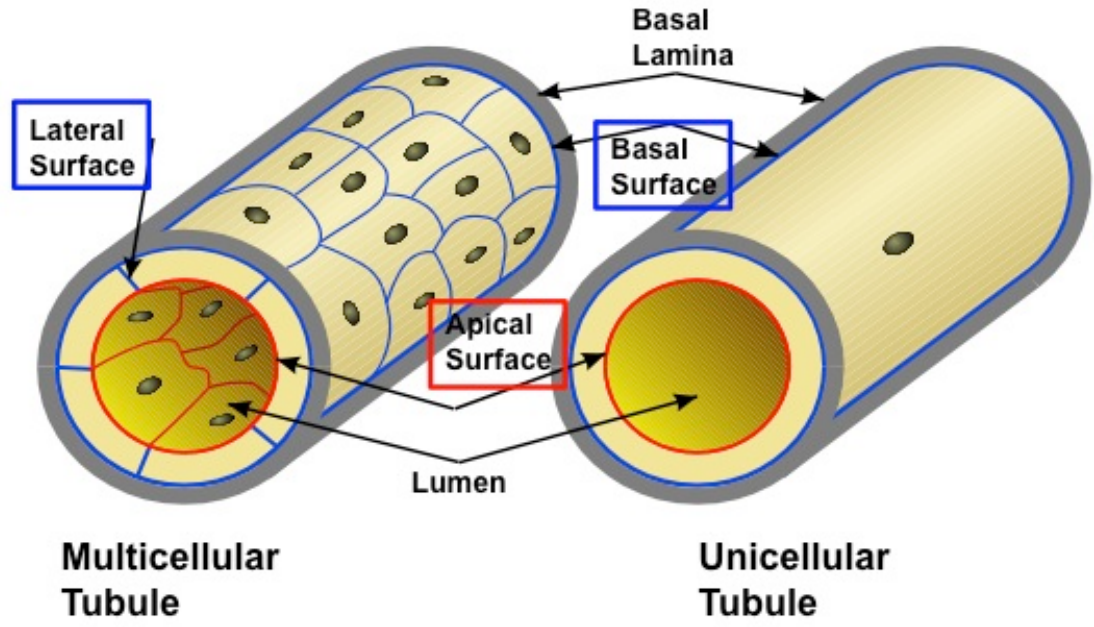

Figure 1.3a Similarities and differences of multicellular and unicellular tubes.
Apical surface shown in red. Basal and lateral surfaces shown in blue. Image adapted from (Buechner, 2002).

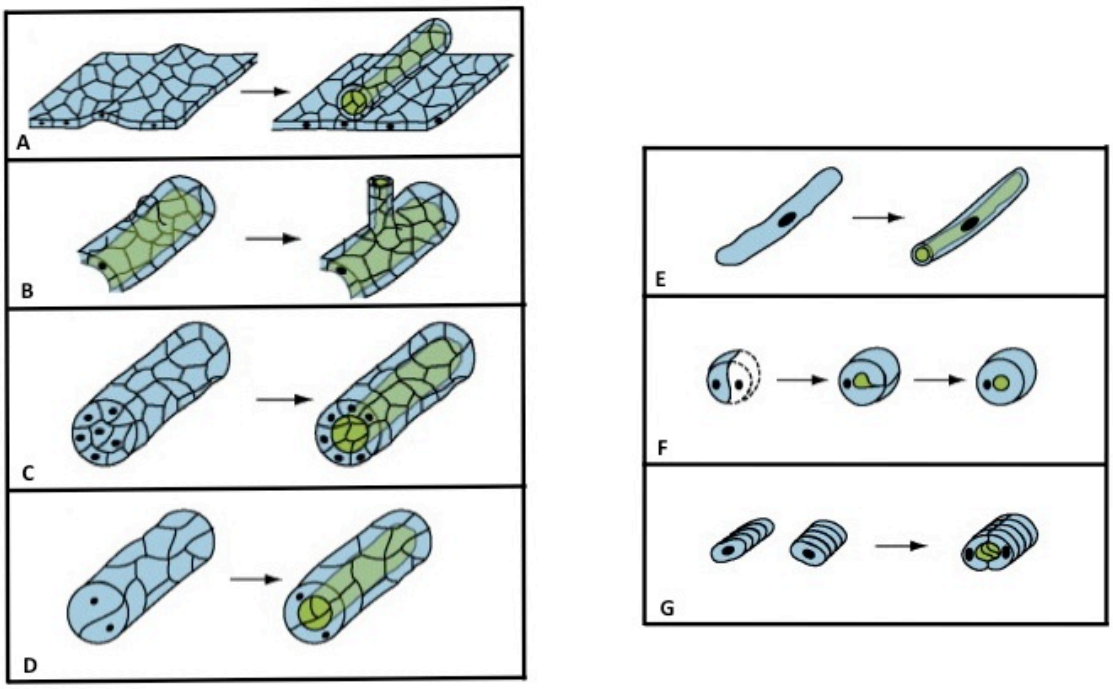

Figure 1.3b Mechanisms of tube formation.
(A-D) Multicellular Tubes: (A) Wrapping (B) Branching (C) Cavitation (D) Cord hollowing. **(E-G)** Unicellular Tubes: (E) Cell hollowing (F) Self Fusion (G) Cell Fusion. Adapted from (Baer et al., 2009).

1.4 *Caenorhabditis elegans*

To get a better understanding of biological tubes, specifically small biological tubes, the nematode *Caenorhabditis elegans* serves as a great model. *C. elegans* has served as a model organism for more than 50 years, and was first chosen as a model to study the nervous system (Brenner, 1974). *C. elegans* provides a great model organism for studies in genetics, developmental and cell biology for many reasons.

C. elegans is a free living, soil-dwelling, roundworm that is about 1 millimeter in length and can be maintained on agar plates with *E. coli* as a food source, making them relatively cheap to study and maintain. This organism is transparent, allowing scientists to see structures within the worm, and through they are relatively simple organisms they do contain most of the major tissues and organ systems that are found in more complex organisms, Figure 1.4a (Brenner, 1974; Wood, 1988).

C. elegans are found in two different sexes; self-fertilizing hermaphrodites (XX) and males (XO). Within a population, males make up the very small percentage of .5%, arising by spontaneous nondisjunction in the hermaphrodite germ line. A higher frequency of males (50%) occurs through mating. Because hermaphrodites are self-fertilizing, maintenance of homozygous traits is easy, as the progeny of the hermaphrodite are genetically identical. The process of introducing mutations or markers into different strains is easily done through mating of males to hermaphrodites and plenty of progeny are made. Hermaphrodites can produce about 300 progeny through self-fertilization and many more if mated (Wood, 1988).

The life cycle of the worm is relatively fast, about 3 days, if all conditions are optimal. There is an embryonic stage, followed by four larval stages (L1-L4) and

adulthood, with a cuticle-molting process occurring between each stage (White, 1987). *C. elegans* can enter an alternative developmental stage, called the dauer stage, if they are in unfavorable environmental conditions such as overcrowding, or low food supply. While entering this dauer stage, the worm closes up its mouth and anus and does not require any food, allowing the worm to survive for a longer time. This dauer worm will return to normal larval stages if returned to favorable conditions (Cassada and Russell, 1975; Riddle and Albert, 1997).

Another advantage of *C. elegans* is that their genome is sequenced (Consortium, 1998) and the cell lineage is known (Sulston and Horvitz, 1977). Hermaphrodites are made of 959 somatic cells while the male has 1031 somatic cells, and we know when every cell is born and where it will travel to and if it will divide, making it an ideal system for studying mutants.

Because *C. elegans* has served as a model organism for many years there are very useful resources available for investigators. wormbase.org is a source of information about the genome and genetics of the worm (Stein et al., 2001). wormbook.org serves as a great source of information about research techniques in worms, along with chapters discussing different topics, such as cell biology and signal transduction. (Girard et al., 2007). Also available is wormatlas.org that supplies many figures and images of *C. elegans,* which is very helpful when attempting to identify cells and structures within *C. elegans,* especially for beginning scientists *(*D. H. Hall, wormatlas.org).

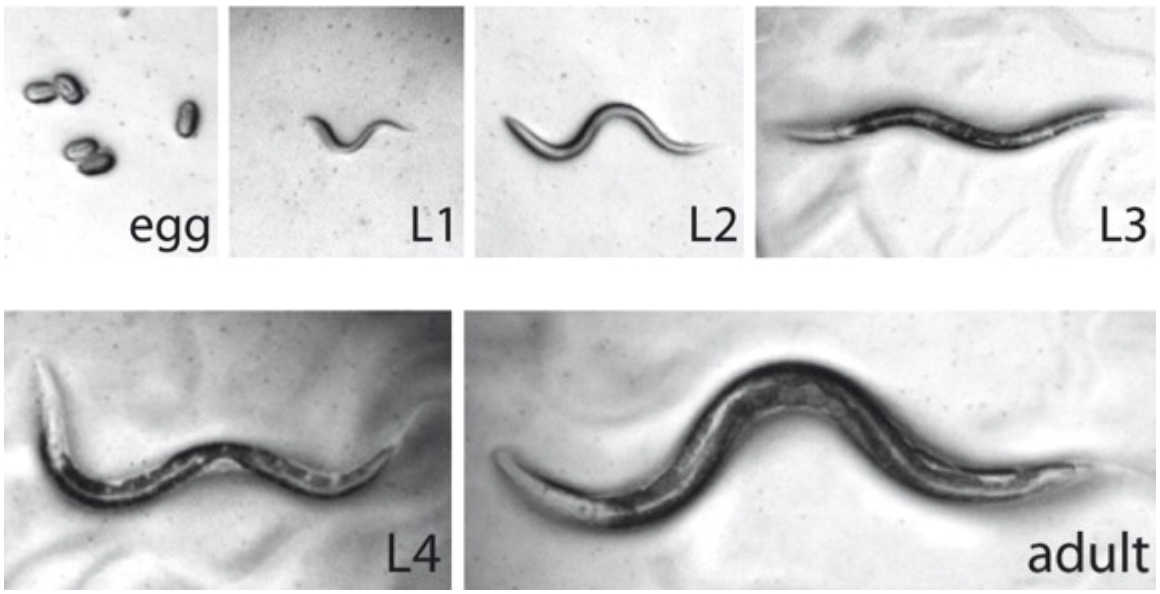

Figure 1.4a *C. elegans* life stages.

Images of *C. elegans* eggs, all the larval stages, and adult stage. Stages are distinguishable by size and gonad development. The dauer stage is not pictured here, dauer stage occurs between L2 and L3, and are relatively small and narrow. Dauer worms also exhibit a 'clearer' body phenotype, because they do not require food during this time. Adapted from (Fielenbach and Antebi, 2008).

1.5 *Caenorhabditis elegans* excretory canal

The *Caenorhabditis elegans* excretory canal serves as an excellent model to study both tubulogenesis and maintenance of tubule shape, Figure 1.5a. The excretory canal is a large single-celled epithelial tube that functions to regulate osmolarity and hydrostatic pressure within the worm (Nelson et al., 1983a; Nelson and Riddle, 1984). By being a single-celled tube, it removes many of the complexities found in multicellular tubes, such as adherens junctions, cell growth and division, which can alter tube structure. The excretory canal is part of the excretory system that is composed of the canal cell, gland cells and the excretory duct and pore cells, Figure 1.5a. The excretory canal acts as the kidney of the worm, taking up fluids and waste from the worm, passing it through the canal to the duct cell, and finally excreting out the excretory pore. If the excretory canal is laser ablated, the worm will fill up with water pressure and die (Nelson and Riddle, 1984).

The excretory canal is born half way through embryogenesis, shortly after vesicles start to form and coalesce, coming together to form the lumen of the canal. Once the lumen is formed, the canal will send out two processes, one to the left and one to the right side of the worm. The right and left canals then transverse the basement membrane of the hypodermis and bifurcate to form an anterior and posterior canal, making a large H-shaped structure. The anterior canals are shorter and narrower relative to the posterior canals, 100μm in length by 1μm in diameter and 800-900 μm in length and 2μm in diameter, respectively. By the time of hatching, the canal will be approximately half the length of the worm. By the end of larval stage 1, the canal will have completely grown, terminating near the tail of the worm. As the worm ages, the canal grows passively with

the worm, maintaining an open lumen throughout growth and development, Figure 1.5b (Buechner et al., 1999a; Nelson et al., 1983a)

As the canal grows out, it responds to different extracellular guidance cues. Some of the cues are also required for axon guidance, such as netrin and its receptor (UNC-6 and UNC-5) and the Wnt receptor, Frizzled (LIN-17) (Buechner, 2002). These molecules explain how the tube itself grows out but it does not explain how the lumen grows out.

Single-cell tubulogenesis and maintenance of narrow tubule structure depends on the interplay of multiple proteins acting in a concerted manner. Several recent studies suggest that the growth of the narrow apical surface of the excretory canal depends on osmotic activity to provide turgor pressure to extend the canals (Khan et al., 2013; Kolotuev et al., 2013; Schottenfeld-Roames and Ghabrial, 2013). The excretory canal lumen is surrounded by a series of small canalicular vesicles, (Figure 1.5c), containing vacuolar ATPase (VHA proteins) and Aquaporin 8 (AQP-8). During growth or hypoosmotic shock, vesicles dock with the apical lumen, where the AQP-8 allows release of water to the lumen as well as binding of ERM-1 (Ezrin-Radixin-Moesin homologue) to stimulate growth of actin filaments to guide the direction of luminal growth. These studies give us an idea of how the excretory canal goes through tubulogenesis, growing out and forming its lumenal shape, but much remains to be known about how the excretory canal maintains that lumenal shape once it is formed.

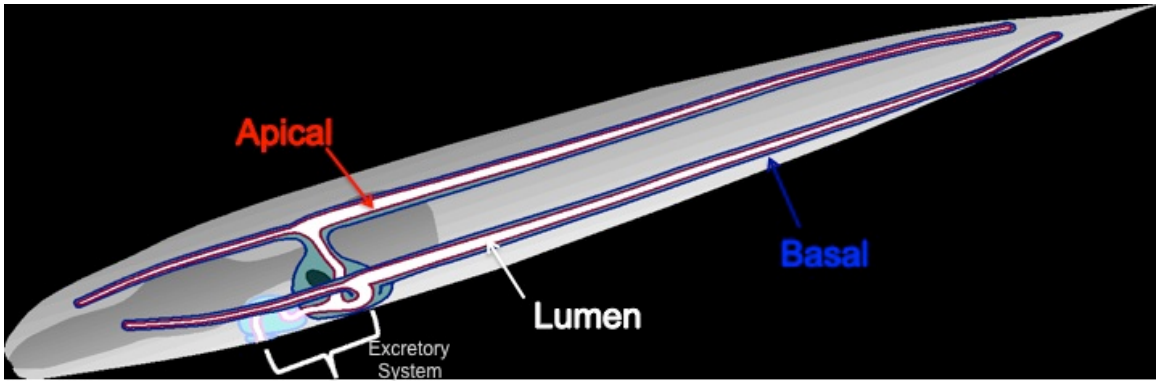

Figure 1.5a *C. elegans* excretory canal.
Apical surface shown as red, basal in blue. Excretory system; composed of the excretory canal, two gland cells (not shown), a duct cell and pore cell are indicated. Adapted from (Buechner, 2003).

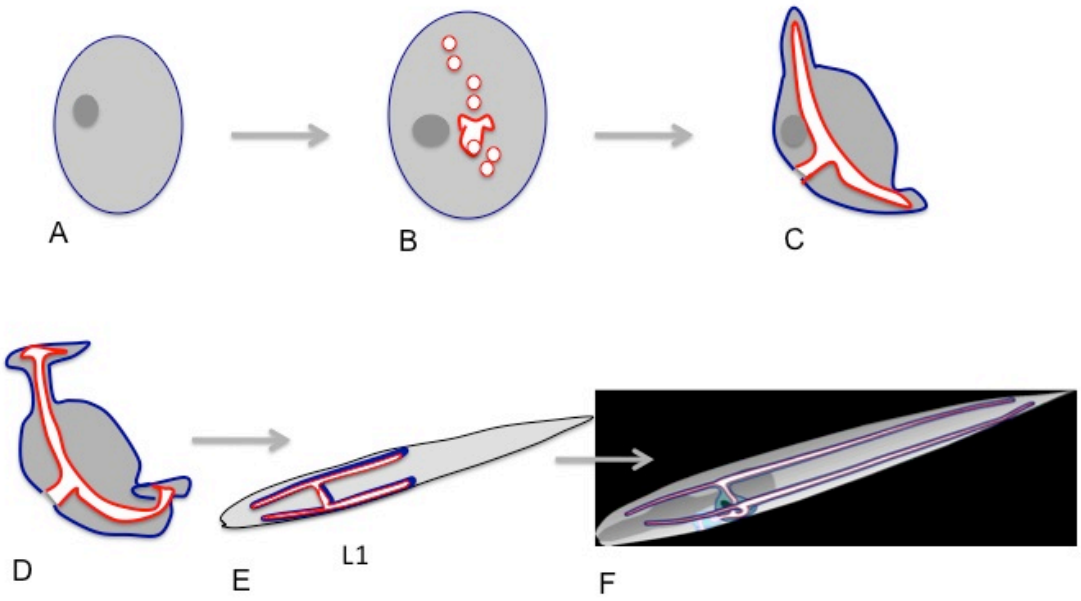

Fibure 1.5b Development of the excretory canal.
(A-D) Display lumen formation and canal growth within the excretory cell. (E-F) Display canal growth within the worm, after hatch (at the beginning of L1 – (E)) to adulthood (F), step by step process described in reading. Adapted from (Buechner, 2003).

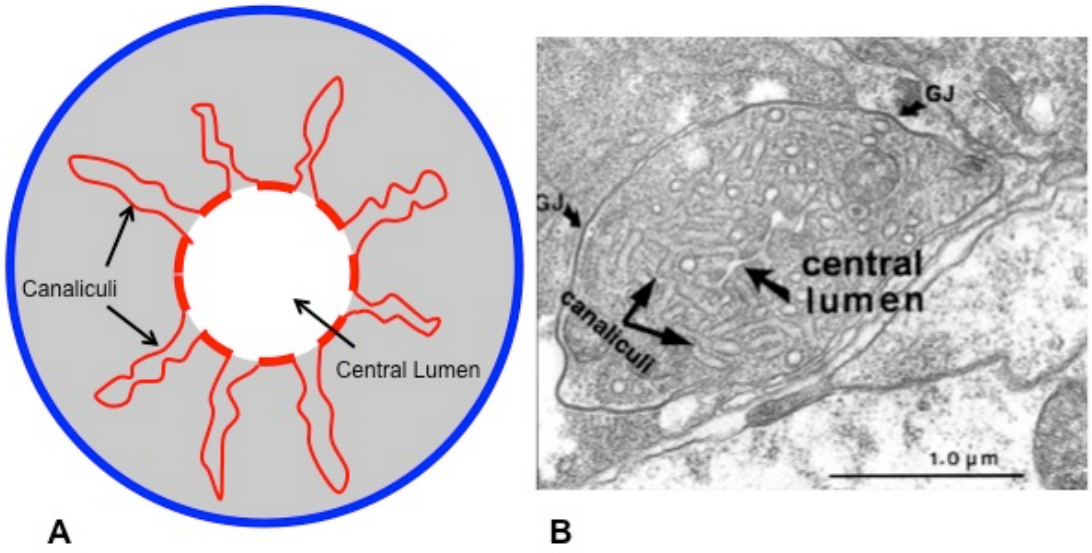

Figure 1.5c Cross section of excretory canal.
(A) A schematic of a cross section of the excretory canal to represent the canaliculi and central lumen (B) an electron micrograph of the excretory canal showing the canaliculi that extend into the cytoplasm, adapted from (Buechner *et al*., 1999).

1.6 *exc* mutants

To get a better understanding of how the excretory canal maintains its narrow lumenal structure we study a group of mutants, the EXcretory Canal abnormal (*exc)* mutants. In the *exc* mutants the worm seems to form the canal normally initially, but loses the ability to regulate luminal diameter, resulting in fluid filled cysts. There are nine genes within the *exc* group (*exc-1 – exc-9*). Cloned genes encode proteins that anchor the terminal web to the apical membrane, regulate osmotic pressure and bind to mRNA (discussed more in chapter 5). Also, in the past few years; identification of a set of EXC proteins that regulate intracellular trafficking within the canal has come together, *exc-1, 5, and 9*. The main focus of this dissertation will discuss the work that I have carried out on mapping, cloning and characterizing the gene *exc-1*, which encodes a GTPase homolog belonging to the family of Immunity-Related GTPase proteins (IRGP). Below shows a model displaying what was known about the family of *exc's* at the beginning of my studies, Figure 1.6. At the end of this manuscript a model including how my work has contributed to understanding the mechanism of maintenance in tubule shapes is given.

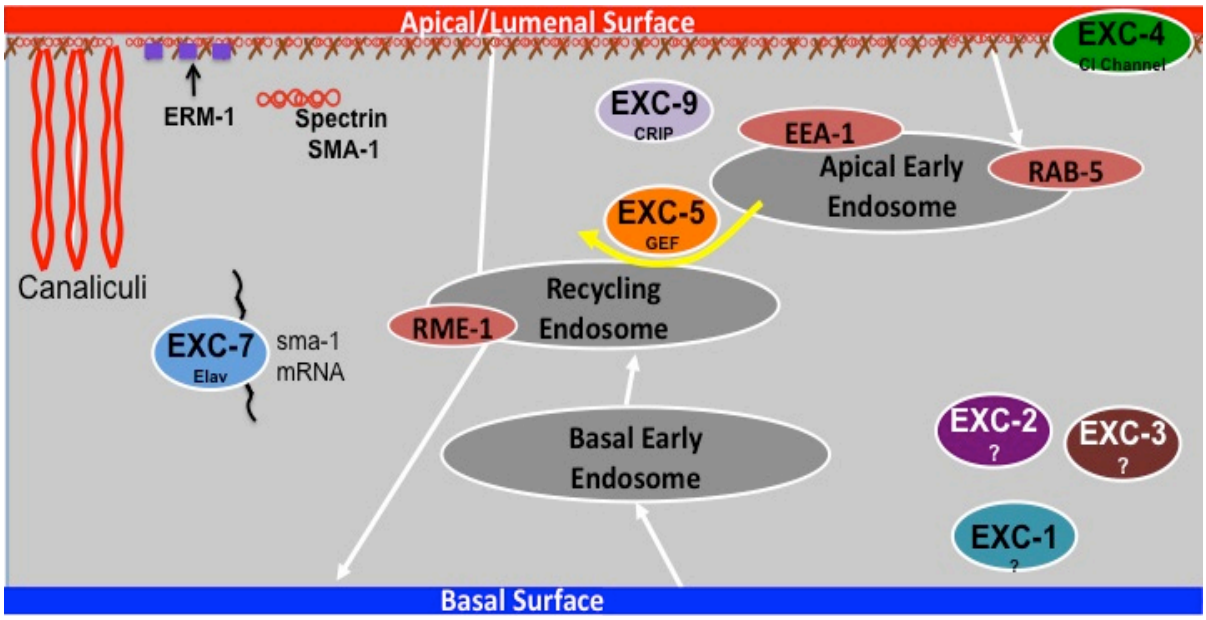

Figure 1.6 Model of the canal at the beginning of my studies.
exc-4 was identified to encode a Chloride channel, to regulate ion concentrations in the canal (Berry et al., 2003) . Cytoskeletal genes encoded by *sma-1*, and *erm-1* are involved in actin binding, which were identified by other labs (Gobel et al., 2004; Praitis et al., 2005). *exc-7* encodes a mRNA binding protein that binds to *sma-1* mRNA (Fujita et al., 2003). *exc-5*, the FGD4 homologue, regulates membrane trafficking with the possible help from genetically upstream gene, *exc-9*. *exc-1*, *2*, 3 and 6 remained to be identified.

Chapter 2

Mapping and Cloning of *exc-1*

.

Chapter 2: Mapping and Cloning of *exc-1*

2.1 Abstract
2.2 Introduction
2.3 *exc-1* phenotype
2.4 Mapping of *exc-1*
2.5 Rescue of *exc-1* with C46E1.3
2.6 *exc-1* mutation and cDNA analysis
2.7 *exc-1* acts cell autonomously
2.8 Alleles of *exc-1*
2.9 Summary
2.10 Materials and Methods
2.11 Complications with mapping

2.1 Abstract

To get a better understanding of the genetic and molecular mechanisms required to maintain a tubule shape, the Buechner lab studies a group of *exc* (EXcretory Canal abnormal) mutants, *exc-1 – exc-9*. Some of these mutants have been mapped and cloned, and some remain to be identified. This chapter discusses the process of characterizing the cystic phenotype, and the mapping and cloning of *exc-1*.

2.2 Introduction

exc mutants vary in severity of cystic phenotype. Some have lumens just wider than wild-type and some mutants have cysts that expand to the entire diameter of the worm, Figure 2.2a. *exc-1* is unique in that it exhibits varied phenotypes that ranges from a very mild phenotype, almost looking wild-type, to a severe cystic phenotype, often associated with very short canals. This section describes the characterization of *exc-1,* in

regard to both cyst size and number, along with canal length. By having an understanding of the phenotype of *exc-1,* I was able to use this information to carry out mapping studies.

There are many different techniques and methods that can be used for mapping a gene (Fay, 2006). Nowadays, for financial and timing reasons, it is common to sequence the entire genome of the organism in question and look for the mutation; unfortunately this is not the technique that was not feasible at the time *exc-1*. *exc-1* was mapped by more of a 'classical mapping' approach. Prior to my joining the lab, *exc-1* had been narrowed to a region of 282kb located on the right end of the X chromosome by 3-factor and deficiency mapping (Buechner et al., 1999a). *exc-1* was predicted to be between the genes *jud-4* and *dyn-1,* X:15284208-15568916, a region that contained 31 predicted genes. Proceeding with mapping of *exc-1,* I used a variety of techniques, including deficiency mapping, and attempts to rescue the *exc-1* cystic phenotype with cosmids, yeast artificial chromosomes (YAC's) or fosmids. RNAi techniques were used as well, to knockdown genes within this region in hopes to identify a phenotype similar to *exc-1*. In the beginning of my studies only one allele of *exc-1* existed, *rh26,* which is the allele I used to carry out all of my studies and characterizations. Throughout the years other alleles have been found, which is discussed in this section.

I was able to successfully map and clone *exc-1* to the predicted gene C46E1.3; from there I carried out sequencing and cDNA analysis of this gene, which is described here as well.

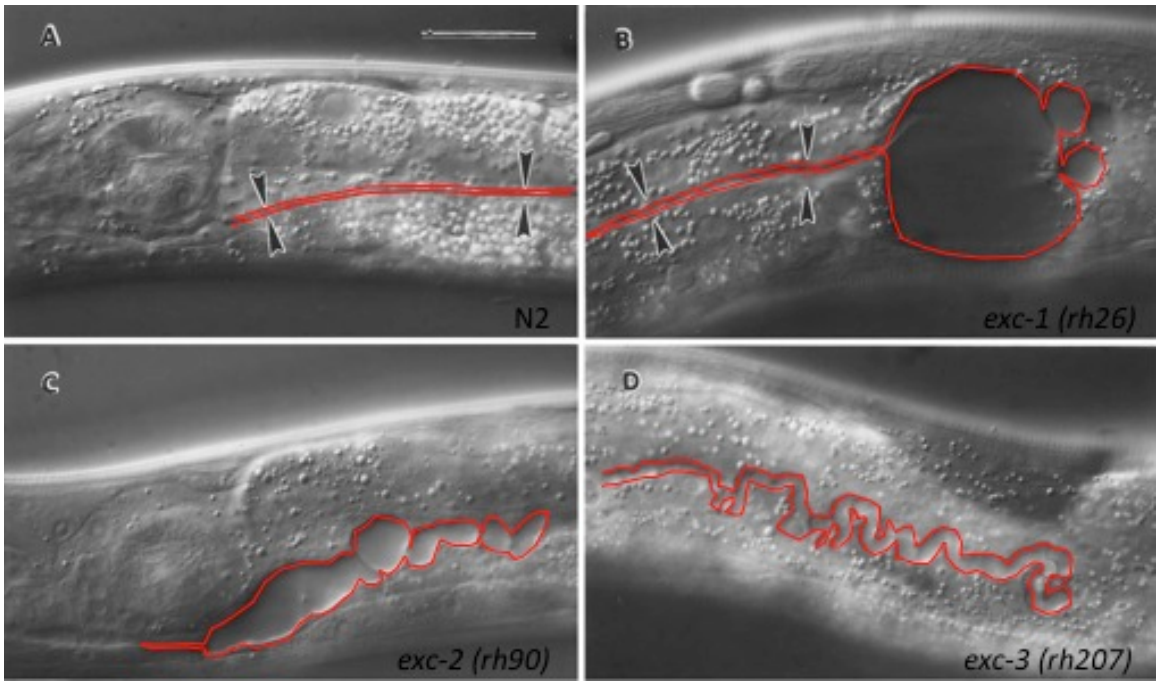

Figure 2.2a *exc* mutants
Wild-type canal and *exc* mutant canals displaying various cystic phenotypes, adapted from Buechner *et al*., 1999. Lumen of the canal is outlined in red, and arrowheads indicate canal regions of normal width. Scale bar, 10μm.

2.3 *exc-1* phenotype

exc-1 (rh26) is a recessive trait that is 100% penetrant; all worms carrying two defective alleles will display a cystic phenotype. The severity of cystic phenotype can vary, from cysts not much wider than a normal lumen, to cysts that expand to the entire diameter of the worm (Figure 2.3a). One consistent phenotype of *exc-1* is the presence of a cyst located at the end of every posterior canal, whether it is the only cyst or one of many (Figure 2.3a). This invariable phenotype of having a cyst located at the end of the canal is found in *exc-5 (rh232)* mutants as well.

To characterize this cystic phenotype of *exc-1* worms I carried out measurements of severity (according to size) and number of cysts, along with canal length. The scale for measuring these standards was first described by former graduate student, Xiangyan Tong (Tong and Buechner, 2008). *exc-1* worms occasionally display canals extending the full length of the worm (7%). However, most *exc-1* canals end earlier, Figure 2.3b. Cysts found within *exc-1* worms are often small, 84% of the time, with only 3% of the cysts observed being large, Figure 2.3c. Mutant worms often exhibit many small cysts located throughout the canal. When characterizing the number of cysts per canal, 66% of them showed between one and five cysts per canal, Figure 2.3d. Other than the cystic phenotype, there is no other obvious phenotype in *exc-1* worms; they mate with no problems and produce the same amount of progeny as wild-type.

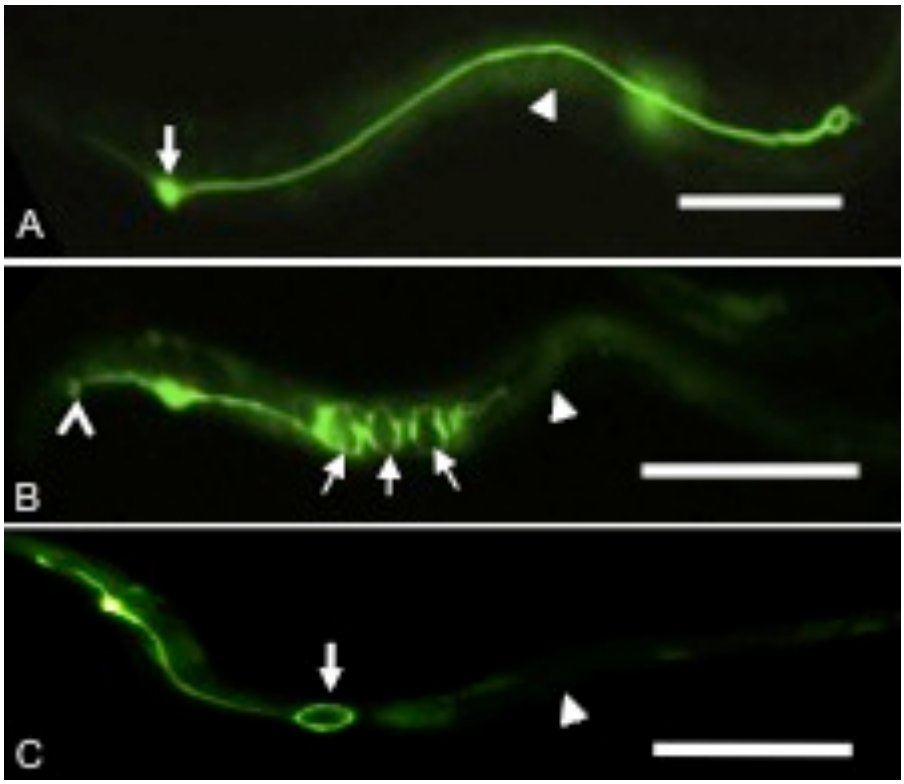

Figure 2.3a *exc-1* phenotypes. (A-C) Canal marked by stable cytoplasmic $P_{vha\text{-}1}$::*gfp* construct in wild-type animal (B), and in *exc-1*(*rh26*) animals showing variable effects with mild (C) or severe (D) effects on tube diameter and length. Wide arrows, excretory cell body; arrowheads, position of vulva at center of animal; narrow arrows, large fluid-filled cysts. Bars, 100 mm.

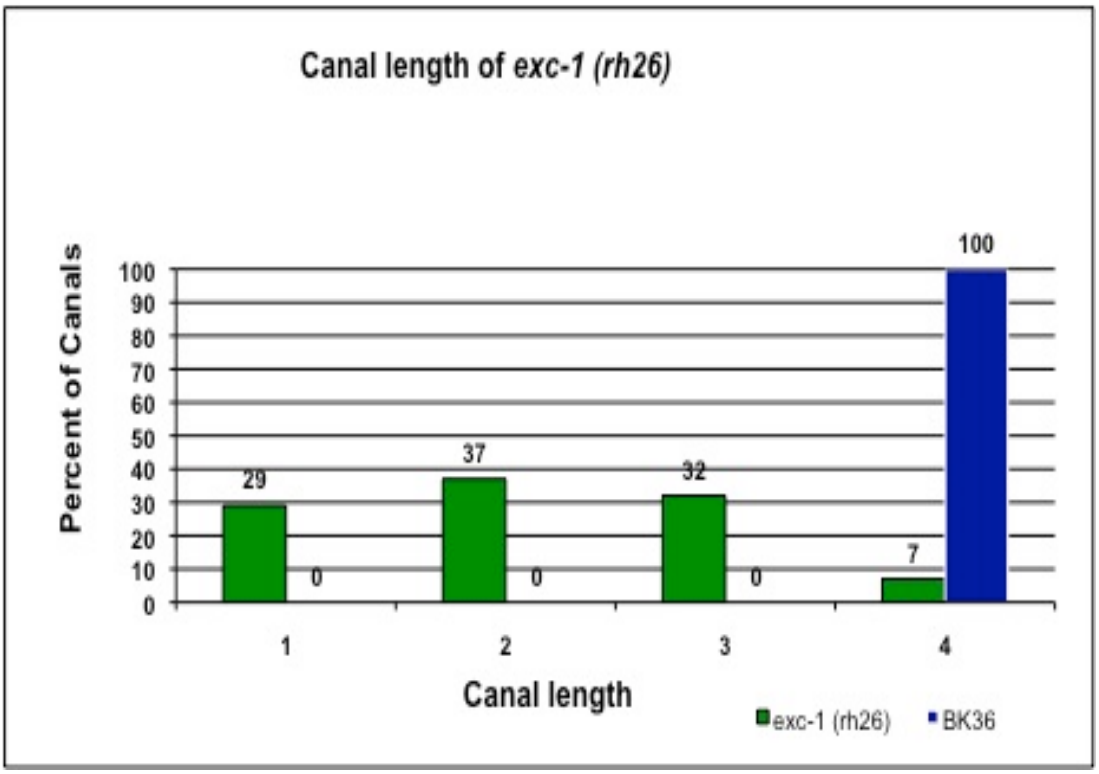

A

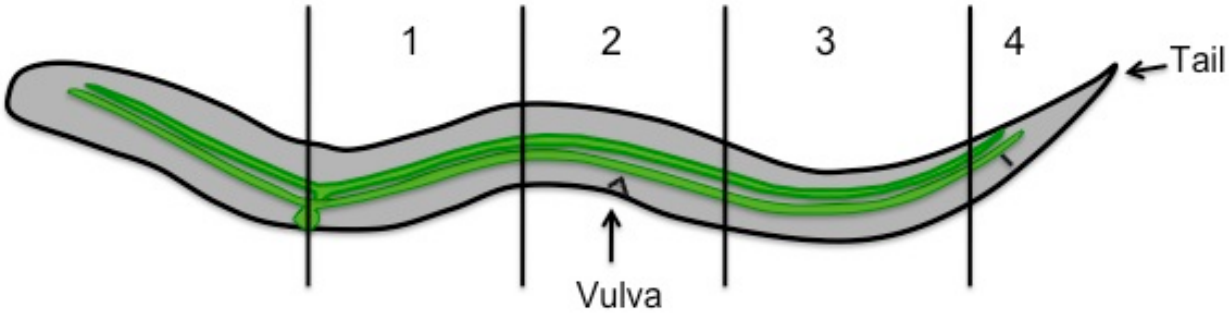

B

Figure 2.3b *exc-1* canal length.

Measurements carried out as described in materials and methods. **(A)** shows graphical representation of data collected, n=100. BK36 strain contains the cytoplasmic canal marker GFP under the control of *vha-1* promoter. **(B)** is a schematic of the scale used for determining canal length.

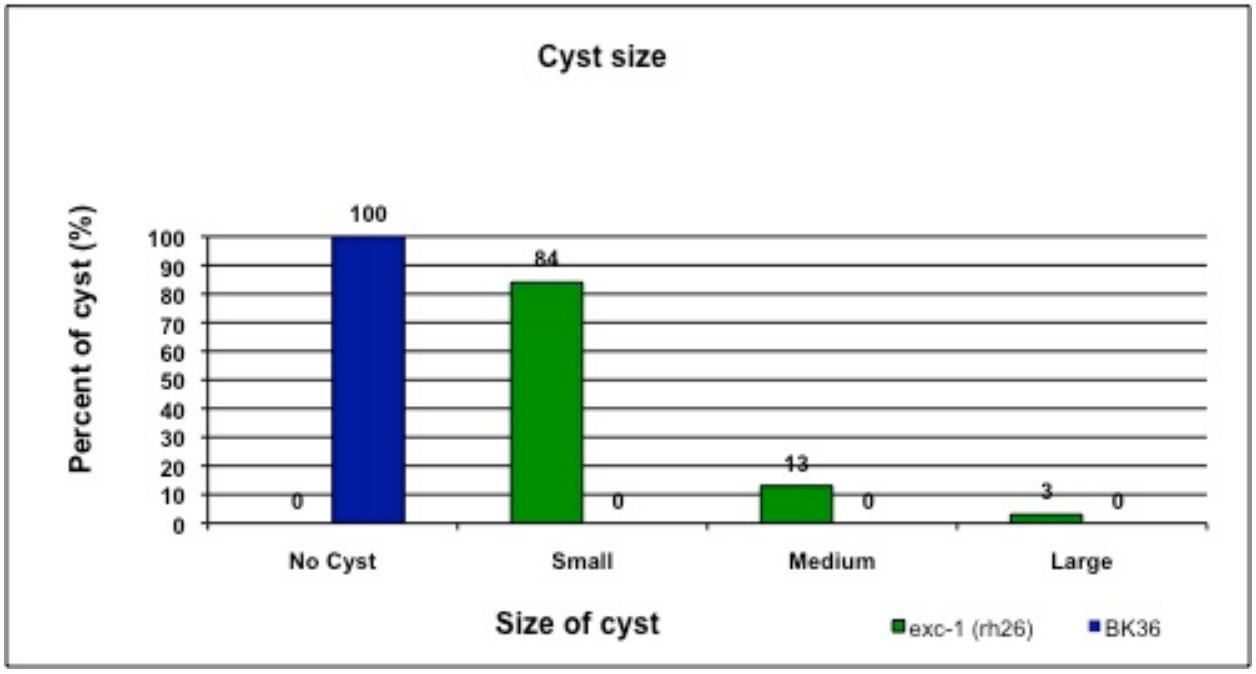

A

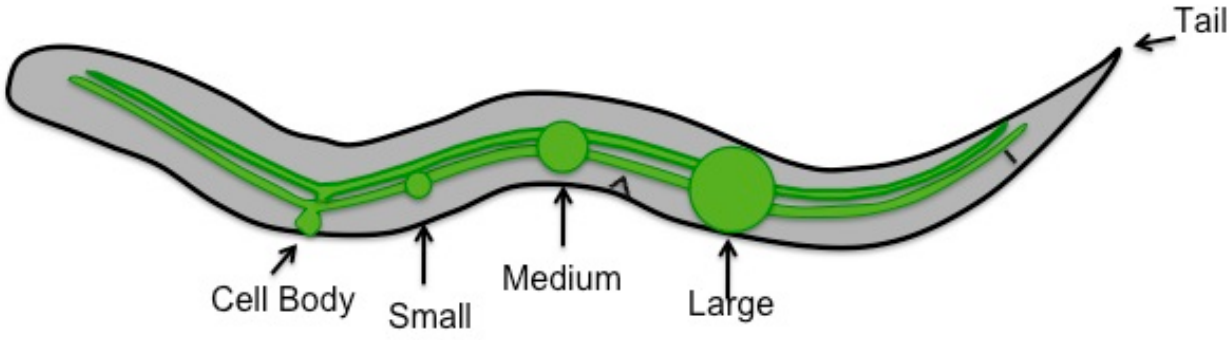

B

Figure 2.3c *exc-1* cyst size.

Determination of small, medium and large cysts was carried out as described in material and methods. **(A)** graphical representation of data collected, n=100. **(B) a** schematic of different sized cysts that was used as a guidance for cyst measurement.

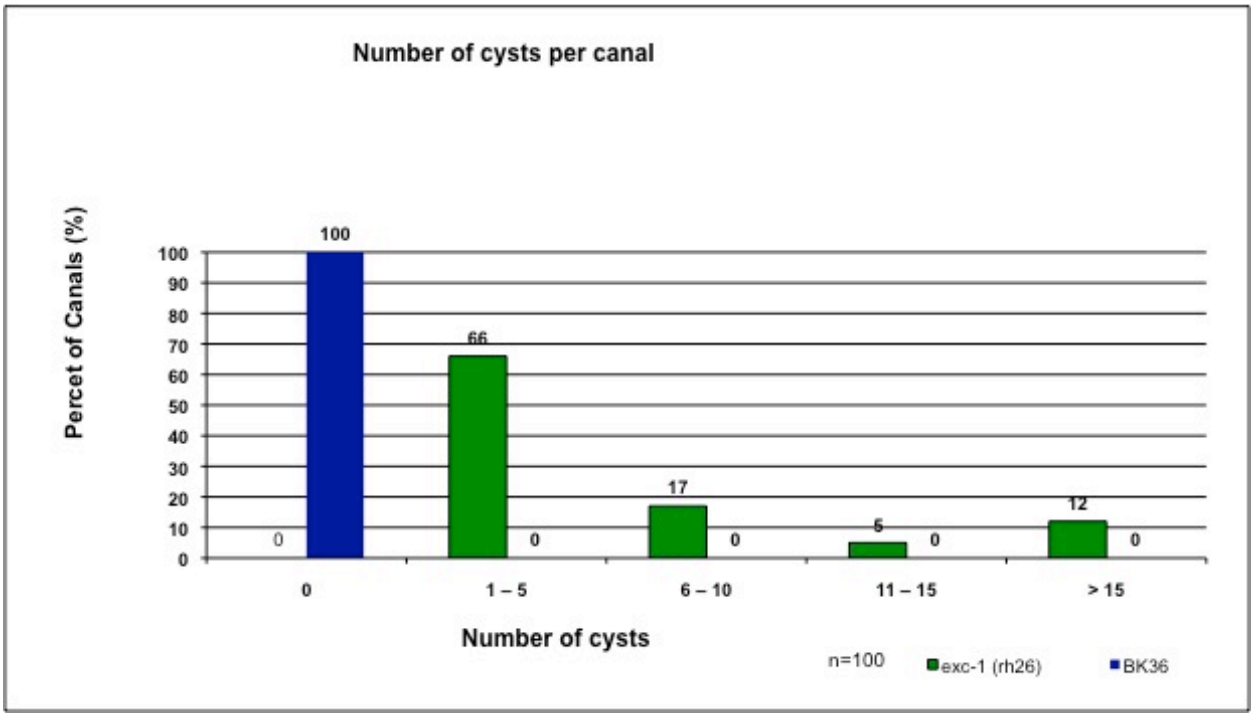

Figure 2.3d Number or cysts per canal in *exc-1* mutant worms, n=100.

2.4 Mapping of *exc-1*

My initial attempt to map *exc-1* was with use of cosmids and Yeast Artificial Chromosomes (YAC) spanning the region where *exc-1* was predicted to be located. Both cosmids and YACs are designed to carry large amounts of DNA, Table 2.4a. After preparation and isolation of these constructs, I found that many were not completely intact and missing large pieces of DNA, making it difficult to use for experiments. Though attempts were carried out to rescue the *exc-1* phenotype, by injection of these incomplete cosmids and YACs, nothing showed signs of possible rescue and I decided to take another approach. I started using fosmids for rescue assays and RNAi techniques.

The region that *exc-1* was predicted to be located in contained 31 predicted genes that were covered by 11 fosmids, Figure 2.4a and table 2.4b. Fosmids are a cosmid vector, based on the *E. coli* F factor replicon. By containing the F factor replicon, the copy number is limited within a host, resulting in a lower chance of recombination events that may result in loss of material. Fosmids can hold large amounts of DNA, up to 40kb in size, containing roughly 4-7 genes (Kim et al., 1992). By using fosmids I was able to inject large pieces of DNA into mutant worms and look for rescue, lowering the number of injections to be carried out. If rescue occurred with a fosmid, I would be able to narrow down *exc-1* to a specific gene located on that fosmid. There were many complications that arose while working with these fosmids; these complications are discussed at the end of this chapter.

Combinations of fosmid injections, and RNAi techniques to knockdown genes in attempt to phenocopy the *exc-1* mutation were carried out. RNAi is a technique that knocks down gene expression by post-transcriptional silencing (Fire et al., 1998). dsRNA can be

administered to *C. elegans* to induce knockdown of a specific gene by injection (Fire et al., 1998), soaking (Tabara et al., 1998) or feeding (Timmons and Fire, 1998).

Eventually, through injection of dsRNA, knockdown of one of the last genes to be tested showed a cystic phenotype, similar to *exc-1*. The corresponding gene was the predicted gene, C46E1.3, Figure 2.4h. None of the other genes in this region caused a cystic phenotype when knocked down, Table 2.4c.

Table 2.4a Cosmids and YAC's in the region predicted to contain *exc-1*.

Cosmid/YAC	**Region**
CO2D4	X:15273419..15309467
Y15E3A (YAC)	X:15298090..15358349
C33A11	X:15351371..15376630
F39D8	X:15397135..15429293
R03A10	X:15419538..15470684
C46E1	X:15465591..15481691
H13N06	X:15474951..15511937
H30A04	X:15510077..15534574
C02C6	X:15534475..15577853

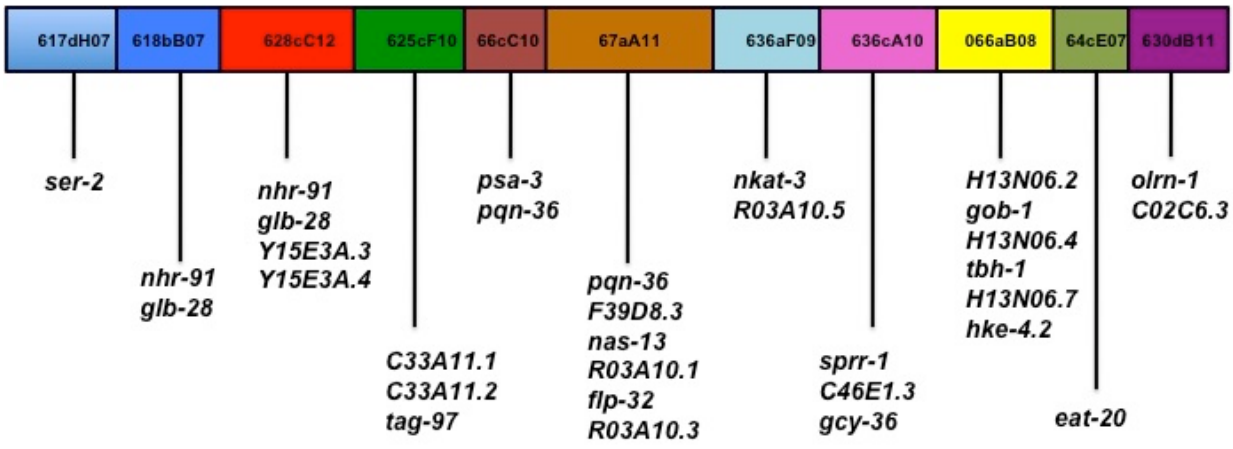

Figure 2.4a Region predicted to contain *exc-1*.
Fosmid indicated by different colors and to scale, the fosmid number is indicated. Listed below each fosmid are the genes located on the corresponding fosmid.

Fosmid	**Genetic location**
WRM0636cA10	X:15453473..15491654
WRM066aB08	X:15477056..15522980
WRM0636aF09	X:15431197..15472039
WRM0625cF10	X:15340030..15383610
WRM064cE07	X:15505066..15546925
WRM0628cC12	X:15301084..15341754
WRM617dH07	X:15258153..15303833
WRM066cC10	X:15369963..15418078
WRM067aA11	X:15411477..15441218
WRM0618bB07	X:1529034..15323445
WRM630dB11	X:15536102..15570596

Table 2.4b Fosmids, including their genetic location, that were used for rescue assays.

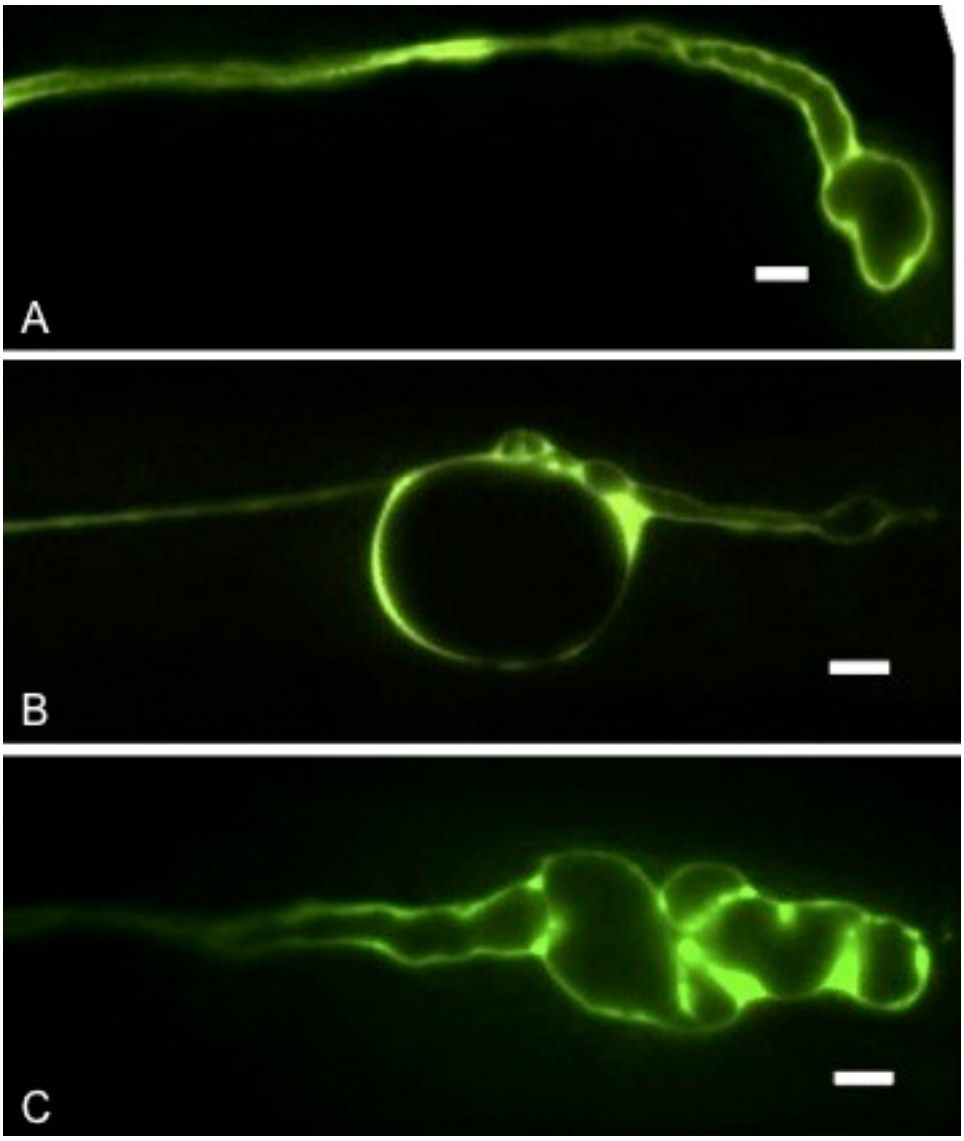

Figure 2.4h. Young adult, F1 progeny from an injected worm.
N2 animal injected with dsRNA corresponding to the 6th exon of C46E1.3 and pCV01 50ng/µl. Knockdown phenocopies the *exc-1 (rh26)* canal, with a wild-type looking canal ending with a small (A) or large (B) cysts, or many cysts (C). Scale bar, 10µm.

Table 2.4c. dsRNAs tested for ability to phenocopy *exc-1* mutants

dsRNA to clone:	Predicted Gene (from wormbase.org)	Forward Primer	Reverse Primer	# Animals Injected	Result
ser-2	SERotonin/octopamine receptor family	TGCATACGAATTTGG	GAGTTACCGTATGCC	38	No canal cysts
nhr-91	Nuclear Hormone Receptor Family	GGACTGCCTAGACCG	TGAGATCTCGTCAGT	60	No canal cysts
glb-28	GLoBin Related	CTTAAAGTTCGCGTG	ATCTTGGAATCGAAT	35	No canal cysts
Y15E3A.3	None	ATATCAGGAAATGAG	ATTCATATTAGAAAA	44	No canal cysts
Y15E3A.4	None	AGCACCCACAAATGT	CAGAACTGGATACGA	45	No canal cysts
Y15E3A.5	None	CGAGTACCTCTTGAC	GCTCTTCAGATCAAT	43	No canal cysts
C33A11.1	None	TGGAAGAACGTGCTT	AATGCTTCTTTGCAA	55	No canal cysts
C33A11.2	None	CTACACTATCGCAGT	TTTGCCACAAAGAAC	59	No canal cysts
tag-97	Temporary Assigned Gene name	ACGCGGGGTTTAACC	TCCTTGGGATTACAA	27	No canal cysts
psa-3	Phasmid Socket Absent	TCAGCAACACTACGC	TACTTGTTTTAAGAA	22	No canal cysts
pqn-36	Prion-like-(Q/N-rich)-domain-bearing protein	TTTTGGTTCTGGTTT	CTGGCTATCAAACTG	25	No canal cysts
F3D98.3	None	GACGAACAGTATTTT	CTATTAATTTCTGTC	61	No canal cysts
nas-13	Nematode AStacin protease	CAATTCTCCCAACTA	CAGTCCACTTTTTGG	27	No canal cysts
RO3A10.1	None	TTAATTATTCGGCGG	ATTTCAGATTGGATA	23	No canal cysts
flp-32	FMRF-Like Peptide	CCAATATTCCAGCCC	ACTAGCAAATTCAGA	25	No canal cysts
mocs-1	MOlybdenum Cofactor Sulfurase	CATTTCTGACGTGAT	AGGAATATCTTCCAT	28	No canal cysts
nkat-3	Nematode Kynurenine AminoTransferase	CATCGAGCCAGCCTA	CACACCCTGTTCTTA	34	No canal cysts
RO3A10.5	None	AGTGCGGAAAAACCG	GCTTTACTAATTCCA	48	No canal cysts
sprr-1	Sex Peptide Receptor (Drosophila) Related	CTATGAAGCTTTGCT	CTGCCGCTGTCGCGC	42	No canal cysts
C46E1.1	None	GATTGCTCAACACAA	TATATCTAGTGTCAC	57	No canal cysts
gcy-36	Guanylyl CYclase	AAACCTATATGAAGA	TTCATTTCCACGTCC	26	No canal cysts
C46E1.3	None	TTTCTTTTCGAAGCC	AAAGCGACGAGGACC	63	Canal, glial cysts
H13NO6.2	None	AACTGAAAACCATCG	AGCGAACTCCAGTCC	41	No canal cysts
gob-1	Gut OBstructed or defective	CTCTTCACCCGAGCA	TTTGAACTCCTAGGG	30	No canal cysts
suox-1	SUlfite OXidase	GAACACAGTTCCATC	TACTGCTTTCGCAAT	40	No canal cysts
tbh-1	Tyramine Beta Hydroxylase	TTGCCCATGCAGCAA	CCAGCCGCTCTCGAG	25	No canal cysts
H13NO6.7	None	ATCAAACTGCGCTGC	TGCATATTCACATT	43	No canal cysts
hke-4.2	Histidine-rich membrane protein KE4 (mouse) homolog	CGCTCATGTCATGA\G	CCTTAATGATCCAAG	56	No canal cysts
eat-20	EATing: abnormal pharyngeal pumping	AGACGAAGATATGAC	TTCCGTACTCGTTTC	67	No canal cysts
olrn-1	Olfactory LeaRNing defective	AATCCCCCAAACTCG	GTTGATGGTTTGAGC	30	No canal cysts
lron-1	eLRR (extracellular Leucine-Rich Repeat) ONly	TGTAATTAGCCGAGA	ACTAATTTGCGCTGG	15	No canal cysts

2.5 Rescue of *exc-1* with C46E1.3

To determine if predicted gene, C46E1.3, truly was *exc-1,* attempts to rescue the cystic phenotype by injections of corresponding gene were carried out. The predicted transcript, as per wormbase, is 6608 bp in length, with the gene *gcy-36* being roughly 1.6kb upstream of C46E1.3. A PCR fragment containing this region of 1.6kb upstream of C46E1.3 and the predicted coding region plus 500bp downstream was amplified. This PCR fragment was then placed into a TOPO TA vector (Invitrogen®, plasmid pBK102). When injected, at 25ng/μl, this construct was able to rescue the cystic phenotype, and even show an overexpression, convoluted canal, phenotype, Table 2.5a and Figure 2.5a.

While injecting the gene C46E1.3 into *exc-1 (rh26)* worms, I recovered a few different phenotypes. Some of the F1 progeny from injected worms showed a rescue back to the narrow, wild-type phenotype, and some showed an overexpression phenotype. This overexpression phenotype results in a convoluted canal. In a convoluted canal the canal seems to polarize normally and have proper formation of the lumen and apical surface, but the basal surface is disrupted and does not extend out from the cell body. This type of overexpression phenotype occurs when overexpressing EXC-5 or EXC-9, as well (Suzuki et al., 2001; Tong and Buechner, 2008).

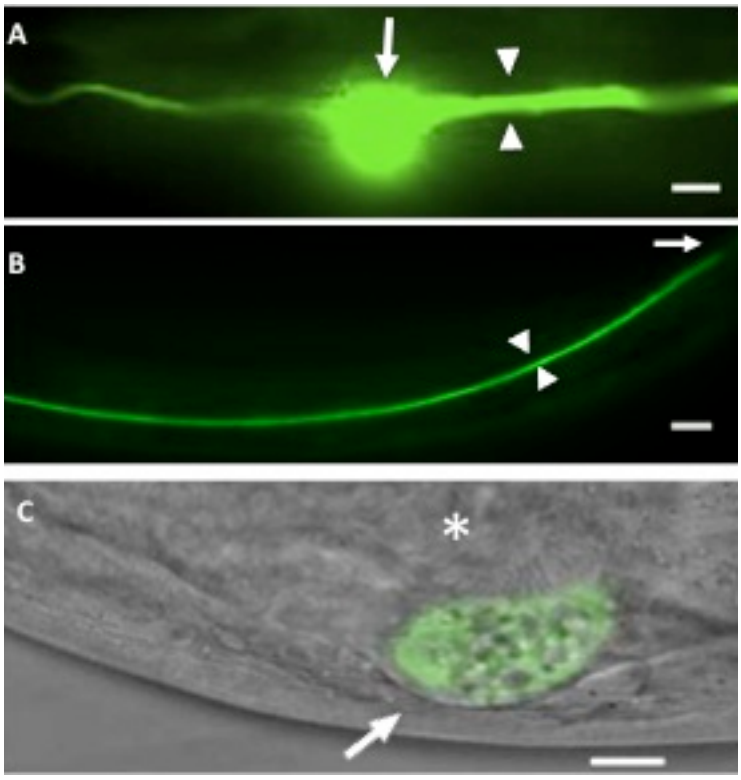

Figure 2.5a. Rescue of cystic phenotype with C46E1.3

(A-C) Microinjection of amplified fragment of fosmid WRM0636cA10 containing the promoter and coding region of C46E1.3 DNA rescues canal phenotype in *exc-1*(*rh26*) mutant. Arrowheads indicate width of canal cytoplasm. (A) Arrow indicates canal cell body, with both anterior and posterior canals visible (anterior to left). (B) Posterior canal extends full-length to the tip of the animal (arrow) and is of normal diameter (C) Arrow indicates overexpression phenotype, the apical surface is maintained, however, the basal surface is unable to extend from the cell body and is located ventrally to the posterior bulb of the pharynx, indicated by asterisk.

Table 2.5a

Strain/Constructs			Canal Lumen Length, Number			Cyst Size, Number			p-value	
Genotype	Injected with	n	No growth and short	Medium (midway and 3/4)	Full-length (WT and convoluted)	Large Medium	Small	None	Lumen Length	Cyst Size
N2		**100**	**0**	**0**	**0**	**0**	**0**	**0**		
exc-1 (rh26)		**100**	**29**	**64**	**7**	**48**	**51**	**1**		
exc-1 (rh26)	***exc-1* + pCV01 (*Pvha-1::gfp*)**	**66**	**0**	**0**	**66**	**0**	**0**	**66**	**1.26×10^{-38}***	**3.78×10^{-46}***
exc-1 (ok5478)		**33**	**13**	**17**	**3**	**22**	**11**	**0**	**0.3897***	**0.1328***

Compared to *exc-1 (rh26)

2.6 *exc-1* mutation and cDNA analysis

To determine the type of mutation in the *exc-1* gene, *rh26* allele, the predicted coding regions were amplified from *exc-1 (rh26)* worms and sequenced. From the sequencing results, compared to wild-type sequence from wormbase, there was a single base-pair mutation (C → T) located near the end of the 11th Exon. This mutation changed the coding sequence from an arginine (ARG) to an early stop, Figure 2.6a.

To determine if the predicted exons, as per wormbase, were correct, I isolated EXC-1 cDNA from wild-type worms. By sequencing the cDNA, it was found that exon 2 of EXC-1 is actually shorter than what was predicted (Figure 2.6a). Many attempts were carried out to determine if there were two different isoforms of EXC-1, however I was only able to extract this shorter sequence, suggesting that this is the only form of EXC-1 and that the predicted exons on wormbase are incorrect. Wormbase predicts the length of EXC-1 to be 763 amino acids in length and I was only able to extract a form that was 738 amino acids in length, 25 amino acids shorter (SLRSFIEETPILLGSSEHSGSSSPP, genomic region X:15477167..15477093).

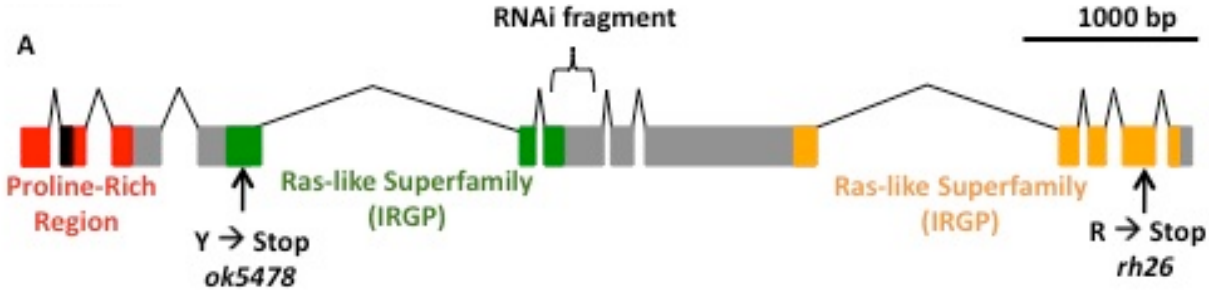

Figure 2.6a. (A) Structure of the *exc-1* coding region and encoded protein. Major domains of the protein are shown in color. Region in black is predicted on wormbase, (bases 58-82 of the predicted cDNA) but not found in the amplified cDNA. Bracket shows area of cDNA used for dsRNA injections. Mutations of *rh26* and *ok5478* alleles are indicated.

2.7 *exc-1* acts cell autonomously

To make sure that this shorter form of cDNA was correct and functional, I tested it for rescue of the cystic phenotype of *exc-1* mutant worms. To do this, the isolated EXC-1 cDNA was placed into the vector pCV01, Figure 2.7a. This vector contains the canal specific promoter *vha-1* with the marker, *gfp*. When this construct was injected into *exc-1 (rh26)* worms it was able to rescue the cystic phenotype, confirming that the sequence of cDNA isolated is sufficient for function, Figure 2.7b. By carrying out this study of using a canal specific promoter expressing EXC-1 in the canal, and showing rescue, it was determined that EXC-1 acts cell autonomously within the excretory canal.

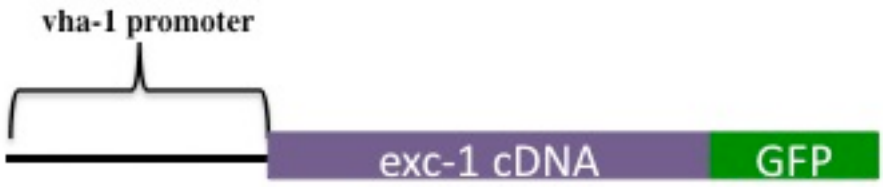

Figure 2.7a cDNA rescue construct.

exc-1 cDNA isolated from N2 worms was ligated N-terminally to GFP in the vector pCV01. The remaining backbone of this vector is not shown.

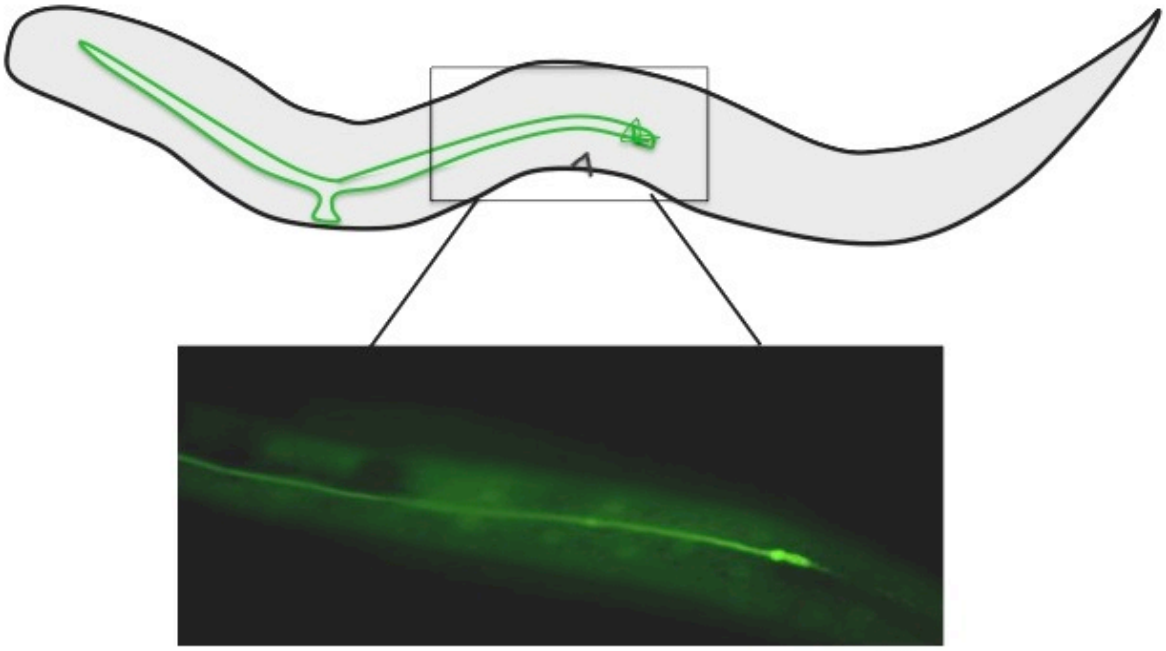

Figure 2.7b. Rescue by EXC-1 cDNA.

Top image shows is a schematic of a worm that has a canal partially grown out ending with a convoluted portion of the canal,. Bottom image is a young adult, F1 progeny of a N2 injected with 25ng/µl of *Pvha-1*::EXC-1cDNA::GFP. Progeny of injected worms also exhibited wild-type length canals and fully convoluted canals

2.8 Alleles of *exc-1*

Because *exc-1 (rh26)* is a nonsense mutation so late in the gene it is a possibility that *rh26* might not be a true null allele. Studies that Dr. Matthew Buechner and I have carried out suggest that *exc-1* is, in fact, a null allele. If *exc-1* is placed over a deletion the severity of the cystic phenotype does not get worse, suggesting that *rh26* is not a partial loss of function.

At the beginning of my studies *rh26* was the only allele of *exc-1* available. Other alleles have been found by the Gene Knockout Consortium (Flibotte et al., 2010; Moulder and Barstead, 1998). One allele, *ok5478*, has a nonsense mutation located in the 4th exon, much earlier than *rh26,* Figure 2.6a. When carrying out phenotypic analysis of this *ok5478* allele I found that the severity of cysts was the same as for *rh26,* Table 2.5a.

Other alleles identified by the Million Mutation project (Consortium, 2012) were ordered from the Caenorhabditis Genetics Center (www.cbs.umn.edu/cgc) and examined for cystic phenotypes, Table 2.8a. All of these alleles contained Missense mutations within the exons of *exc-1* and when observed, they did not exhibit a cystic phenotype. Since this time, 59 new alleles have been identified by this Million Mutation project, though they have not been examined for cystic phenotypes.

Table 2.8a *exc-1* alleles identified by the Knockout consortium or the Million mutation project that were examined for cystic canals.

Strain	**Allele**	**Mutation**		**Reference**
VC20424	*gk303482*	Missense – Exon	544G→E	Million Mutation
VC20161	*gk303483*	Missense – Exon	528R→H	Million Mutation
VC20598	*gk303484*	Missense - Exon	374A→T	Million Mutation
VC300068	*gk303492*	Missense – Exon	212T→A	Million Mutation
VC20491	*gk303494*	Missense – Exon	198P→L	Million Mutation
VC2008	*gk303495*	Missense – Exon	164P→S	Million Mutation
RB5001	*ok5478*	Nonsense	302Y→Stop	KO Consortium (Flibotte et al., 2010)
RB5002	*ok5960*	Missense – Intron	Unknown	KO Consortium (Flibotte et al., 2010)

2.9 Summary

C46E1.3 encodes *exc-1*

This work mapped and identified the *exc-1* gene as C46E1.3. When C46E1.3 is knocked down by RNAi it phenocopies the cystic phenotype of *exc-1*. Also, a PCR amplified product corresponding to C46E1.3 rescues the *exc-1* cystic phenotype. We conclude that C46E1.3 is *exc-1*.

EXC-1 cDNA is shorter than predicted

By isolation of EXC-1 cDNA and sequencing, it was found that the 2nd exon is shorter than predicted. This shortened cDNA is functional and is able to rescue the *exc-1* cystic phenotype. Also, by expressing this cDNA only within the canal we are able to determine that *exc-1* works cell autonomously within the canal.

exc-1 alleles

Allele *rh26* has a single base-pair mutation, within the 11th exon, resulting in an early stop. This allele is a predicted null mutation, because when placed over a deletion, the severity of phenotype does not get worse. Also, allele *ok5478,* which has a nonsense mutation in the 4th exon shows similar cystic phenotype as *rh26*.

2.10 Materials and Methods

Worm strains

Throughout this disseration; *C. elegans* strains were maintained by use of standard culture techniques on lawns of *Escherichia coli* strain BK16 (a streptomycin-

resistant derivative of strain OP50) grown on nematode growth medium (NGM) plates (Sulston and Hodgkin, 1988). Strains were kept at 20°C, unless otherwise noted, and phenotypic analyses were carried out on L4 larvae or young adults.

Characterizing exc-1

Scoring of canal lengths was on a scale from 0 – 4: A score of (4) was given if the canals had grown out to full length; canals that extended past the vulva but not full-length were scored as (3); at the vulva (2); canals that ended between the cell body and the vulva were scored as (1); and if the canal did not extend past the cell body, the canal was scored as (0). Cyst phenotype was measured by count and size relative to normal canal width. Cysts wider than a normal canal up to 1/4 the diameter of the worm were scored as small, cysts larger than ¼ diameter to ½ the diameter of the worm were scored as medium. Any cysts larger than ½ the diameter of the worm were scored as large. This scheme of cyst and canal measurements was used for all phenotypic studies.

To determine if C46E.13 and the short isoforms of EXC-1 cDNA were able to rescue the *exc-1* cystic phenotypes, for both length and cyst severity, results from canal measurements were binned and analyzed via a 3×2 Fishers' Exact Test. A p- value of 0.0001% or lower was regarded as strong statistical significance of rescue; p- values between 0.0001% and 0.01% or less were regarded as partial rescue. Performing statistical analysis was carried out with the assistance of Stuart MacDonald and was first described in the work by former graduate student, Xiangyan Tong (Tong and Buechner, 2008) . This is also the analysis that has been carried out for studies in Chapter 5.

Constructs and mRNA Isolation

YACs and cosmids were supplied by Sanger Institute, Cambridge, UK and fosmids were supplied by Bioscience Lifesciences (Source BioScience Cambridge, UK). The cosmid and fosmid DNA or YAC DNA was isolated using a DNA prep protocol from bacteria and yeast, respectively. Once purified, the DNA was analyzed, to determine if the constructs were intact, via digestion with restriction enzymes and gel electrophoresis.

dsRNA was designed to a 300-400 base pair region that corresponded to an exon within each gene. A PCR of the corresponding region was carried out and then transcribed into dsRNA with the MEGAscript® T7 kit (Life Technologies, Invitrogen™ Grand Island, NY).

A fragment amplified from fosmid WRM0636cA10 via PCR with primers 5'CCACGTCAGAAAAGAAATATTCTCGCTCCG3' and 5' TCACATGTTCATCAAGCGGAAAAGTTCACT3' contained 1.6 kb upstream through 0.5 kb downstream of predicted gene C46E1.3. The amplified region was ligated into pCR®-XL-TOPO® vector (Life Technologies, Grand Island, NY) and microinjected at 25ng/µl into *exc-1(rh26)* mutants.

Isolation of the cDNA was carried out by extracting the mRNA from wild-type worms with a mRNA magnetic bead isolation kit (New England Biolabs, Ipswich, MN). To isolate EXC-1 cDNA, specific primers were used (F: 5'ATGGGACACAAAACCTCAAAAA 3' AND R: 5' TCAATGAACTCCGGCTGTATCTAGAT 3'). Once isolated, cDNA was ligated into a

TOPO vector (Life Technologies, Invitrogen™ Grand Island, NY) and has been maintained it in the lab (plasmid, pBK105).

Injections

Microinjections were carried out by injecting into the distal arm of the worm gonad (Mello et al., 1991). Injected worms were allowed to recover and scoring of canal phenotypes was carried out on their progeny. This microinjection technique is the way every microinjection was carried out throughout this dissertation.

Fosmids were injected at various concentrations to try and rescue the *exc-1* cystic phenotype, starting at 100ng/µl and decreasing to 25ng/µl. All fosmids were co-injected with canal cytoplasmic marker pVC01 (*Pvha-1*::*gpfp*) that expresses GFP only within the canal and head mesodermal cell.

EXC-1 cDNA construct, *Pvha-1*::EXC-1cDNA:GFP was injected at a concentration of 25ng/µl.

Sequencing

Sequencing of C46E1.3 was carried in four regions, designed to include the predicted coding sequences: Exons 1 and 2, Exon 3 and 4, Exons 5-8 and Exons 9-12. These regions were amplified from *exc-1 (rh26)* worms with the following primers:

Region	Forward Primer	Reverse Primer
Exon 1-2	AGTTGGCTTAAACTTGTGCTCAGCC	CCTCTTGTGAGTACGGACGAACC
Exon 3-4	GCCGTCTGATCCGCCTAAAGAT	TTGGGTAAGACTTGGGCGACG

Exon 5-8	GGGTAAACCTTGGGCAAGAGTTGG	ACGTTCAAAATCATCCGAACG
Exon 9-12	CAGGGTGTAGTCCACCTT	TTCTGCTCCATTCCCACC

DNA sequencing was carried out by ACGT, inc (Wheeeling, IL) then aligned with wild-type sequence from wormbase by the program, clustalw (www.ebi.ac.uk/Tools/msa/clustalw2/).

Microscopy Imaging

Live worms were mounted on 2% agarose pads with added 10mM muscimol or 0.5% 1-phenoxy-2-propanol as an anesthetic, as described previously(Sulston and Hodgkin, 1988). Images were captured with a MagnaFire Camera (Optronics) on a Zeiss Axioskop microscope with Nomarski optics.

2.11 Complications with mapping

During my work with fosmid injections it looked like multiple fosmids were able to rescue the *exc-1* cystic phenotype, at first. In the order that I was doing injections (Table 2.11a) it looked like there was some rescue when *exc-1* worms were injected with fosmid WRM064cE07, Figure 2.11a. This was exciting because the fosmid WRM064cE07 contained the gene *eat-20,* a paralog of the Drosophila Crumbs protein. Crumbs functions as an apical determinant in many cell types and has been shown to be important for tubulogenesis and tube shape in *Drosophila melanogaster (Myat and Andrew, 2002)* It is also known that Crumbs interacts with $\beta_{\text{-HEAVY}}$ Spectrin and is

important for properly maintaining equal apical and basal membrane distribution (Wodarz et al., 1995). Deletion strains of *eat-20* (alleles *nc5* and *nc6*) were obtained to check for a cystic phenotype. While observing the *eat-20* mutant strains, I did not observe a cystic phenotype, indicating *eat-20* was most likely not *exc-1*.

Continuing with injections, it looked like WRM618bB07 or WRM628cC12, might have rescued the *exc-1* phenotype, though not at a large percentage, Table 2.11a, Figure 2.11b and 2.11c. Because the gene, *nhr-91,* was located on both of these fosmids studies were carried out to investigate this gene further. Also, previous studies had shown that *nhr-91* was expressed in the canal (Gissendanner et al., 2004), making it an even more attractive candidate. RNAi experiments were carried out to knockdown *nhr-91*. Knockdown of *nhr-91* seemed to disrupt the excretory canal structure, and in some worms there seemed to be small cysts, figure 2.11d and 2.11e. These cysts did not look like *exc-1,* either in number or size, and did not occur very often, so I continued with rescue experiments with other fosmids.

While injecting fosmid WRM677aA11 it looked like it might be rescuing the *exc-1* cystic phenotype, Table 2.11a, Figure 2.11f so studies were carried out to test each individual gene located on the fosmid for rescue; *pqn36, F39D8.3, nas-13, R03A10.1, flp-32* and *R03A10.3*. When injecting these genes individually, many of the F1 progeny from all of the injections looked wild-type, indicating that something was wrong with the strain that was used for injections, Table 2.11b. As mentioned previously, *exc-1* can have a very mild cystic phenotype, almost looking wild-type, however not at the rate observed during these injections. These results suggested that there had either been a reversion, and the mutation in the DNA causing the *exc-1* phenotype was no longer present, or there was

possible a suppression mutation that arose (through later sequencing it was identified as a reversion). There is a possibility of contamination with another strain, but as this was the only worm strain I was working with at the time, this is unlikely. So, I re-thawed one of the initial lines of *exc-1 (rh26)* and continued with the attempts to rescue with fosmids or phenocopy with RNAi.

Table 2.11a Fosmids

Injections of fosmids (with pVC01 as co-injection marker) into *exc-1 (rh26)* worms.

Fosmid	**Genetic location**	**Number of worms injected**	**Canals Scored (n)**	**Percent rescued**
WRM0636cA10	X:15453473..15491654	76	81	0
WRM066aB08	X:15477056..15522980	92	61	0
WRM0636aF09	X:15431197..15472039	85	50	0
WRM0625cF10	X:15340030..15383610	103	62	3
WRM064cE07	X:15505066..15546925	256	123	13
WRM0628cC12	X:15301084..15341754	130	132	10
WRM617dH07	X:15258153..15303833	84	54	11
WRM066cC10	X:15369963..15418078	125	87	7
WRM067aA11	X:15411477..15441218	162	75	48
WRM0618bB07	X:1529034..15323445	142	102	6
WRM630dB11	X:15536102..15570596	153	92	10

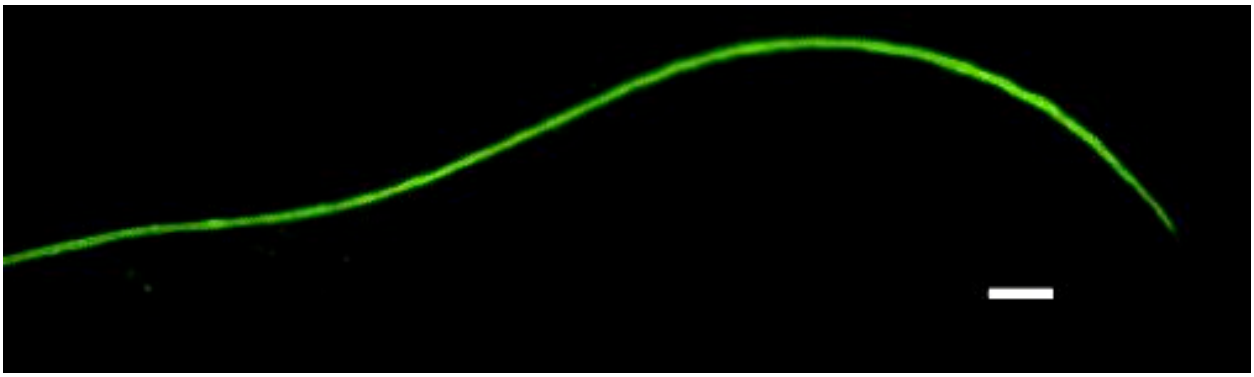

Figure 2.11a Young adult, F1 progeny from injected worm.
Injection of fosmid WRM064cE07 100ng/µl and pCV01 50ng/µl into *exc-1 (rh26)*. Scale bar, 10µm.

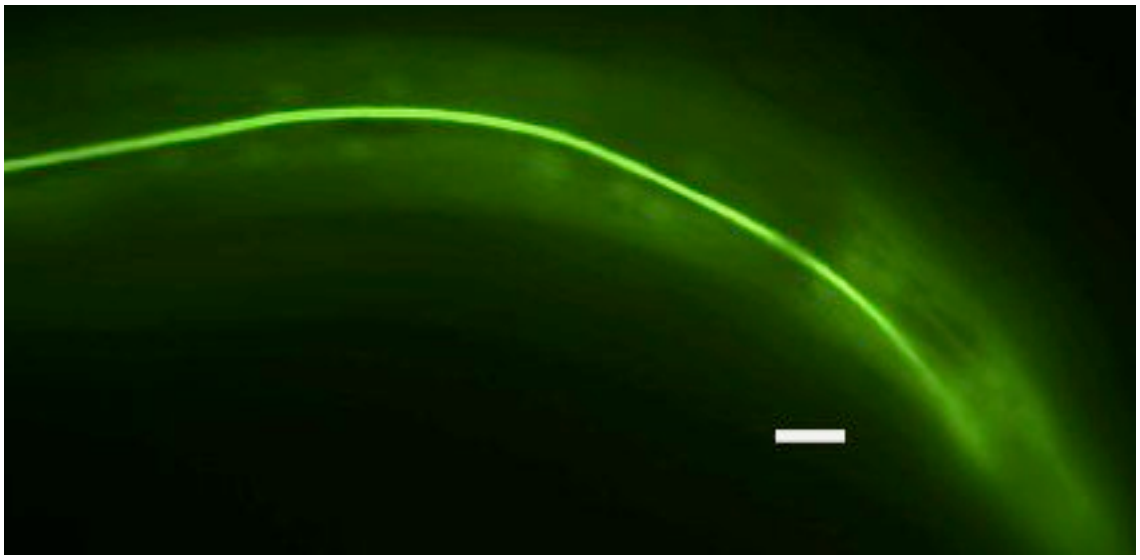

Figure **2.11b** Young adult, F1 progeny from an injected worm.
Injection of fosmid WRM0618bB07 100ng/µl and pCV01 50ng/µl into *exc-1 (rh26)*. Scale bar, 10µm.

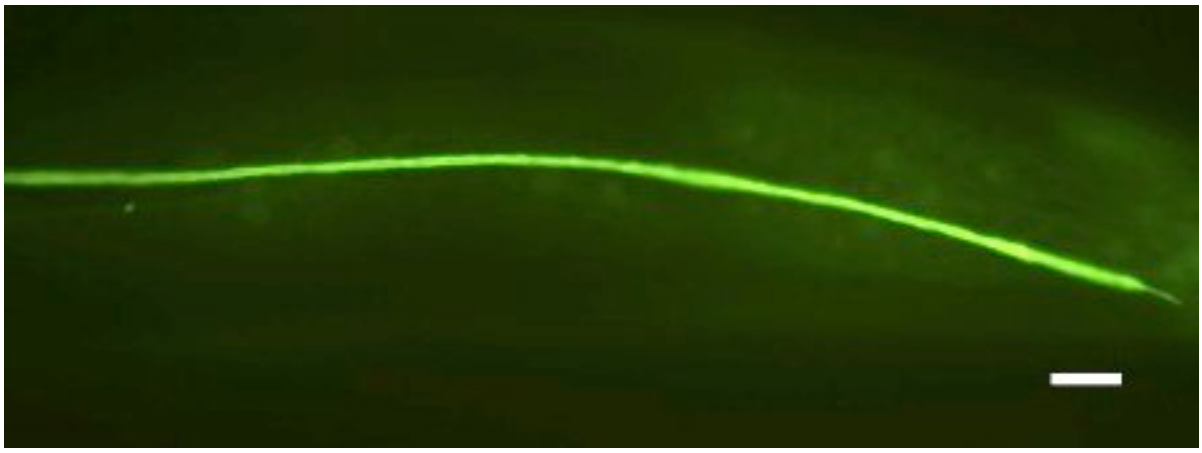

Figure 2.11c Young adult, F1 progeny from an injected worm.
Injection of fosmid WRM0628cC12 100ng/µl and pCV01 50ng/µl into *exc-1 (rh26)* . Scale bar 10µm.

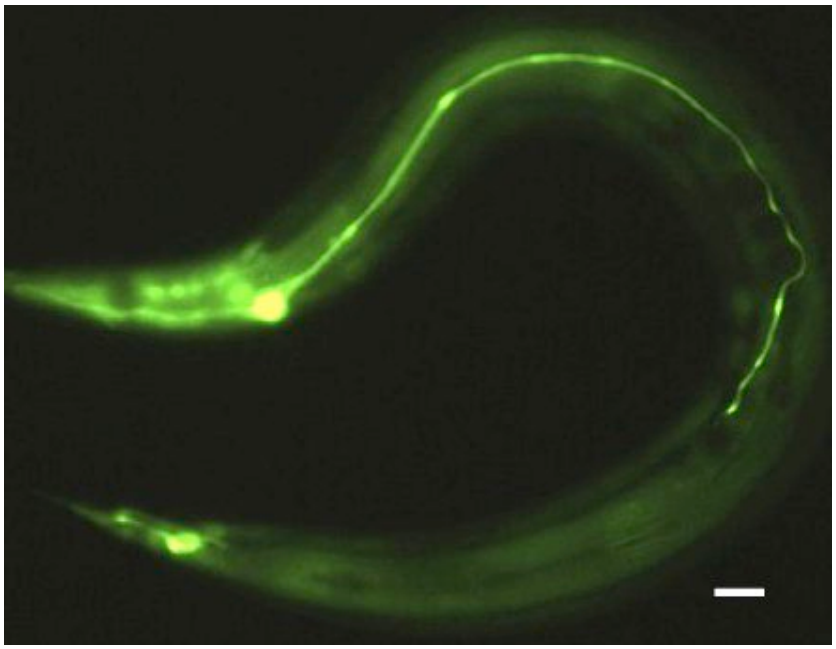

Figure 2.11d Young adult, F1 progeny from an injected worm.
Injection mixture of dsRNA corresponding to gene *nhr-91* and pCV01 50ng/µl into N2 worms. Scale bar, 10µm.

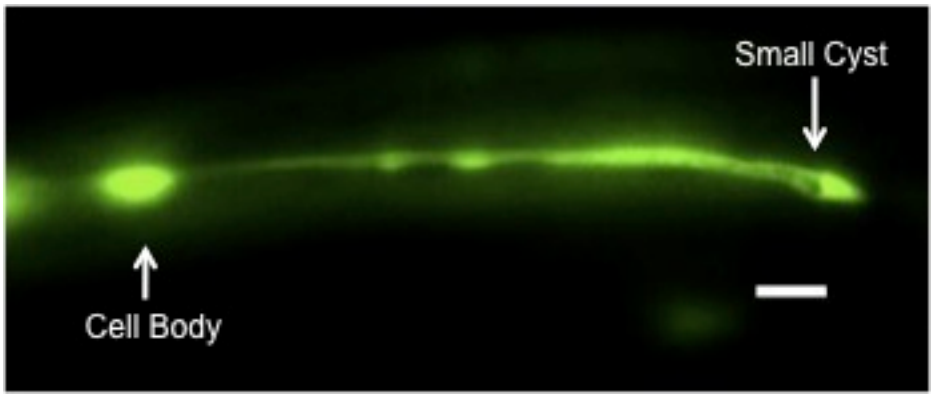

Figure 2.11e Young adult, F1 progeny from an injected worm.
Injection mixture of dsRNA corresponding to gene *nhr-91* and pCV01 50ng/µl into N2 worms. Scale bar, 10µm.

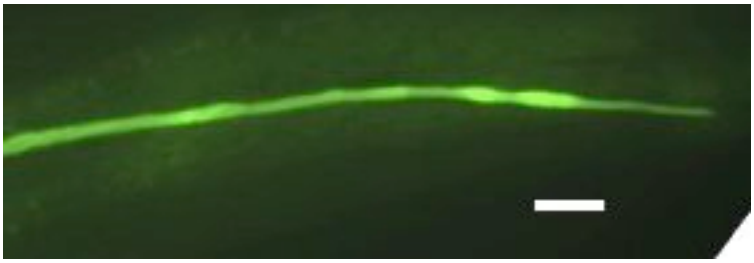

Figure 2.11f. Young adult, F1 progeny from an injected worm. Injection of fosmid WRM0677aA11 100ng/µl and pCV01 50ng/µl into *exc-1 (rh26)* Scale bar 10µm.

Table 2.11b. Genes from fosmid WRM0677aA11 injected into *exc-1 (rh26)* worms.

Gene	**Canals Scored/Injected**	**# Cystic (%)**	**# Rescue (%)**
F39D8.3	23/47	15 (65)	8 (35)
flp-32	27/38	15(56)	12 (44)
R03A10.1	25/48	5 (20)	20 (80)
nas-13	13/26	3 (23)	10 (77)

Chapter 3

EXC-1 in the Amphid Sheath

Chapter 3: EXC-1 in the Amphid Sheath

3.1 Abstract
3.2 Introduction
3.3 Expression pattern of EXC-1
3.4 Dye filling assay
3.5 Structure of amphid sheath in *exc-1*
3.6 Summary
3.7 Materials and Methods

3.1 Abstract

A transcriptional reporter was used to determine temporal and spatial expression patterns of *exc-1*. *exc-1* is expressed within the excretory canal and the glial amphid sheath cells, another tubular-like structure that ensheaths 12 neurons, located near the head of the worm. *exc-1* mutants exhibit occasional small cysts along the processes of the amphid sheath cells, but these did not seem to prevent the amphid sheath from properly wrapping around the amphid neurons.

3.2 Introduction

Once regarded as strictly structural support, the function and role of glial cells has been overlooked for decades. After discoveries that these neuronal supportive cells are involved in signaling as well, they have emerged as essential components to understand the complex working of the nervous system (Araque et al., 1999; Haydon, 2001; Kuffler and Potter, 1964). And although it is estimated that there are five glial cells for every neuron, in humans, research on these intricate cells has been slightly neglected. (Oikonomou and Shaham, 2010). One of the biggest challenges in study glia is the vital role they play in neuronal survival. In most organisms, glia is necessary for neuronal survival, so defects within the corresponding glia may result in no neuron to study. In *C*.

elegans, glial cells are not required for neuronal survival; through they play a role in neuronal development and function (Bacaj et al., 2008b; Shaham, 2006). The interaction of glial cells and neuronal cells is less complicated in *C. elegans* as well. In the adult hermaphrodite there are 302 neurons and 56 neuronal supportive cells, allowing for a simpler model to study glia.

The bilateral amphids, located within the head of the worm, make up the largest sensory organ in *C. elegans* (Sulston, 1983; Ward et al., 1975). Each amphid contains 12 sensory neurons, one sheath cell that ensheaths the neuronal dendrites, and one socket cell wrapping around the distal part of these dendrites. Through an opening, formed by the sheath and socket cells, most of these neurons are exposed to the outside environment Figure 3.2a. These 12 sensory neurons exhibit specific responses to different stimuli, playing roles in chemotaxis, mechanosensation, osmotaxis and dauer pheromone sensation (Bargmann, 2006). Of the 12 neurons, 8 of them pass through the amphid sheath and are exposed to the outside environment. The remaining 4 neuronal dendrites terminate within the amphid sheath, in a hand-in-glove fashion, Figure 3.2b. The amphid sheath is attached anteriorly with the amphid socket via an adherens junction, forming the amphid channel, the only tubular portion of the sheath cell Figure 3.2b. (Perkins et al., 1986; Ward et al., 1975).

EXC-1 is expressed within the amphid sheath. *exc-1* mutants exhibit occasional cysts located along the axon-like process. In this section I describe the studies and results of characterizing EXC-1 within the amphid sheath.

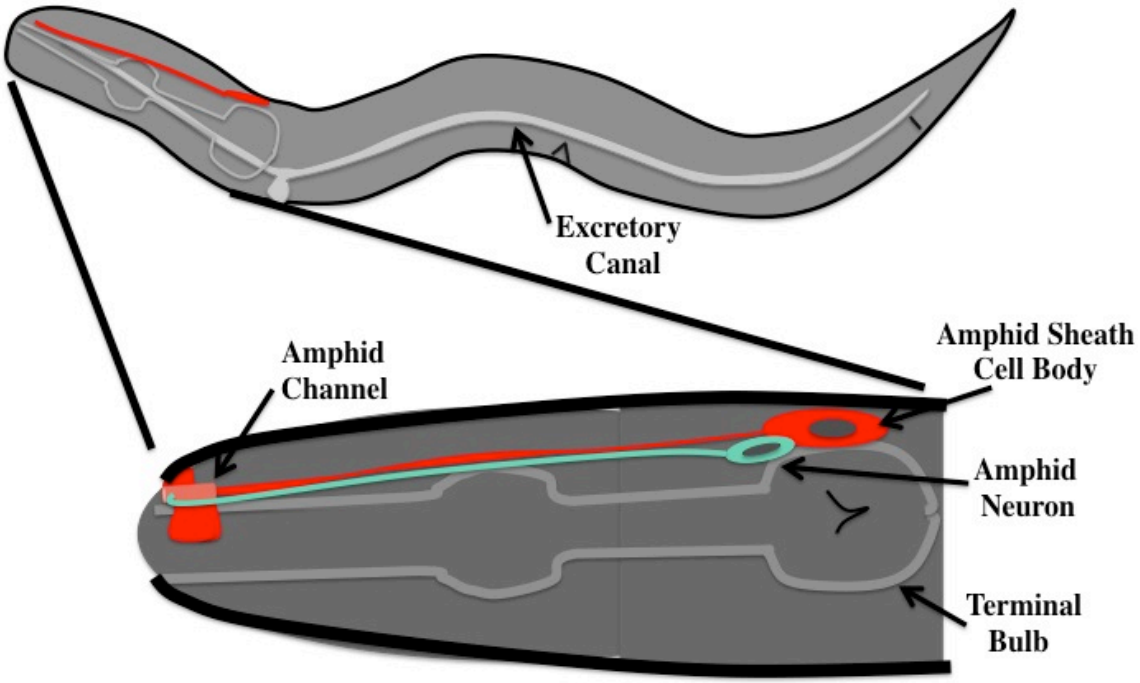

Figure 3.2a *C. elegans* amphid sheath.

A schematic to diagram the location of the amphid sheath and amphid channel. Only the right amphid sheath is shown. In the close up section, the amphid sheath cell body, process and region contributing to the amphid channel is shown. Only one of the amphid neurons is shown for clarity, the neuron cell body is located near the amphid sheath cell body and sends its dendrite towards the head, where it will either pass through into the amphid channel or remain within the sheath.

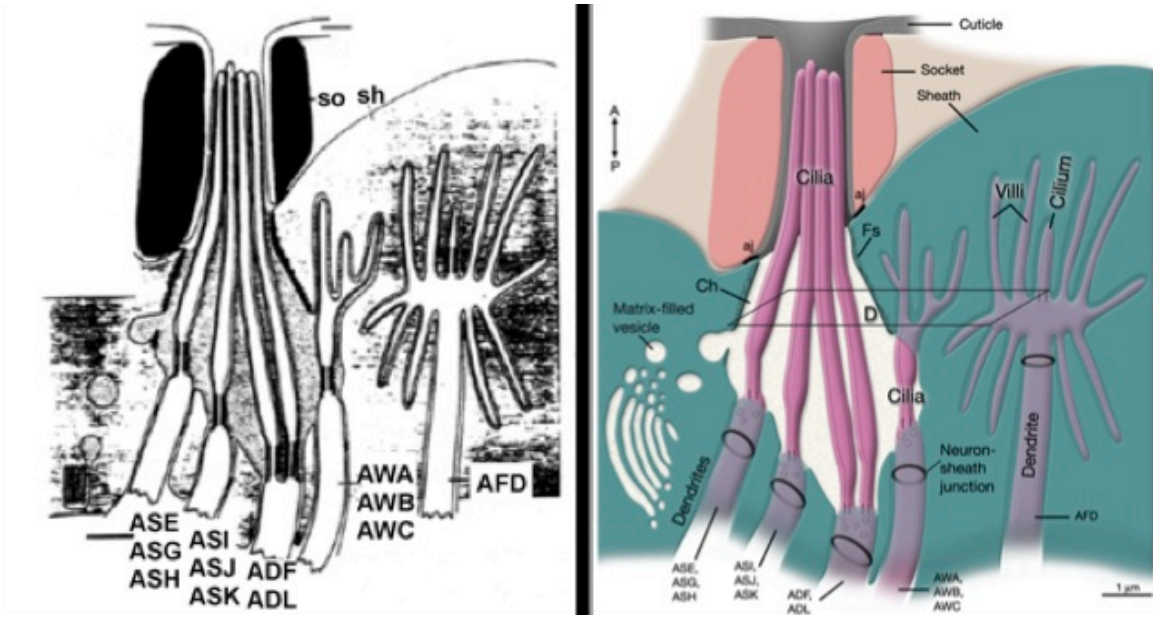

A **B**

Figure 3.2b Amphid channel

(A) One of the original diagrams displaying the amphid sheath (sh) and amphid socket (so) along with the dendrites of neurons that pass through the channel (ASE, ASG,ASH, ASI, ASJ, ASK, ADF and ADL) or stay embedded in the amphid sheath (AWA, AWB, AWC, AFD) (Perkins et al., 1986). **(B)** diagram similar to (A) for clarity reasons**,** image from wormatlas.org.

3.3 Expression pattern of EXC-1

To determine where EXC-1 is expressed, a GFP reporter construct was made. This transcriptional vector contained the 1.6 kb region upstream of *exc-1*. This sequence of DNA was chosen because of location of neighboring genes. I cloned this promoter region into the vector L3691 (a gift from Andy Fire) and injected it into wild-type worms. Animals carrying this extrachromosomal array show expression within the excretory canals and in the glial, amphid sheath cells, Figure 3.3a. Expression within the excretory canals begins shortly after the cell is born, and persists throughout the lifetime of the animal. Expression within the amphid sheath cells was not as strong, but also persisted throughout the lifetime of the animal.

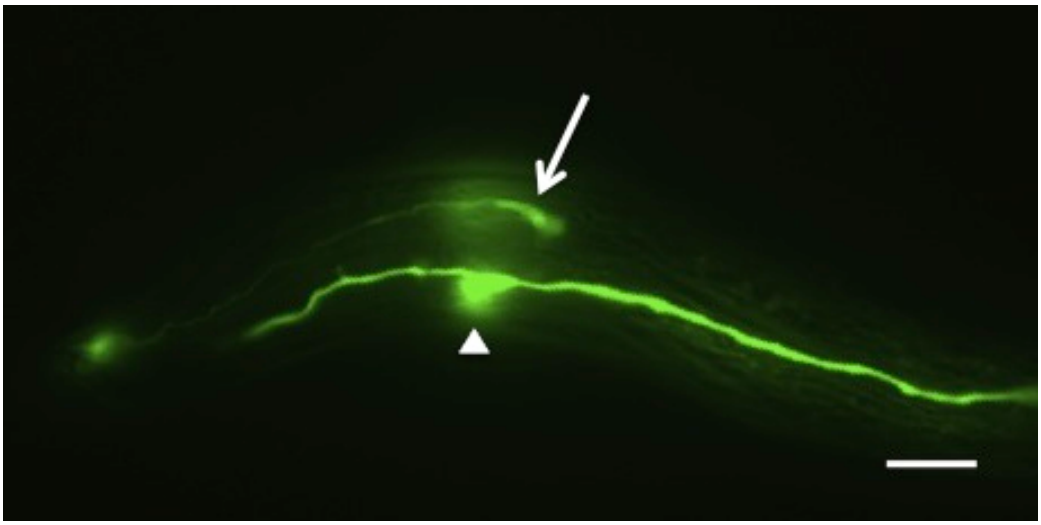

A

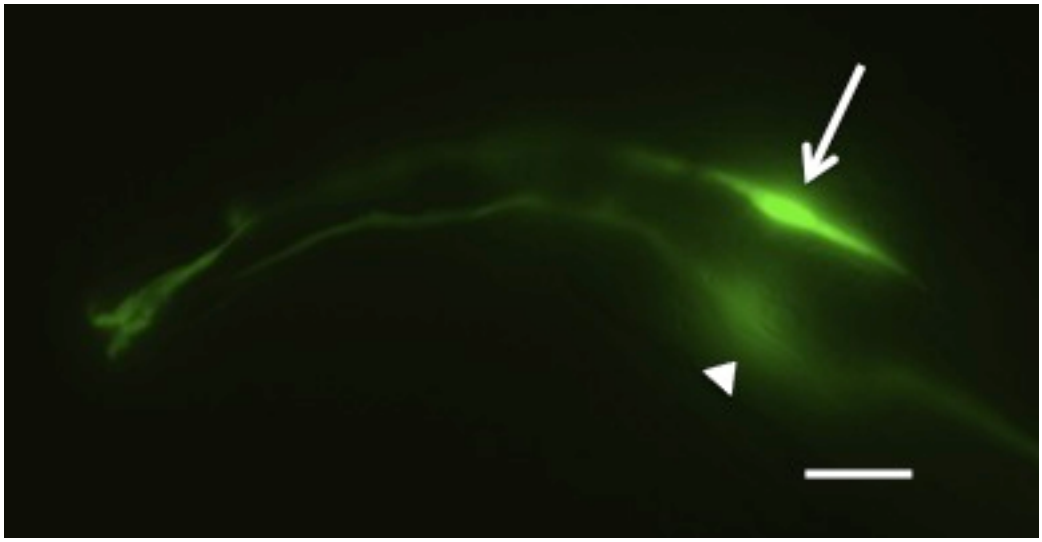

B

Figure 3.3a *exc-1* is expressed in the excretory canal and amphid sheath.

(A) L2 worm **(B)** Young Adult. Both carrying the extrachromosomal array *Pexc-1::gfp*. Expression is shown in both the amphid sheath (cell body indicated by arrow) and the excretory canal (cell body indicated by closed arrowhead). Scale bar 10μm.

3.4 Dye-filling assay

Because the amphid sheath forms a tube like structure as well, this result of EXC-1 expression here was very exciting. Other studies have identified genes that are required for the tubular structure in both the amphid sheath and excretory canal (Perens and Shaham, 2005). Because of some overlap in structure and gene requirement, I wanted to determine if there were structural defects within the amphid sheath of *exc-1* mutants, along with the defects in the canal.

When living wild-type animals are exposed to fluorescent lipophillic dyes, six of the eight pairs of amphid neurons fill with dye, allowing for visualization of these neuronal processes and cell bodies via fluorescence microscopy (Hedgecock et al., 1985; Perkins et al., 1986). This lipophillic dye enters through the amphid channel, staining the amphid neurons by lateral diffusion in the plasma membrane. This dye does not affect the viability, development or basic physiological properties of the neurons. Mutations with structural defects within the opening of the amphid channel often reduce or abolish the amount of dye filling. A class of mutants that are unable to take up this dye are known as *dyf* (DYe Filling) mutants.

To determine if the structure of the amphid sheath contributing to the amphid channel is maintained, I carried out dye-filling assays. *exc-1* mutant worms were able to take up the dye, staining the neuronal processes and cell bodies, indicating that the amphid channel is remains open, Figure 3.5a. This result isn't too surprising, as *exc-1* mutants do not exhibit mutations in response stimuli such as mechanosensation (ASH neuron) and dauer formation (ASI, ADF, ASG and ASJ neurons), which are controlled by amphid neurons passing through the amphid channel (Bargmann, 2006).

3.5 Structure of amphid sheath in *exc-1*

Though the opening of the amphid channel is still maintained in *exc-1* worms, I wanted to get a better look at the amphid sheath structure. With a sheath cell marker, *P::vap-1::dsRED,* (a gift from Shai Shaham) I was able to do this. While observing *exc-1* mutant worms I discovered there are small cysts, or cyst like structures, located within the process of the amphid sheath, in 60% of the worms observed, Figure 3.5a. The amphid sheath process extends from the cell body, distally, to the amphid channel. Though this structure is long and slender like the excretory canal, it does not contain a lumen. Though *exc-1* does not seem to be disrupting the lumen of the amphid sheath, it may still be playing a similar role as in the excretory canal.

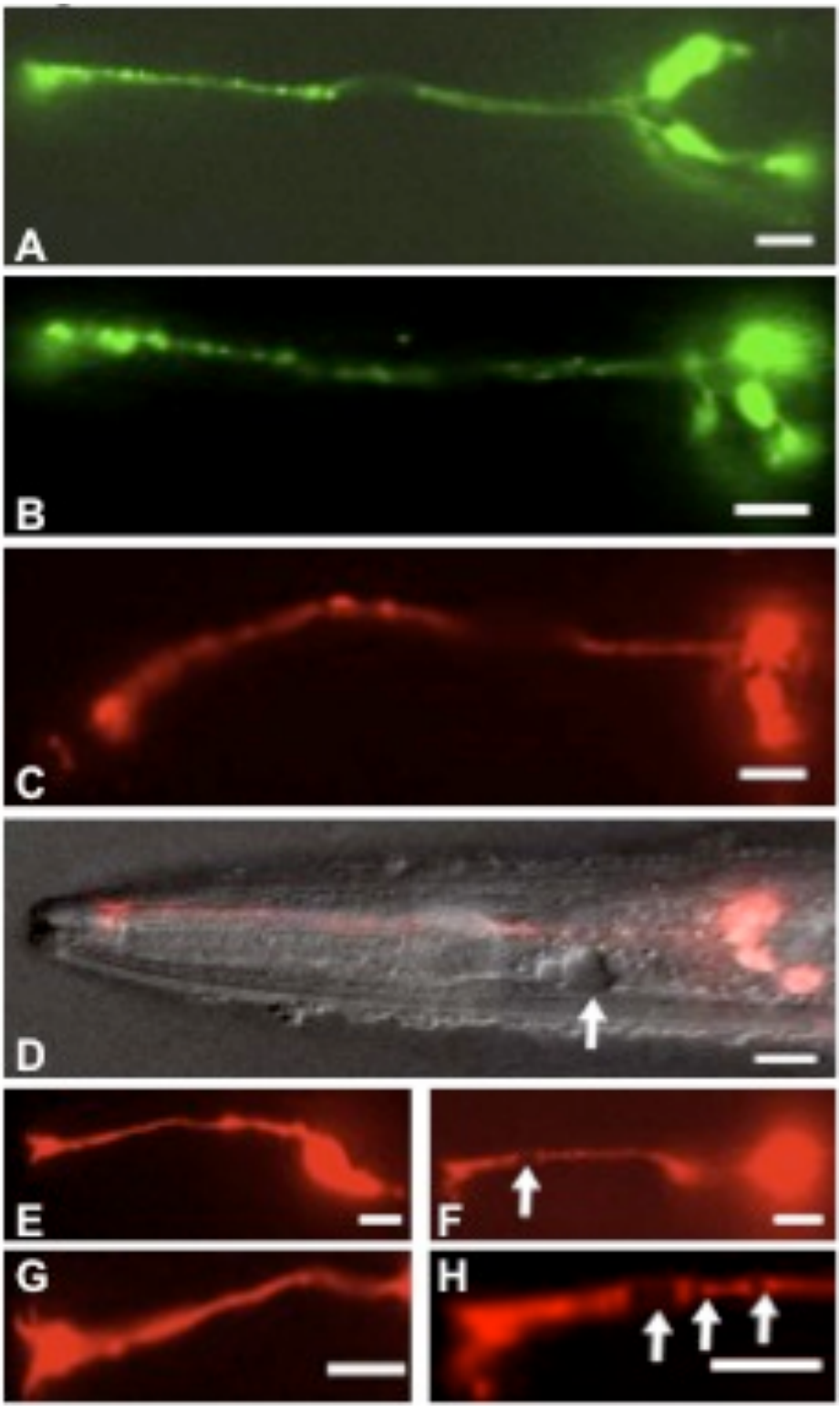
A
B
C
D
E
F
G
H

Figure 3.5a *exc-1* mutation has minor effects on amphid sheath cell structure.

(A-D) *exc-1* mutants are able to take up dye from the outside environment indicating that the amphid channel remains open. (A,B) Stained with DiO (C-D) Stained with DiI. (A and C) Wild-type worm (B and D) *exc-1 (rh26)* worms. (E-H) Amphid sheath with the cell specific marker, *Pvap-1::dsRED* (gift from Shai Shaham) in (E and G) wild-type worms show a smooth, axon-like process. However, in (F and H) *exc-1 (rh26)* worms this thin process is disrupted and exhibits cyst-like structures along its length. (G and H) are close-ups of E and F to indicated the cyst-like structures. Fluorescence in all panels have been brightened to show position of amphids and cysts within. Scale bars, 10μm.

3.6 Summary

EXC-1 is expressed amphid sheath and causes cyst like structures

By use of a transcriptional, GFP reporter, EXC-1 shows expression in both tube-like structures, the excretory canal and the amphid sheath. Though EXC-1 does not seem to be required to maintain the tubule structure at the distal region of the amphid sheath, it is needed for proper structure of the amphid process. In 60% of *exc-1* mutant worms, there is a cystic-like phenotype found within the amphid process. Continued studies need to be carried out to determine what this cyst-like structure is, possibly a build up of material.

This cystic like phenotype within the amphid sheath is very interesting and is something that hasn't been noticed by the lab of Shai Shaham, a lab that studies the structure and function of the amphid sheath. (Max Heiman, personal communication).

3.7 Materials and Methods

Reporter construct

The 1.6kb region predicted region to contain the *exc-1* promoter was amplified from N2 DNA, with the following primers:

Forward Primer with *BamH1* cut site added	Reverse Primer with *BamHI* cut site added
5' GCGTCGGATCCTCCTAAAAAATTCA AGTTGAA	5' CCGCCGGATCCTCATCAAAAATTTT ATTATCC

This PCR amplified product was then cut and ligated into the backbone of plasmid L3691, This final construct remains in the lab as pBK101.

Expression analysis

Wild-type worms were injected with 75ng/µl of pBK101 and their progeny were viewed and imaged via DIC and Fluorescence microscopy. Determination of structures with GFP expression were identified with the help of wormatlas.org and the *C. elegans* t images that are available (Sulston and Horvitz, 1977)

Dye-filling assay

These assays were carried out by methods based on original assays performed (Hedgecock et al., 1985; Perkins et al., 1986). Worms were grown on NGM agar plates according to common practice, then rinsed off the plates with M9 buffer and moved to an eppendorf tube containing .01mg/mL lipophilic dye solution. The worms were then allowed to soak in this dye solution by rotation at room temperature, in a light-limiting tube, for 1.5hrs. Worms were then rinsed with M9 to remove excess dye and transferred to an agar plate for recovery. Worms were then observed under fluorescence microscopy. The N2 strain served as a positive control, allowing stain to enter through the amphid channel and stain the amphid neurons. *dyf-11 (mn392)* served as a negative control. *dyf-11* mutants have obstructed amphid channels and are unable to take up dye from the outside environment (Bacaj et al., 2008a; Perkins et al., 1986; Starich et al., 1995).

Microscope Imaging

Live worms were mounted on 2% agarose pads with added 10mM muscimol or 0.5% 1-phenoxy-2-propanol as an anesthetic, as described previously(Sulston and Hodgkin, 1988). Images were captured with a MagnaFire Camera (Optronics) on a Zeiss

Axioskop microscope with Nomarski optics. Confocal images were taken on an FV1000 Confocal microscope (Olympus) laser scanning confocal microscope, with lasers set to 488 nm excitation (GFP) or 543 nm excitation (mCherry). Images were captured via FluoView optics, and analyzed with ImageJ software.

Chapter 4

EXC-1 is an IRGP homologue

Chapter 4: EXC-1 is an IRGP homologue

4.1 Abstract
4.2 Introduction
4.3 IRGPs
4.4 EXC-1 Ras domains
4.5 Different forms of EXC-1
4.6 Summary
4.7 Materials and Methods

4.1 Abstract

The *exc-1* gene encodes a large (738 amino-acid) protein with little obvious homology along its entire length. Two regions, however, show homology to the IRG (Immunity-Related GTPase) family of GTPases, both genetically and structurally. The first Ras homology domain shows closer homology to IRG, seems to be acing like a true GTPase domain, which is required to cycle between both GTP and GDP bound forms.

4.2 Introduction

exc-1 encodes a large 738 amino-acid protein. With the use of BLAST (Basic Local Alignment Search Tool) analysis, EXC-1 did not show strong homology along its entire length; though two regions showed homology to the family of Immunity-Related GTPases, Figure 4.2a. These two regions of homology contain putative Ras homology domains. EXC-1 also contains a proline-rich region located on its N-terminus. The history of IRGPs and their role as a family of GTPases is discussed here.

The Ras superfamily of GTPases regulate diverse cellular functions including membrane trafficking, cytoskeletal control, cell division, cell signaling and nuclear import and export (Macara et al., 1996). GTPases carry out these vital roles by cycling between

GTP-bound and GDP bound states. A GTPase is considered in its 'active state' when a GTP is bound and in its 'inactive state' when GDP is bound, at what is known as its G-domain. GTPases switch between these two forms with the aid of guanine nucleotide-exchange factors (GEFs) and GTPase-activation proteins (GAPs). GEFs catalyze the conversion of 'inactive' RAS to its 'active' form by removing a GDP from the GTPases, allowing GTP to bind. GAPs accelerate the rate of hydrolysis of bound GTP to GDP, Figure 4.2b. Because EXC-1 contains two of these RAS-like G domains, it adds to its complexity and possible conformational states within the canal, Figure 4.2c.

Sequence homology among members of the Ras superfamily tends to be very low. However they share strong structural homology at the G domain, a region recognized by four to five conserved sequence motifs, G1-G5 (Bourne et al., 1990, 1991). G1 (also known as the P loop domain) has a conserved sequence of GX_4GKS/T with the main-chain NH groups and the lysine in contact with the phosphates of the nucleotide. G2 (also known as switch I) contains a threonine (T) and is important for guanine base specificity, along with G3 domain (DxxG) and G4 domain (N/TKxD). The Asp of DxxG (G3, also known as switch II), makes a water-mediated contact with the Mg^{2+} and is important for GTP hydrolysis; in some G proteins the Asp can be replaced with Glu (E). G5 may play a role with binding to guanine as well, but is weakly conserved. Both of the EXC-1 Ras domains clearly contain the characteristic GTP- and GEF/GAP-binding G1, G2, and G4 domains, with lower homology to the G3 and G5 guanine-interaction domains. The structure of EXC-1's two Ras homology domains is discussed here with comparisons to the canonical Ras and IRGP families.

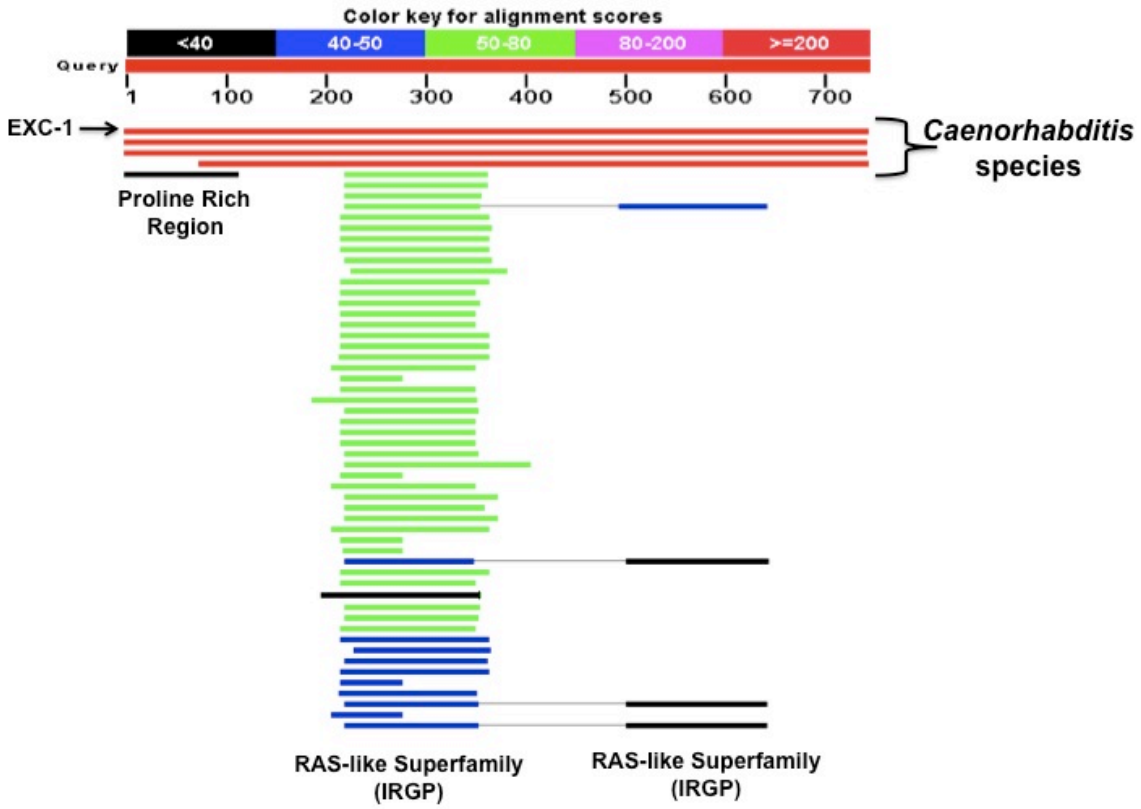

Figure 4.2a BLAST results of EXC-1.

BLAST results indicate three homologus regions along its length; an N-terminus proline-rich region followed by two Ras homology domains, specifically the IRGP family.

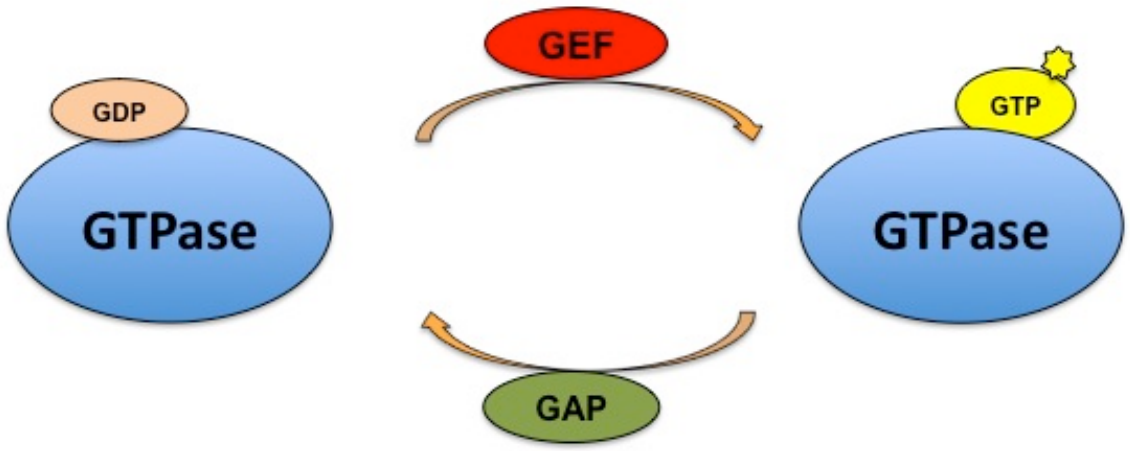

Figure 4.2b GTPase cycle

GTPases cycle between its GTP bound form, by the assistance of GEFs, and its GDP bound form, by the assistance of GAPs.

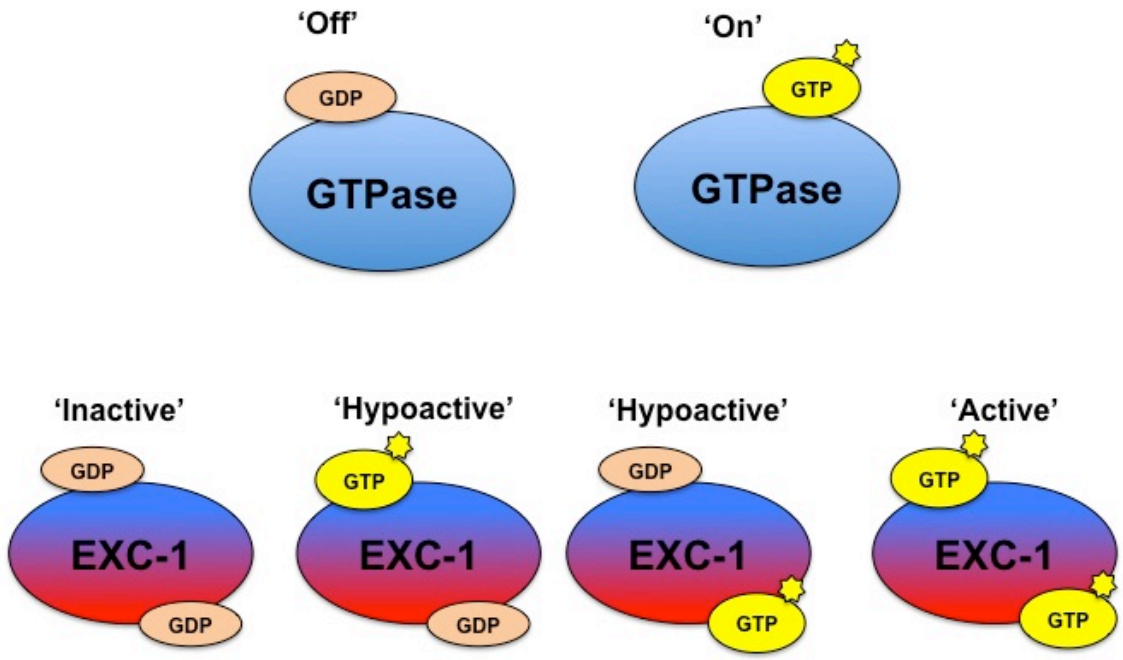

Figure 4.3c EXC-1 contains two Ras homology domains

GTPases can be found in a GTP or GDP bound state (A). Because EXC-1 contains two GTPase domains it adds to its complexity and number of possible states it can be found in (B).

4.3 IRGPs

Immunity-Related GTPase Proteins (IRGPs) make up one subgroup of the large family of Interferon Inducible GTPases (IIGP) (Martens and Howard, 2006). Like their name suggests, members of this IIGP family were identified and grouped together by their shared responsiveness to interferon stimuli (Boehm et al., 1998; Gilly and Wall, 1992; Lafuse et al., 1995; Taylor et al., 1996). Since their initial discovery, the family has expanded immensely, and can be broken up into four subgroups based on their homology, relative size, and different responses to interferons: Mx (Myxovirus resistance), guanylate binding protein (GBP), very large inducible GTPases (VLIG) and Immunity-Related GTPases (IRGP) (Martens and Howard, 2006). EXC-1 only shows homology to IRGPs.

Members of the IRGP family were initially identified in mice as important components in resistance against different intracellular pathogens, working in a pathogen-specific manner. In mice, IRGPs have been show to be involved in pathogen clearance of *Listeria monocytogenes, Toxoplasma gondii, Mycobacterium tuberculosis, Salmonella typhimurium* and *Chlamydia trachomatis (Al-Zeer et al., 2009; Bernstein-Hanley et al., 2006; MacMicking et al., 2003; Taylor et al., 2000).*

Members of the IRGP family were identified in a piecemeal fashion and it wasn't until 2005 that they were identified and described as a related group (Bekpen et al., 2005). 23 IRGPs have been identified in mice, of which 20 are functional, suggesting the IRGPs play a pivotal role in immune response in mice (Taylor, 2007).

IRGPs have also been identified in other organisms and vertebrates, including *Danio rerio* (11 IRGP genes), the pufferfish *Tetraodon nigriviridis* (2 IRGP genes) and

the dog *Canis familiaris* (8 IRGP genes) and humans. To much surprise, humans only encode for two IRGPs. The two IRGP members in humans, IRGC and IRGM, are homologous to the mice IRGPs, *Irgc* and *Irgm,* respectively. When first identified, by the Eichler group, both IRGC and IRGM were predicted to be nonfunctional in relation to interferon response (Bekpen *et al.,* 2005).

IRGC encodes a full-length protein with a G-domain located in the middle of the protein. However, IRGC is not inducible by interferon and, as of yet, has only been shown to have high expression in the male testis (Bekpen et al., 2005). Because of IRGC's absence from immunity response, in both mice and humans, it hasn't been the focus of many studies, unfortunately. EXC-1 shows strongest homology to IRGC.

IRGM encodes a small protein (178 amino acids) that has been severely truncated on both N and C terminus, when compared to the mouse homologue, and has a very interesting history. IRGM still retains its G domain, but was originally thought to be a pseudogene. Later it was found that IRGM is expressed in humans but not under the control of interferon stimulus. Interestingly, IRGM is constitutively expressed in many tissues but shows high expression levels in the testis, along with its IRGC counterpart (Bekpen et al., 2005; Bekpen et al., 2009).

From studies carried out by the Eichler group, it has been proposed that the IRGM gene has undergone a unique 'death and resurrection'. It is believed that IRGM was pseudogenized about 50 million years ago, as a result of Alu insertions, resulting in a non-functional IRGM. IRGM is non functional in all Old World and New World monkeys but is functionally restored in both apes and humans. This function has been restored as a

result of an integration of an ERV9 element (endogenous retrovirus), upstream of the IRGM locus (Bekpen *et al.,* 2009.

Cellular role of IRGPs

IRGM and mice IRGPs have been shown to play a role in antiviral autophagy (Huett et al., 2009; Petkova et al., 2012; Singh et al., 2006; Singh et al., 2010; Zhao et al., 2009). In normal conditions, IRGPs show various membrane localizations within the cell, many of them being found at the Golgi or the endoplasmic reticulum. Once a pathogen has invaded, these IRGPs relocalize, often requiring it be in its GTP-bound state (Martens and Howard, 2006; Papic et al., 2008). Most IRGPs contain a myristoylation sequence for insertion into membranes, though some IRGPs lack this signal and still are able to bind lipids (MacMicking, 2004; Tiwari et al., 2009; Zhao et al., 2010). EXC-1 does not contain a myristoylation sequence or any identifiable signal for membrane binding.

IRGM binding partners

IRGM has been shown to play a role in autophagy and is a main target of many infecting pathogens to either inhibit or promote this process for its own benefit. Studies carried out in the Faure lab found that IRGM interacts with autophagy proteins ATG5, ATG10, MapILC3B and SH3GLB1, all involved with autophagosome formation and cytoskeletal interactions (Gregoire et al., 2011). Another study was carried out, showing that the mouse homolog *Irga6* (IIGP) binds to a microtubule interacting protein, hook3, and may play a role in intracellular trafficking (Kaiser et al., 2004).

This suggests that the family of IRGPs play a role in lipid membrane binding, because of their myristolyation and membranous compartment formation, particularly the autophagosomes. Plus, because they have been shown to interact with the microtubules through protein interactions they may play a role in intracellular trafficking as well.

Through genome-wide association studies, IRGM has been shown to be associated with Crohn's Disease and Inflammatory Bowel Syndrome. IRGM is important for induction of autophagy and clearance of intracellular bacteria and with a loss of this function it is believed that this is what induces inflammation within the GI tract of these patients (Parkes et al., 2007; Prescott et al., 2010).

EXC-1 shows strongest homology to IRGC, not IRGM. As stated, unfortunately there is not a lot known about IRGC either in mice or in humans, other than it's high expression level in testis. One thing that is exciting about this information is the structure of the male testis. The male testis is largely composed of small tubules, the seminiferous tubules. Though it is now known what IRGC might be doing on the cellular level, it could be something similar to IRGM, such as membrane binding or endosome formation or trafficking within the cell.

4.4 EXC-1 RAS domains

As stated, EXC-1 has two Ras homology domains, with strongest homology to the family of IRGPs. Table 4.4a shows the consensus sequence found within IRGP G-domains, and the homologous regions in the 1st and 2nd RAS-like domains of EXC-1. The first Ras homology domain contains higher homology than the 2nd, particularly at the G3

motif, which is important for guanine base specificity and GTP hydrolysis. However, both seem to contain strong homology to the G1, G2 and G4 domains and less homology to G5 domains.

There is only one solved structure of the IRGP family, the mouse IRGP, *Irga6* (also known as IIGP)(Ghosh et al., 2004). *Irga6* contains two domains, the G domain and a helical domain; EXC-1 only has homology to the G domain. The topology of the *Irga6* G domain is identical to the Ras G domain but contains different loop insertions and deletions, and is a six-stranded β sheet surrounded by six α helices; while the typical G domain contains 5 α helices. *Irga6* is also found in a dimer formation, which brings the two molecules' myristoylation sequences together, possibly helping with stabilizing membrane localization. This dimerization only occurred when *Irga6* was in the presence of GTP or the non-hydrolyzable analog of GTP, GppNHp. They also found that that this dimer is required for GTP turnover and GTP-dependent oligomerization of *Irga6*. EXC-1 lacks this helical domain required to dimer formation, but likely does not need one, as it contains two G domains that are already physically linked.

Because there is low sequence homology across Ras members but high structural homology I wanted to determine if the Ras homology domains of EXC-1 were structurally similar to solved IRGP structure. To do this I used the program I-TASSER. I-TASSER is an open online server that makes model predictions by the use of protein threading sequence comparison of known structures within the Protein Data Base (PDB) (Zhang, 2008).

The complete sequence of EXC-1 was run through I-TASSER. The protein predicted to have the highest structural similarity in the PDB was the crystal structure

Irga6, suggesting that EXC-1 has both sequence and structural similarity to the family of IRGPs. When comparing the structure solved for *Irga6* to the predicted model of EXC-1 from I-TASSER there was a RMSD (root-mean-square deviation) of 1.50. RMSD is the measurement of the average distance between the atoms of the two proteins. After *Irga6*, the next top hit had a RMSD score of 8.40 suggesting that EXC-1 does not have strong structural homology outside of IRGP. See Figure 4.4a for predicted structure of EXC-1.

To determine how closely related each Ras homology domain of EXC-1 is to the G domain found within the structure of IRGP, I ran the sequence for each predicted domain alone through I-TASSER. Both RAS-like domains of EXC-1 have high similarity to the G domain of *Irga6* of structural similarity, as well.

When merging the structures of the G domain from IIGP and the 1st Ras homology domain, they were very similar with many of the motifs aligning very well, including G1-G4, though G5 did not seem to line up as well. This misalignment of G5 motif is not that unusual as this motif shows the least conservation across G domains, Figure 4.4b.

When carrying out the same thing for the 2nd Ras homology domain and merging its predicted model with the solved structure of IIGP, they also had a very similar structure, and alignment of domains Figure 4.4c, though two regions that seemed to extend away with no structural homology to *Irga6*.

	G1	G2	G3	G4	G5
Consensus Ras protein	GxxxxSGKS/T	T	DXXG	N/TKxD	SAK
IRGC	GESGAGKS	T	DLPG	TKVD	SNL?
EXC-1 1st Ras Domain	GRSGSGKS	D	EIPY	TKSD	SAR?
EXC-1 2nd Ras Domain	GGRGVGKS	T	ELPY	SKCD	SRR?

Table 4.4a Ras domain sequence homology

The specific subdomains found in a consensus Ras protein, human IRGC, and the first and second Ras homology domains of EXC-1.

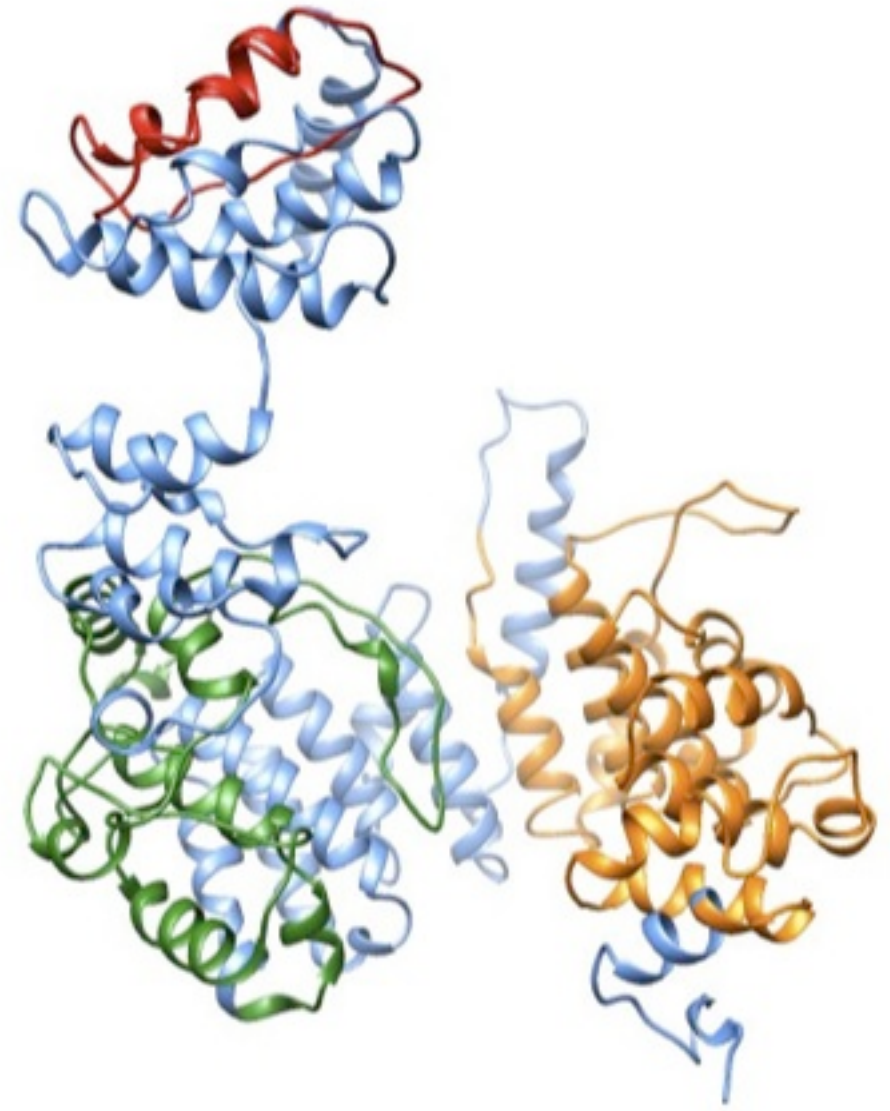

Figure 4.4a Predicted structure of EXC-1

A model of the predicted structure of EXC-1 from I-TASSER. EXC-1 contains a N-term proline-rich region (red) and two tandem Ras homology domains (1st shown in green and 2nd in orange).

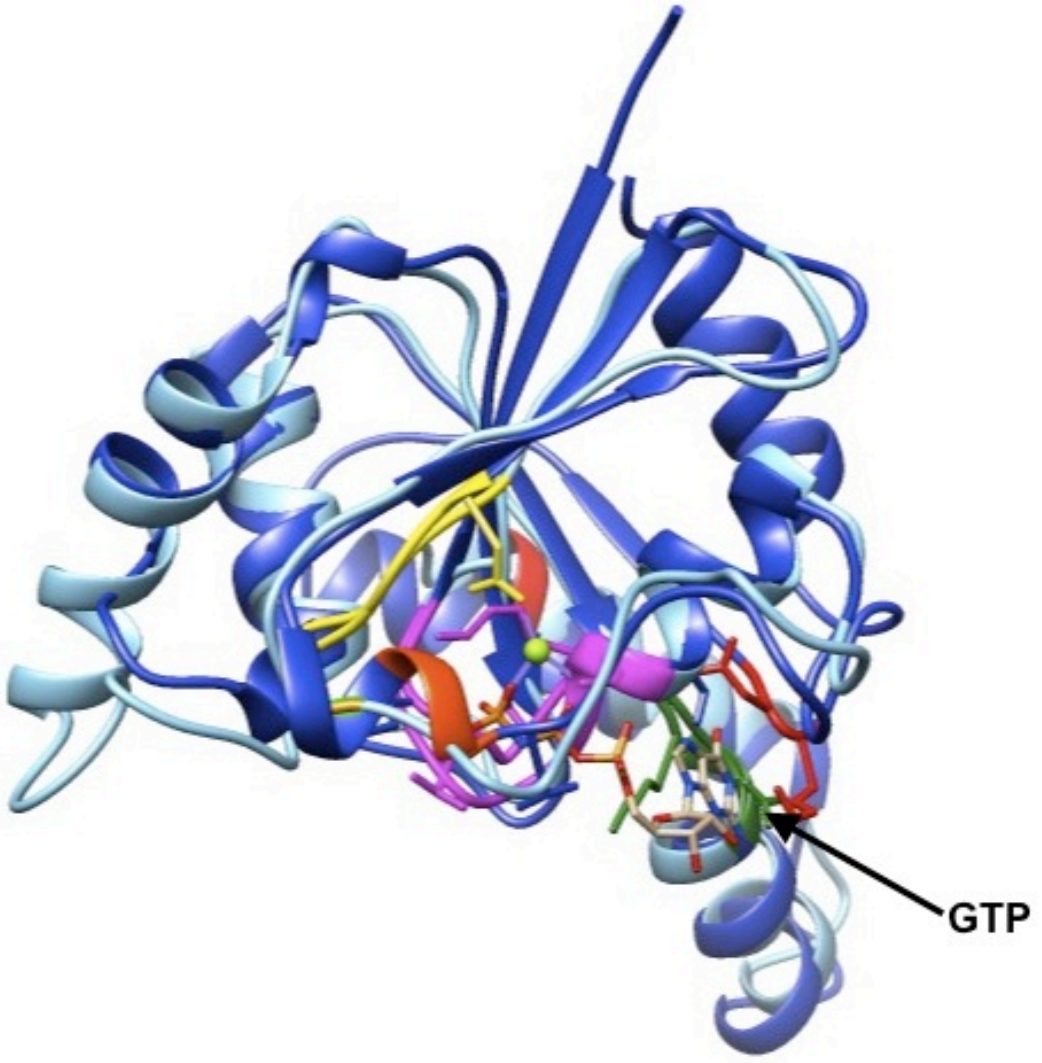

Figure 4.4b 1st Ras homology domain merged with *Irga6* (IIGP) G-domain

Colors of the subdomains are as labeled in table 4.4a; G1 (Pink), G2 (Orange) G3 (Yellow), G4 (Green) and G5 (Red). All subdomains show close positional alignment, with the exception of the G5 motif. *Irga6* (IIGP) is indicated in dark blue and 1st Ras homology domain indicated in light blue.

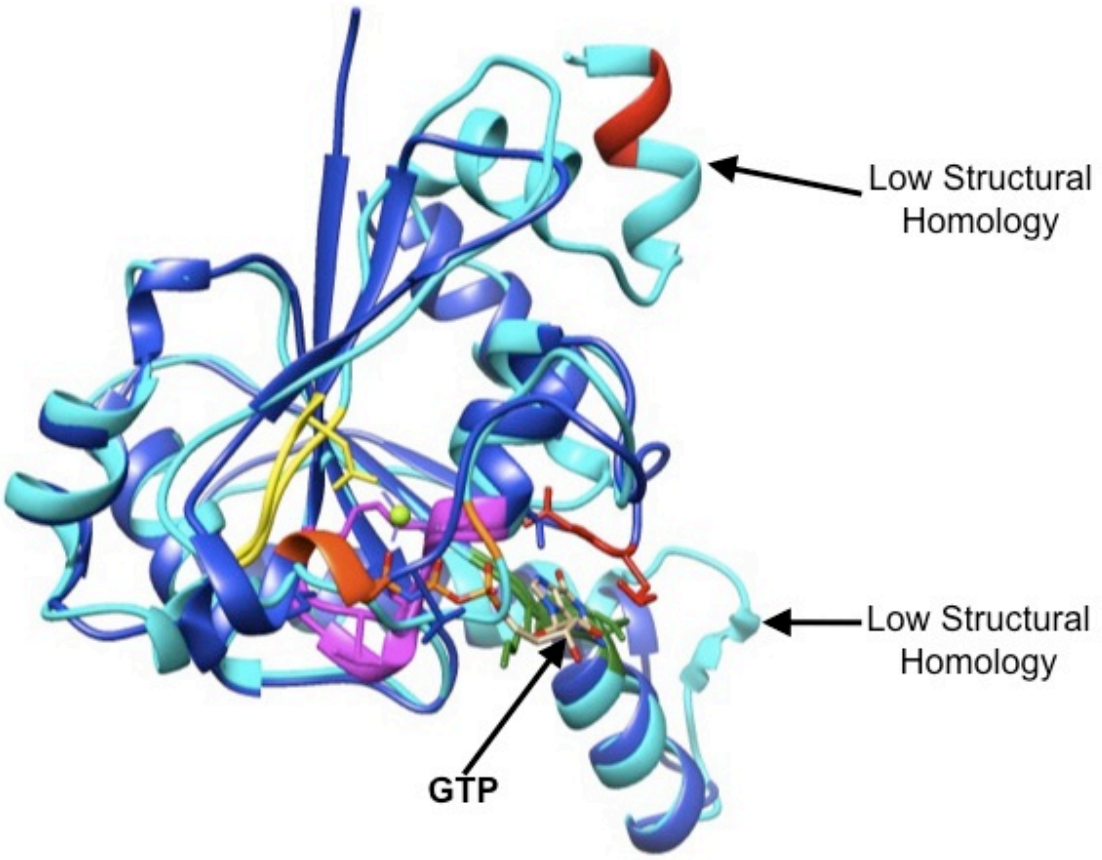

Figure 4.4b 2nd Ras homology domain merged with *Irga6* (IIGP) G domain.

Colors of the subdomains are as labeled in table 4.4a; G1 (Pink), G2 (Orange) G3 (Yellow), G4 (Green) and G5 (Red). All subdomains show close positional alignment, with the exception of the G5 motif. The 2nd Ras homology domain also contains two regions that extend from the G domain that show low structural homology to *Irga6*. *Irga6* (IIGP) is indicated in dark blue and 1st Ras homology domain indicated in light blue/cyan.

4.5 Different forms of EXC-1

Because EXC-1 is a GTPase and a GTPase typically carry out different functions within the cell depending on its GTP/GDP bound state, I wanted to determine if there was an effect on the canal depending on the conformation of EXC-1. I carried these studies out on the 1st RAS domain, as it has higher sequence homology to IRGP compared to the 2nd domain, because of the stronger homology of sequence and structural.

There are well known mutations that can lock a GTPase in a specific nucleotide-bound form. Mutations exist that abolish GTPase activity resulting in a GTPase found always in its active state (constitutively active). Mutations that block the interaction of the GTPase effectors result in an always inactive state (dominant negative) (Bourne et al., 1990, 1991). Site-directed mutagenesis was carried out on the 1st RAS-like domain, specifically at the G1 motif. The mutation of altering the conserved Ser in the G1 box to an Asp (S257N), locks the G domain in a GDP-bound, inactive form. By altering the G1 box of the two conserved Gly to Val, G250V and G255V, (GX4GKS to VX4VKS) it abolishes the GTPase activity causing to be in a constitutively active form.

I was able to make these mutations in the plasmid that contained the genomic sequence for *exc-1,* allowing me to use its native promoter to express these alternate forms. When the CA form was injected into *exc-1* worms it was able to rescue the cystic phenotype. However, it did not result in convoluted canals as occurs with normal *exc-1* overexpression injections. This suggests that *exc-1* may be required to have the ability to cycle between active and inactive states for proper function. When the DN form was injected into *exc-1* worms it was unable to rescue the cystic phenotype. Also, when

injected into wild-type worms, it induced a *exc-1* cystic phenotype. This demonstrates that the 1st RAS indeed has biological function.

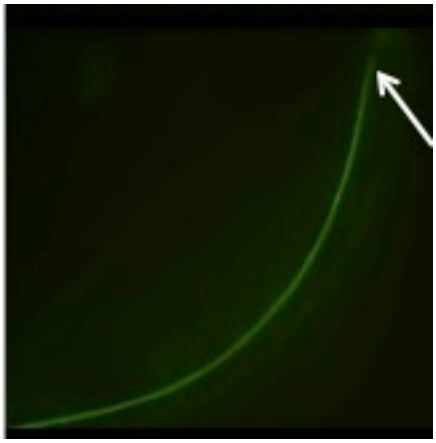

Figure 4.5a EXC-1 CA is able to rescue *exc-1 (rh26)*

Young adult, F1 progeny of injected worm. Injection mixture of 25ng/µl of CA form of pBK102 (*P::exc-1::exc-1)* plus 50ng/µl of pCV01 (*P::vha-1;;gfp)*. Arrow indicates tip of posterior canal length, with no cyst present.

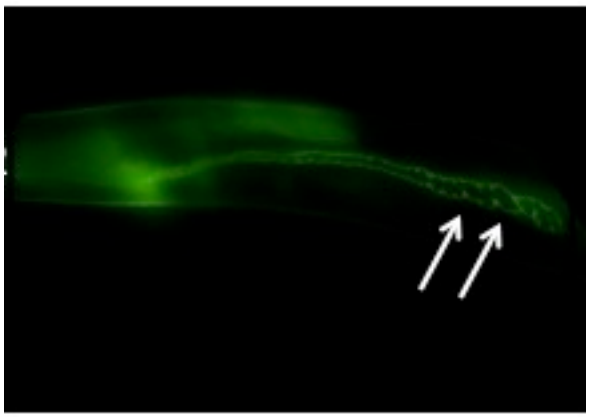

Figure 4.5b EXC-1 DN is unable to rescue *exc-1 (rh26)*

Young adult, F1 progeny of injected worm. Injection mixture of 25ng/µl of DN form of pBK102 (*P::exc-1::exc-1)* plus 50ng/µl of pCV01 (*P::vha-1;;gfp)*. Arrows indicate cysts along the canal.

4.6 Summary

EXC-1 shows both sequence and structural similarity to the G domain within the family of IRGPs. There are only two members of IRGPs within humans, one with known immunity function and the other of unknown function. IRGPs of known function seem to be playing a role in autophagy. It is yet to be determined how EXC-1 and IRGPs may be similar at the cellular and functional level, outside of sequence and structural similarity.

The first RAS seems to act as a functional G-domain, as it carries out different functions depending on its GTP/GDP-bound state.

4.7 Materials and Methods

CA and DN constructs

Constitutively active (G250V, G255V) and dominant-negative (S257N) changes to the cloned gene were produced through use of the QuikChange® II XL Site-Directed Mutagenesis kit (Agilent Stratagene, Santa Clara, CA). Injections of these constructs were at 25mg/μl, the same concentration that wild-type EXC-1 is able to rescue *exc-1* cystic phenotype.

Structural predictions

Structural predictions were carried out with the program I-TASSER, (http://zhanglab.ccmb.med.umich.edu/I-TASSER/)

Modeling manipulation was carried out with the Molecular Modeling Program, Chimera (http://www.cgl.ucsf.edu/chimera/).

Merged structures of solved *Irga6* (IIGP) Ras domain with predicted EXC-1 1st and 2nd Ras homology domain structures were also carried out with Molecular Modeling Program, Chimera. Chimera merges models passed on pairwise sequence alignments based on Needleman-Wunch (Needleman and Wunsch, 1970) and Smith – Waterman algorithms (Meng et al., 2006; Smith and Waterman, 1981).

Chapter 5

Genetic Interactions between *exc-1* and other *exc* genes

Chapter 5: Genetic Interactions between *exc-1* and other *exc* genes
5.1 Abstract
5.2 Introduction
5.3 *exc-1* does not interact with *exc-2, 3,4, 6* or *exc-7*
5.4 *exc-1* interacts genetically with *exc-5* and *exc-9*
5.5 Summary
5.6 Material and Methods

5.1 Abstract

Cloned *exc* genes encode proteins that are all required for the maintenance of tubule shape within the excretory canal but can even be further divided by their subcellular roles. The function of EXC proteins vary by anchoring the terminal web to the apical membrane, regulate osmotic pressure of the canal lumen, and regulate movement of mRNA and endosomes within the cell. By carrying out genetic interaction studies we found that *exc*-1 works in a pathway with *exc*-9 and *exc*-5.

5.2 Introduction

Some of the genes identified necessary for maintenance of tubule shape within the canal include structural proteins, such as *sma-1* which encodes an the β_H heavy chain of spectrin, an actin cross-linking protein that supports the shape of the canal (McKeown et al., 1998). The Buechner lab cloned *exc-7* which is an mRNA-binding protein that binds to *sma-1,* regulating its expression (Fujita et al., 2003). Loss of *exc-7* results in small cysts all along the length of the canal. ERM-1 (Ezrin, Radixin, and Moesin homolog), another structural, actin-binding protein, was found to be necessary for proper canal shape as well (Gobel et al., 2004). *exc-2* has been studied by a fellow graduate student within the

Buechner lab, Hikmat Al-Hashimi, and whole-genome sequencing suggests that *exc-2* may encode an intermediate filament (though this has not been verified through rescue assay as of yet – personal communication). Intermediate filaments are structural proteins that act as dimers (Lazarides, 1980), and in fact, it has recently been shown that intermediate filament (IF), *ifb-1,*another IF isoform, is required for canal structure (Kolotuev et al., 2013). It will be exciting to verify that *exc-2* is an intermediate filament and determine its role in the maintenance of the tubule shape. Recently, the Grenwald lab, has identified *exc-6* and found that it encodes a formin protein. Formins assist in actin polymerization, de-polymerization and microtubule stability (Wallar and Alberts, 2003).

Other genes affecting the structure of the canal, resulting in large cysts, have included a Chloride Channel, EXC-4 (Berry et al., 2003) and apically secreted proteins, including the mucin protein LET-653 (Jones and Baillie, 1995)

Genes *exc-5* and *exc-9* been studied in the Buechner lab and they seem to be playing a role in intracellular trafficking (see chapter 7). Former grad student, Xiangyan Tong, cloned EXC-9. *exc-9* mutant worms are characterized by variable wide and short canals, often found with septations Figure 5.2a. *exc*-9 encodes a small LIM-domain protein that is homologous to the human CRIP, Cysteine Rich Intestinal Protein (Tong and Buechner, 2008). *exc*-9 is expressed in other tissues than the canal, including the tail spike, uterine seam cell (UTSE), distal tip cells, intestine, ALM and PLN neurons, and nerve ring.

exc-5 encodes a Rho GTPase GEF (Guanine nucleotide Exchange Factor) that is homologous to the human protein FGD4, Facial Genital Dysplasia 4 (Mattingly and Buechner, 2011). *exc*-5 shares expression pattern with *exc*-9, being expressed in the

canal, but is found in additional locations, including the pharynx, rectal epithelial cells, and some head and tail neurons (Suzuki et al., 2001). *exc*-5 mutants are characterized by often having a severe cystic phenotype with cysts located at the end of the canal, similar to *exc-1,* Figure 5.2b.

To test for genetic interactions with other *excs* I attempted rescue assays of the corresponding *exc* mutants' cystic phenotype. To do this the construct pBK102 was injected into other *exc* mutants and observed for rescue of the cystic phenotype. pBK102 is a TOPO vector containing the genomic region of *exc-1* plus 1.6kb upstream and 500 bp downstream; this is the same vector that shows rescue and overexpression in *exc-1* mutants (See chapter 2).

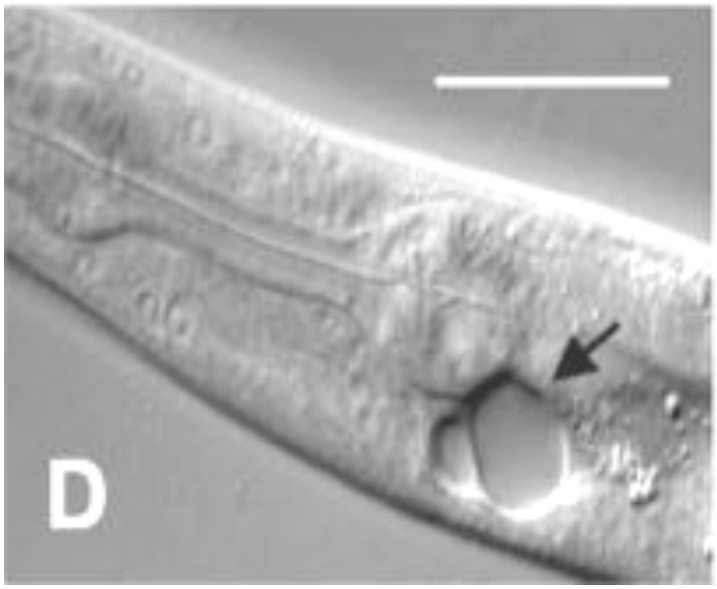

Figure 5.2a *exc-9* mutants can exhibit severe cystic phenotypes

exc-9 (n2669) loss of function worm, arrow indicates cyst near cell body. Image from (Tong and Buechner, 2008).

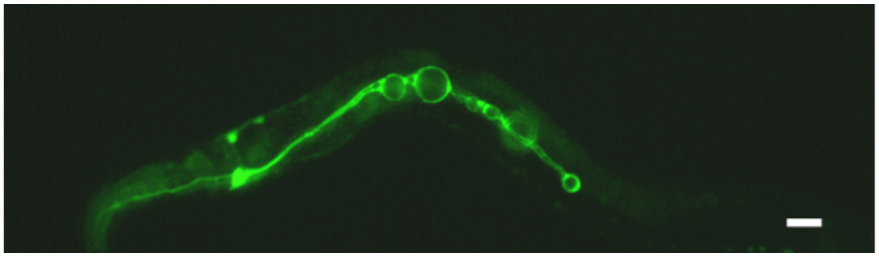

Figure 5.2b *exc-5 (rh232)* mutants show cyst along the canal and at end.

exc-5 (rh2320 loss of function worm with cysts located along the length of the canal. Scale bar is 10μm.

5.3 *exc-1* does not interact with *exc-2, 3,4, 6* or *exc-7*

When injecting *exc-1* into each individual strain: *exc-2, exc-3, exc-4, exc-6,* and *exc-7* there were no signs of rescue or improved cystic phenotype. This could suggest a couple different things. It is possible that EXC-1 might be working upstream of these genes and no matter how many copies of *exc*-1 are put into the mutant worm it will not be able to rescue the cystic phenotype. The other possibility is that *exc*-1 and these EXC proteins work in different pathways for maintaining the tubule shape within the canal.

5.4 *exc-1* interacts genetically with *exc-5* and *exc-9*

It was previously shown that *exc-5* overexpression prevents cyst formation and causes convoluted tubules in *exc-9* mutants, while *exc-9* overexpression has no effect on the large cystic canals of *exc-5* mutants (Tong and Buechner, 2008). We examined similar interactions for *exc-1* mutants. *exc-5* overexpression prevents cyst formation and creates convoluted tubules in *exc-1* mutant excretory canals, while *exc-1* overexpression had no effect on *exc-5* mutant cysts Figure 5.4a. *exc-1* overexpression prevented the formation of cysts in *exc-9* mutants, Figure 5.4b, and caused convoluted canals in these animals. Conversely, *exc-9* overexpression had no effect on the formation of cysts or length of tubules in *exc-1* animals. We conclude that *exc-1* acts downstream of *exc-9* but upstream of *exc-5* to maintain tubule diameter, Figure 5.4c and Table 5.4a. All three work together genetically, but show different expression patterns that seem to only overlap in the canal, which suggests that other proteins interact with *exc-1* within the amphid sheath.

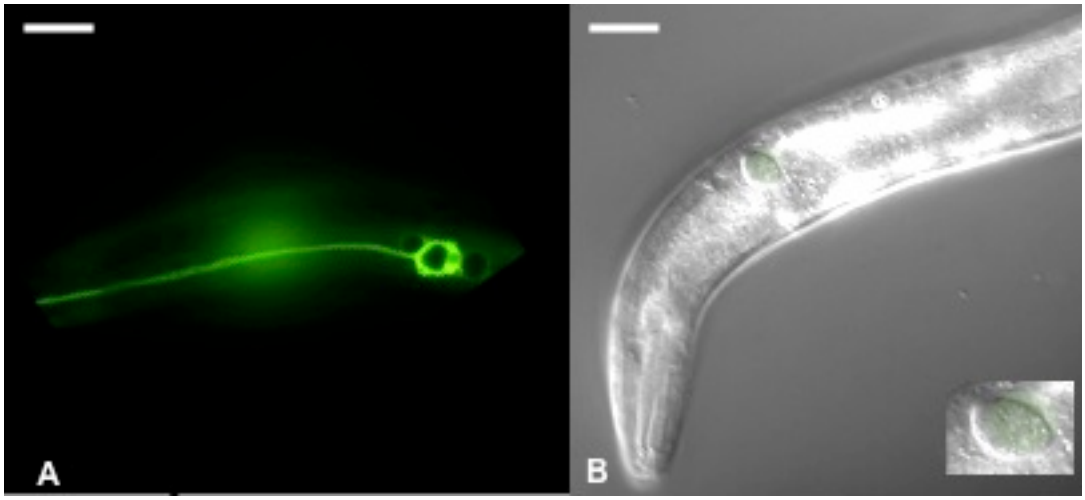

Figure 5.4a *exc-1* and *exc-5* interact genetically

(A) *exc-1* does not rescue *exc-5 (rh232)* cystic phenotype
Young adult, F1 progeny from an injected worm. Injection mixture was 25ng/µl *Pexc-1::exc-1,* and 75ng/µl of pCV01, *Pvha-1::gfp*..

(B) *exc-5* rescues *exc-1's* cystic phenotype and causes overexpression.
exc-1, F1 progeny from an injected worm. Inset shows a close up of a convoluted canal with GFP expression located near the cell body. Injection mixture: 25ng/µl *Pexc-5::exc-5::GFP*. Image from Brendan Mattingly.

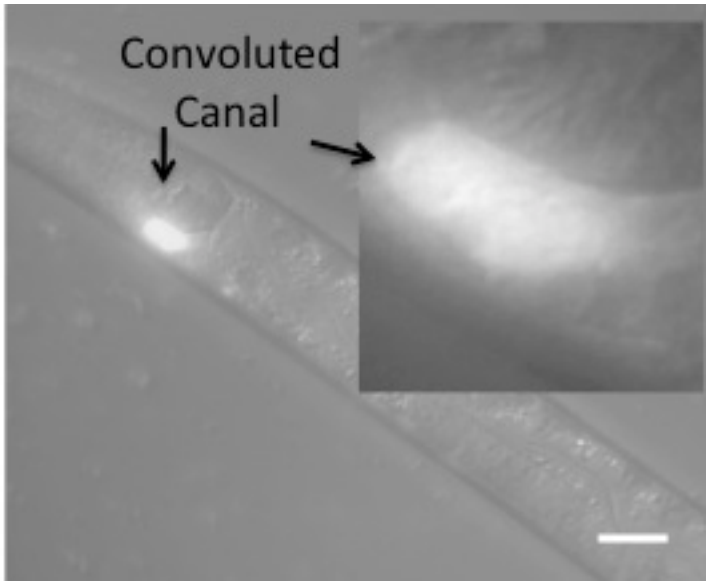

Figure 5.4b *exc-1* rescues *exc-9's* cystic phenotype
exc-9 (n2669) young adult, F1 progeny from an injected worm. Injection mixture was 25ng/µl *Pexc-1::exc-1*, and 75ng/µl of pCV01, *Pvha-1::GFP*.

Figure 5.4c Proposed pathway
From genetic analysis EXC-9 works upstream of EXC-1 and EXC-5. Also, EXC-1 works upstream of EXC-5.

Table 5.4a

Strain/Constructs			Canal Lumen Length, Number			Cyst Size, Number			p-value	
Genotype	Injected with	n	Almost none (no growth and short)	Medium (midway and 3/4)	Full-length (WT and convoluted)	Large + Medium	Small	None	Lumen Length	Cyst Size
exc-5 (rh232)		**87†**	**79**	**8**	**0**	**45**	**38**	**4**		
exc-5 (rh232)	***exc-1* + pCV01 (*Pvha-1::gfp*)**	**57**	**45**	**12**	**0**	**37**	**20**	**0**	**0.05179+**	**0.1134+**
exc-9 (n2669)		**66†**	**0**	**0**	**66**	**0**	**0**	**66**	**1.26x10-38***	**3.78x10-46***
exc-9 (n2669)	***exc-1* + pCV01 (*Pvha-1::gfp*)**	**33**	**13**	**17**	**3**	**22**	**11**	**0**	**0.3897***	**0.1328***

+ Compared to exc-5 (rh232) *Compared to exc-9 (n2669) †Numbers from (Tong and Buechner, 2008)

5.5 Summary

From genetic analysis *exc-1* does not interact with *exc-2, 3, 4, 6* or 7, at least not downstream of them in a genetic pathway. Continued work would have to be carried out to determine if EXC-1 worked upstream of any of theses genes.

EXC-1, EXC-5 and EXC-9 work together in a genetic pathway, determined by work from former graduate students and studies carried out here. The proposed pathway of this interaction is *exc-9* upstream of both *exc-1* and *exc-5* and *exc-1* upstream of *exc-5,* in a *exc*-9 → *exc*-1 → *exc*-5 → pathway. This work gives us a better understanding of how these three proteins may be functioning in the excretory canal and how they are carrying out roles together in the same pathway to maintain tubule shape.

5.6 Materials and Methods

Constructs and Injections

Construct containing the coding region for *exc-1,* the promoter (1.6kb upstream) and 500bp downstream placed in the TOPO vector (pBK102) was injected into *exc* mutant strains at a concentration of 25ng/µl with a co-injection marker pCV01 at a concentration of 75ng/µl. Injected worms were allowed to recover and their progeny were observed to canal phenotype and determination of possible rescue and genetic interaction. The canal measurements were carried out the same way as described in Chapter 2 material and methods.

Xiangyan Tong carried out injection of *exc*-9 into *exc-1* or *exc-5* worms and Brendan Mattingly carried out injection of *exc-5* into *exc-1* or *exc-9*.

Microscope Imaging

Live worms were mounted on 2% agarose pads with added 10mM muscimol or 0.5% 1-phenoxy-2-propanol as an anesthetic, as described previously (Sulston and Hodgkin, 1988). Images were captured with a MagnaFire Camera (Optronics) on a Zeiss Axioskop microscope with Nomarski optics.

Chapter 6

Binding partners of EXC-1

Chapter 6: Binding Partners of EXC-1
6.1 Abstract
6.2 Introduction
6.3 Results of Yeast-two hybrid studies
6.6 Summary
6.7 Materials and Methods

6.1 Abstract

It has been shown that *exc-1, exc-5* and *exc-9* interact genetically with *exc-9* upstream of both *exc-1* and *exc-5*, and *exc*-1 upstream of *exc*-5 in a predicted pathway of *exc-9* → *exc-1* → *exc-5*. Yeast two-hybrid assays indicate EXC-1 binding to EXC-9, and that this binding is dependent on EXC-1's activity.

6.2 Introduction

Yeast Two-Hybrids

Because *exc-1, exc-9* and *exc*-5 have been shown to interact genetically from work that I have carried out, along with former graduate students Brendan Mattingly and Xiangyan Tong, binding assays were carried out to determine if they interacted directly. To do this, I used the yeast two-hybrid system. This is a project that I pioneered in the lab and a system that will continue to be used successfully.

Yeast two-hybrids are often used as a screening method, screening through a library of proteins to find binding partners. This was not my intention; I used a candidate approach based on what we discovered from our genetic interactions. I used a system based on the Dup-LEXA™ system (Gyuris et al., 1993). The Dup-LexA™ system is a LexA based version of the original Gal4-UAS system (Fields and Song, 1989). In this

original yeast two-hybrid system, Fields and Song exploited the use of the yeast transcriptional activator protein, Gal4. Gal4 has two different domains; the activation domain (AD) and the DNA binding domain (DBD), both required for proper transcription. Transcriptional activation only occurs when the DNA-binding domain is bound to its corresponding DNA sequence and is in close proximity to the activation domain. The two-hybrid system involves fusing a protein of interest, "X" to the DBD and a protein of interest, "Y" to the AD. If proteins "X" and "Y" are binding partners and an interaction occurs, this will tether the DBD to the AD and induce transcription. This Gal4 DBD is placed upstream of a reporter gene (such as LacZ) to determine possible interactions.

Instead of using the transcriptional activator, Gal4, the Dup-LexA™ system uses the *E. coli* protein, LexA DNA binding protein and an activation protein, the acid blob domain B42. Neither LexA nor B42 are able to induce transcription alone. By bringing LexA and B42 together in close proximity, transcription of the reporter gene will occur. Another advantage is that using prokaryotic proteins instead of eukaryotic, largely reduces the number of false positives.

The reporter gene for my assays was the LEU2 gene that is required for production of amino acid Leucine. The reporter construct of LexA-binding sites upstream of the LEU2 gene is integrated into the yeast strain EGY48. This allows for easy detection of a protein interaction. When the yeast is grown on plates that lack Leucine they will only be able to survive if they activate the LEU2 gene and produce it themselves. With the design of this system only yeast with binding interactions will produce Leucine when placed on –LEU plates. The general set up of this system is shown in Figure 6.2a.

To carry out these assays, I designed constructs according to Table 6.2a. The bait construct (plasmid pEG202) contains a protein of interest in frame with the LexA DNA-binding protein along with the HIS3 gene. The presence of the HIS3 gene allows for confirmation of proper transformation of the plasmid into the yeast. This also allows for indication that protein of interest is produced and is not lethal to the yeast. The prey construct (plasmid pJG4-5) contains a protein of interest in frame with the acid blob domain B42. This construct also included the TRP1 gene, allowing detection of proper transformation and non-lethality. All of the empty bait and prey constructs were provided from Barth Grant at Rutgers University.

Gateway System

In this yeast two-hybrid system, I also used another relatively new technique for the lab, the Gateway® Cloning technique. This Gateway® system manipulates the recombination properties found in bacteriophage lambda and the integration and excision of phage λ from *E. coli* bacterial genome (Nunes-Duby et al., 1989). It manipulates the DNA recombination sequence found within lambda and *E. coli* (*att* sites) and the proteins that mediate the recombination event, the site-specific recombinase (Int) Excisionase (Xis) and *E. coli* Integration Host Factor (IHF). These proteins bind to the specific *att* sites, bringing these sites together, which then go through cleavage and recombination by assistance of the other proteins. Recombination events will occur at these *att* sites, which are conservative, and result in no loss or gain of nucleotides. The reactions carried out involved the *att* sites, L and R. The Gateway® system allows for these recombination events to occur between vectors containing these sites, the entry vector and destination

vector. The entry vector will contain the gene or sequence of interest flanked by *att*L sites. The destination vector will contain *att*R sites flanking the lethal gene, *ccdB*. With the destination vector containing the *ccdB* gene, when recombination occurs, the sequence of interest will be inserted into the destination vector and the by-product, entry vector, now containing the *ccdB* gene, will be eliminated when grown in normal *E. coli* cells, such as DH5α, see Figure 6.2b.

The Gateway® system is great for many reasons. With this system you don't have to deal with the challenges of typical cloning and use of restriction enzymes. You don't have to worry about use of a restriction enzyme that may have a recognition sequence in your gene of interest. There is no designing of primers containing cut sites and everything remains in frame. You also avoid a lot of the clean up and screening process that occurs with typical cloning because of the selectable *ccdB* gene. And the quality I find most important and valuable is the time that is saved by using this system.

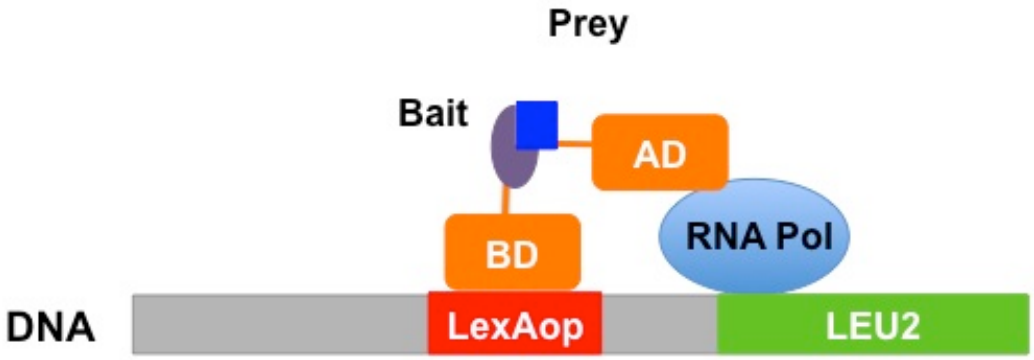

Figure 6.2a Design of Y2H

The bait consists of the protein or sequence of interest in-frame with the LexA DNA-binding domain (BD). The BD binds to the LexA operator site on the DNA, upstream of the LEU2 gene that is incorporated in yeast strain, EGY48. The prey consists of the Blob 42 activation domain that will interact with RNA polymerase and is in frame the protein or sequence of interest. If interaction occurs everything will come together and activate transcription the LEU2 gene.

Table 6.2. Yeast Two-hybrid studies

Bait	Prey	Interaction?
Empty Vector	Empty Vector	No
Empty Vector	EXC-1	No
Empty Vector	EXC-5	No
Empty Vector	EXC-9	No
Empty Vector	EXC-1 1st RAS CA	No
Empty Vector	EXC-1 1ST RAS DN	No
Empty Vector	EEA-1	No
Empty Vector	RME-1	No
Empty Vector	EXC-1 Region 1	No
Empty Vector	EXC-1 Region 2	No
Empty Vector	EXC-1 Region 3	No
Empty Vector	EXC-1 Region 4	No
EXC-1	Empty Vector	No
EXC-1	EXC-1	No
EXC-1	EXC-5	No
EXC-1	EXC-9	Yes
EXC-1	EXC-1 1st RAS CA	No
EXC-1	EXC-1 1ST RAS DN	No
EXC-1	EEA-1	No*
EXC-1	RME-1	No
EXC-1	EXC-1 Region 1	No
EXC-1	EXC-1 Region 2	No
EXC-1	EXC-1 Region 3	No
EXC-1	EXC-1 Region 4	No
EXC-1 1st RAS CA	Empty Vector	No
EXC-1 1st RAS CA	EXC-1	No
EXC-1 1st RAS CA	EXC-5	No
EXC-1 1st RAS CA	EXC-9	Yes
EXC-1 1st RAS CA	EXC-1 1st RAS CA	No
EXC-1 1st RAS CA	EXC-1 1ST RAS DN	No
EXC-1 1st RAS CA	EEA-1	No*
EXC-1 1st RAS CA	RME-1	No*
EXC-1 1st RAS DN	Empty Vector	No
EXC-1 1st RAS DN	EXC-1	No
EXC-1 1st RAS DN	EXC-5	No
EXC-1 1st RAS DN	EXC-9	No
EXC-1 1st RAS DN	EXC-1 1st RAS CA	No
EXC-1 1st RAS DN	EXC-1 1ST RAS DN	No
EXC-1 1st RAS DN	EEA-1	No
EXC-1 1st RAS DN	RME-1	No
EXC-5	EXC-1	No
EXC-5	EXC-5	No
EXC-5	EXC-9	No
EXC-5	EXC-1 1st RAS CA	No
EXC-5	EEA-1	No*
EXC-5	RME-1	No*
EXC-9	Empty Vector	No

EXC-9	EXC-1	Yes
EXC-9	EXC-5	No
EXC-9	EXC-9	No
EXC-9	EXC-1 1st RAS CA	Yes
EXC-9	EXC-1 1ST RAS DN	No
EXC-9	EEA-1	No*
EXC-9	RME-1	No*
EXC-9	EXC-1 Region 1	Yes
EXC-9	EXC-1 Region 2	Yes
EXC-9	EXC-1 Region 3	No
EXC-9	EXC-1 Region 4	No
EEA-1	Empty Vector	No
EEA-1	EXC-1	No
EEA-1	EXC-5	No
EEA-1	EXC-9	No*
EEA-1	EXC-1 1st RAS CA	No
EEA-1	EXC-1 1ST RAS DN	No
EEA-1	EEA-1	Yes
EEA-1	RME-1	No
RME-1	Empty Vector	No
RME-1	EXC-1	No
RME-1	EXC-5	No
RME-1	EXC-9	No
RME-1	EXC-1 1st RAS CA	No
RME-1	EXC-1 1ST RAS DN	No
RME-1	EEA-1	No
EXC-1 Region 1	Empty Vector	No
EXC-1 Region 1	EXC-1	No
EXC-1 Region 1	EXC-9	Yes
EXC-1 Region 2	Empty Vector	No
EXC-1 Region 2	EXC-1	No
EXC-1 Region 2	EXC-9	Yes
EXC-1 Region 3	Empty Vector	No
EXC-1 Region 3	EXC-1	No
EXC-1 Region 3	EXC-9	No
EXC-1 Region 4	Empty Vector	No
EXC-1 Region 4	EXC-1	No
EXC-1 Region 4	EXC-9	No

*Indicate combinations that have been tested only once, and may need to be retested for confirmation. Remainders were tested on two separate events and transformation combinations.

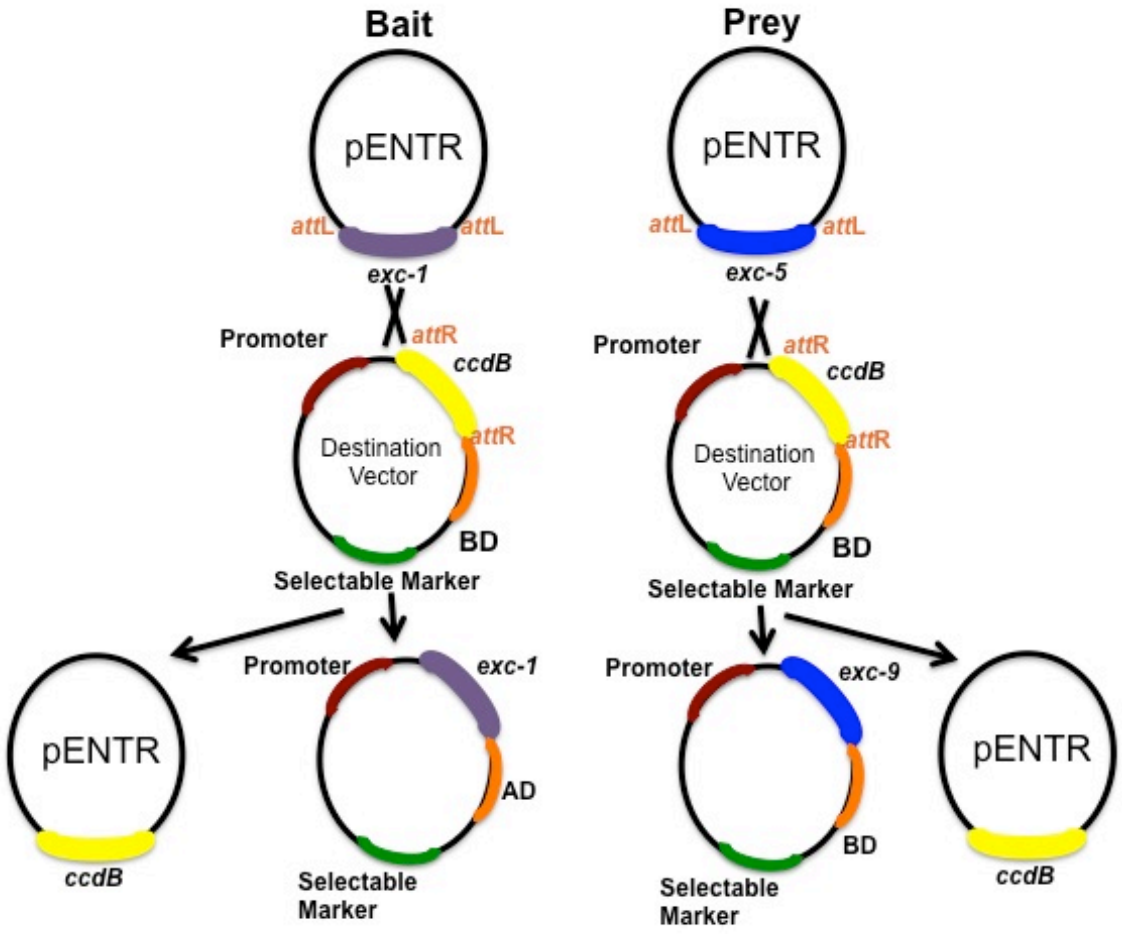

Figure 6.2b. Design of Gateway reactions

The Gateway® system allows for efficient transfer of sequence of interest into desired destination vector. Selection of desired construct is achieved by insert of *ccdB* gene into undesired pENTR vector. Description of process found in the reading.

6.3 Results of Yeast-two hybrid studies

Through the use of the Gateway system, many different constructs were made in both the prey and bait vectors, Table 6.2a. To test for interactions, I tested one protein of interest, "X" as bait and the other protein of interest, "Y" as the prey. I also carried out the reverse test, "Y" as bait and "X" as prey, for most.

As expected, many of the proteins and combinations were tested did not show an interaction, except for EXC-1 and EXC-9 Figure 6.3b. When this combination of EXC-1 and EXC-9 were carried out in either conformation, (EXC-9 – Bait, EXC-1 Prey and EXC-1 – Bait and EXC-9 – Prey) binding occurred and transcription of the reporter gene was observed. Because EXC-1 is a GTPase it is thought that it can be found in many different forms, active and inactive. And because EXC-1 has two predicted GTPase domains it adds to the number of possible forms and complexity. I wanted to determine if EXC-1 needed to be in a certain state to interact with EXC-9.

Most of the studies carried out in regards to active or inactive GTPase domains were focused on the 1st Ras-homology domain, for a few reasons. First, this region shows higher homology to the family of IRGP's. The other reason that I focused on the 1st G domain was because of many failed attempts to make CA and DN mutations to the second G domain.

When testing for interactions with EXC-9, it was found that EXC-1 was required to be in its wild-type state, when it had not been altered, and when EXC-1 was in its CA form (G250V and G255V) but not in its DN form (S257N). This suggests that the 1st G domain, in fact, is functional and that it does carry out different roles whether it is found in its active or inactive state.

To determine the location of binding of EXC-1 to EXC-9, I broke up the EXC-1 protein into regions and tested for interactions with EXC-9. The regions are as follows:

Region1: ATG (aa1) to before 1st RAS domain (aa228)

Region2: The 1st RAS domain (aa222-aa355)

Region 3: Region between the two RAS domains (aa340-aa517)

Region 4: 2nd RAS to stop codon (aa507-aa738)

See Figure 6.3a.

When these different regions of EXC-1 were tested for interaction with EXC-9 the region 1 and region 2 showed binding, Figure 6.3b. Region 1 contains the proline rich region, and since proline-rich regions have been found to be important for protein binding, these results weren't that surprising (Williamson, 1994). It is interesting that the region containing the 1st RAS binds EXC-9. This is interesting because when EXC-1 is in the DN form it does not bind to EXC-9. This could mean a few different things. First, EXC-9 might be binding to a region that spans these two regions tested. The second is that EXC-1 might undergo a conformational change depending on its conformation that would change the binding properties. When looking at the predicted structure of EXC-1 (See Figure 4.4a) it seems like EXC-1 could very likely undergo a conformational change and possible bending between the proline-rich region and the 1st Ras homology domain, which may affect its binding when in active or inactive state. More studies would need to be carried out to test these possibilities.

From work described in Chapter 7, it was found that EXC-1 and EXC-5 seem to be playing a role in trafficking within the excretory canal and seem to be working in a pathway that disrupts trafficking molecules, EEA-1 and RME-1. Because of this, I also

carried out yeast two-hybrids to determine if there was any binding occurring between EEA-1 or RME-1 with EXC-1, EXC-5, or EXC-9. Results indicate that there is no direct binding occurring between any of these molecules, except for homodimerization between EEA-1, which is known to occur within the cell for proper function in trafficking (Callaghan et al., 1999),

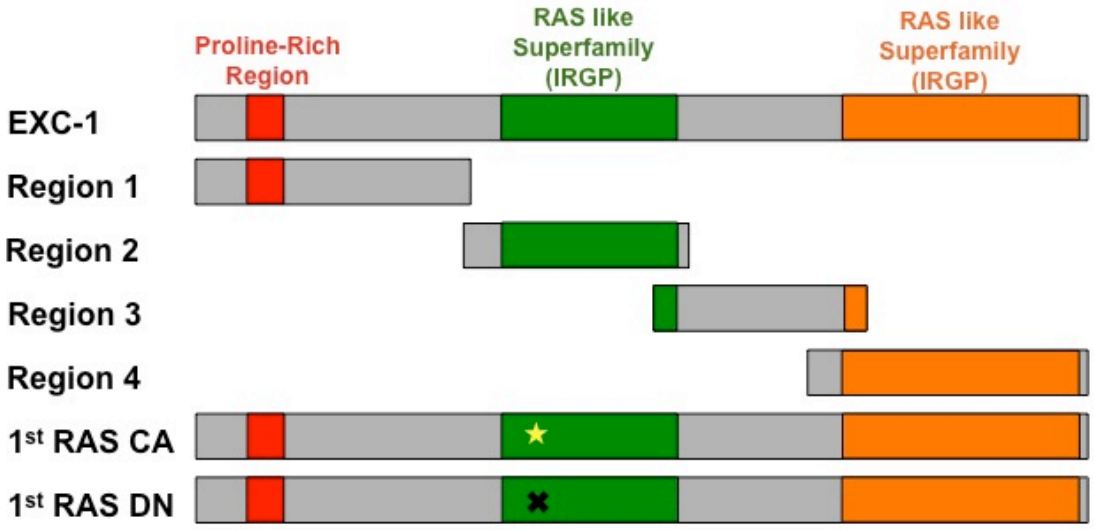

Figure 6.3a Different EXC-1 constructs

The constructs that were tested for binding interactions with EXC-9 are diagramed here, red indicates the proline-rich region, green the 1st Ras homology domain, and orange the 2nd Ras homology domain. Star indicates site of mutation to a constitutively active form and 'x' indicates site of mutation to a dominant-negative form.

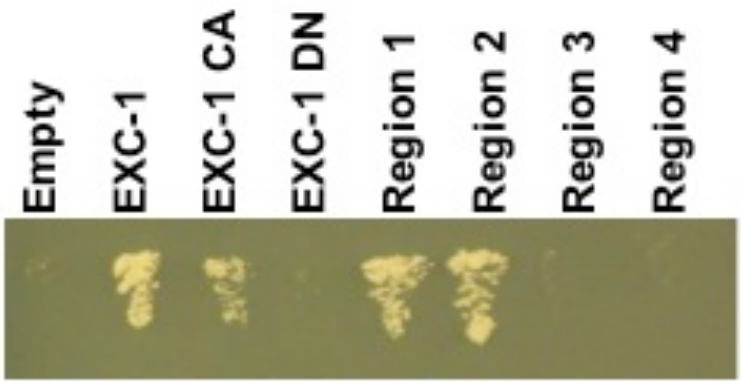

Figure 6.3b EXC-9 and EXC-1 binding
EXC-9 does not bind to the empty prey vector, EXC-1 DN, or Region 3 or 4 of EXC-1, however, it does bind to EXC-1 in wild-type and CA forms. EXC-9 specifically binds to Region 1 (proline-rich) and the Region 2 (the 1st Ras homology domain).

6.5 Summary

Since *exc-1* shows genetic interactions with *exc-5* and *exc-9*, we performed yeast 2-hybrid assays between EXC-1 and these other two proteins. We expressed wild-type *exc-1* in yeast plasmids as well as engineered mutants that contained the presumably constitutively active G249V, G254V or dominantly negative S257N forms of the first Ras-homology domain, as the second Ras-like domain has lower homology to that of IRG proteins. No form of EXC-1 showed hybridization to EXC-5. In contrast, both the wild-type and constitutively active forms of EXC-1 indicated binding to EXC-9. To confirm these results, we are currently testing interactions with a GST-expression assay.

We conclude that activated EXC-1 interacts downstream of EXC-9 through direct binding to effect trafficking at the early endosome, and these proteins stimulate EXC-5 through an indirect mechanism.

6.6 Materials and Methods

Constructs

For yeast 2-hybrid studies, various forms of the EXC-1 protein were cloned into the pENTR vector (Invitrogen), then moved via Gateway recombination reaction into plasmid pEG202 two-bait vector in-frame with the LexA DNA-binding domains, and into plasmid pJG4-5 in-frame with the activation protein's acid blob domain B42 fused to an HA tag (OriGene Technologies, Rockville, MD).

mRNA from N2 animals was isolated via Magnetic mRNA Isolation Kit® (New England Biolabs, Ipswich, MA), reverse transcribed to cDNA with Finnzymes' Phusion®

RT-PCR Kit (New England Biolabs, Ipswich, MA) and were PCR-amplified with primers to various sections of the *exc-1* gene.

(5' end of the coding region: 5'CACCATGGGACACAAAACCTC3' and

5'CTACCCACTTCTTCCACAAAATCC3';

1st Ras-like domain: 5'CACCGGATTTTGTGGAAGAAGTGGGT3' and

5'CTAGTTTTCTCGGTTTTCTGCGTC3';

center: 5'CACCCTCCTAACAAAAAGCGAC3' and

5'CTATCTTCCTCCAATAAATCCG;

2nd Ras-like domain and 3' end of the coding region:

5'CACCACATGCTTCAACTACGGA3' and

5'TCAATGAACTCCGGCTGTATCTAG3').

Transformations and Y2H

All assays began with the yeast strain EGY48 that contains the LEU2 gene downstream of the LexA operator site integrated into the genome. Also within this strain was the reporter plasmid pSH18-34 that contains 8 operator sites of LexA upstream of LacZ and the URA3 coding region. This reporter plasmid indicates strong binding when plated on plates containing Galactose and X-gal. (indicated by blue colonies).

The bait plasmid was transformed first into this EGY48 strain with the reporter plasmid and then grown on –URA-HIS plates for selection of yeast colonies that contained the plasmid, which was then used for continued assays. Then the prey plasmid was transformed into this corresponding strain and grown on –URA-HIS-TRP plates for selection of yeast colonies that contained all there plasmids. Three colonies were chosen

from this transformation for final assays to determine binding interactions. Each yeast strain was streaked onto different plates: Glucose –URA-HIS-TRP served as a positive control, Galactose –URA-HIS-TRP plus X-gal was used to determine strong binding interactions (indicated by blue colonies). Plates Galactose –URA-HIS-TRP-LEU were test plates. Controls were carried out with empty plasmids, which should not show growth on the test plates, and did not in these studies.

Chapter 7

exc-1 is necessary for trafficking

Chapter 7: *exc-1* is necessary for trafficking
7.1 Abstract
7.2 Introduction
7.3 Subcellular localization of EXC-1
7.4 Subcellular Markers
7.5 Electron Micrograph Images
7.6 Summary
7.7 Materials and Methods

7.1 Abstract

With a group of subcellular markers, EXC-1 was found to be required for proper trafficking within the excretory canal, specifically trafficking from the early to recycling endosomes, indicated by build-up of early endosome marker, EEA-1, and loss of recycling endosome marker, RME-1. This disruption of trafficking at this location was also found in *exc-5* loss of function. This section discusses trafficking within polarized epithelial cells and how loss of *exc-1* affects trafficking within the excretory canal determined with the use of nine subcellular markers.

7.2 Introduction

Within a cell, proteins and molecules are constantly being synthesized and recycled; many of these are being shuttled between cellular compartments, neighboring cells and the surrounding environments through exocytosis and endocytosis pathways. Though exocytosis is clearly important in the excretory canal, and every cell, the focus of this chapter will be on endocytosis.

Cells internalize material from the outside environment, along with lipids and proteins within the plasmid membrane, by endocytosis. Once endocytosed, material can travel onto different pathways. Material can continue through the typical, and well-

characterized pathway, to the lysosome for degradation. Or material can be returned to the plasma membrane, through a less characterized pathway, the recycling pathway. Because the plasma membrane and the molecules located within it are constantly being turned over, both production and maintenance of these molecules that are being recycled need to be properly coordinated and efficient. In fact it is estimated that cells internalize the equivalent of their cell surface as many as five times an hour! (Grant and Donaldson, 2009; Steinman et al., 1983) Things are even more complicated in polarized cells. In polarized cells material is take up from the two distinct surfaces, the apical and basal surfaces. For the return of material to these separate surfaces, things need to be regulated so it goes to the proper surface and the amount of material is correct and maintained (Maxfield and McGraw, 2004; Rodriguez-Boulan et al., 2005).

There are many regulators of both exocytic and endocytic pathways, particularly the family of Rab GTPases. As mentioned in chapter four, GTPases function by cycling between two different forms, the active, GTP bound form and the inactive, GDP bound form. These Rab proteins are distributed to distinct intracellular compartments and carry out different roles in transporting materials. There are many Rab proteins, making up the largest family of small GTPase proteins, of which humans have more than 60 (Zerial and McBride, 2001).

Material can be internalized through a clathrin-dependent or clathrin-independent manner (Pearse, 1976; van Deurs et al., 1993). Once internalized, material is passed to early endosomes. The early endosome is the site of cargo sorting; it is here the decision is made whether material will continue on to be degraded or will be recycled back to the plasma membrane. Early endosomes are identified by the presence of the GTPase RAB-5.

RAB-5 plays a role in regulation of both endosome motility and heterotypic and homotypic fusion of endocytic vesicles and early endosomes (Bucci et al., 1992; Gorvel et al., 1991; Zahraoui et al., 1989). Functional RAB-5 requires the presence of EEA-1 for endosome fusion. EEA-1 is a RAB-5 effector that contains a FYVE domain involved in binding to PI3P; this membrane binding allows EEA-1 to act a tether to assist in membrane fusion (Maxfield and McGraw, 2004; Mu et al., 1995; Simonsen et al., 1998)

If material continues through the pathway on its way to degradation it will stay within the early endosomes and this endosome will mature into a late endosome, by changing both shape and internal environment. A late endosome is characterized by both the shape and acidity, along with the presence of RAB-7. RAB-7 replaces RAB-5 as the GTPase, and membrane organizer, as the early endosome matures into the late endosome. This process is carried out by a Rab 'conversion' or 'switch' that involves RAB-5 bringing in effectors that will ultimately result in the activation of RAB-7 (Del Conte-Zerial et al., 2008; Rink et al., 2005). The material will then continue to the lysosome where it will be degraded.

Molecules may also return to the plasma membrane, and can do this through two possible routes. Material can return to the plasma membrane directly, through a process that is called 'rapid recycling', or can recycle through the recycling endosome and then eventually back to the plasmid membrane through the process termed 'slow recycling' (Maxfield and McGraw, 2004). The mechanisms and steps of these two pathways are less characterized than the degradation pathway.

Rapid recycling returns material to the plasma membrane directly from the early endosomes, is known to involve RAB-4 and RAB-35 for this process (Grant and Donaldson, 2009).

If material is recycled and goes through the 'slow recycling' pathway, material will be passed from the early endosome to the common recycling endosome (CE), also known as the subapical compartment (SAC), which is enriched with Rab-11 (Hoekstra et al., 2004; Ullrich et al., 1996). This common recycling endosome is where material received from both apical early endosomes (AEE) and basal early endosomes (BEE) will merge. In *C. elegans,* RME-1 (Receptor Mediated Endocytosis-1) is needed for trafficking of material from the recycling endosome back to the plasma membrane; it has also been shown for trafficking to the golgi (Grant et al., 2001; Grant and Caplan, 2008; Lin et al., 2001).

Though RABs are the main drivers behind trafficking within a cell, they require the assistance of many effectors to carry out their roles (Grosshans et al., 2006). These effectors assist in different processes of trafficking with RABs, including vesicle budding, vesicle delivery, tethering and fusion of the vesicles. Because RABs bind directly to the membrane of their corresponding compartments, many of these effectors localize there as well. These localized effectors may assist in the formation and bending of membranes for proper trafficking (Jean and Kiger, 2012)

Because many members of the IRGP family have shown localization with intracellular membranes and structural proteins (Kaiser et al., 2004; Petkova et al., 2012; Singh et al., 2006) it was thought that maybe EXC-1 is playing a similar role within the canal.

Within the Buechner lab we have a group of markers that label certain subcellular components; these markers were made by former graduate student Brendan Mattingly (Mattingly and Buechner, 2011). All of the markers are under the control of *exc-9* promoter. This promoter was chosen because the sequence and regions are well characterized and shows moderate levels of expression within the canal (Tong and Buechner, 2008). Because *exc-9* is also expressed within other tissues within the worm the markers do show up in other tissues including the uterine seam cell and in some head neurons. However, none of these tissues lay over the canal obstructing vision of the canal when doing microscope work. Under the control of the promoter is an N-terminal mCherry marker that will have the marker of interest in frame with the mCherry. All of these markers were integrated with the help of undergraduate, Elinor Brown. There are nine different markers, Figure 7.2a labeling different compartments and molecules within the canal, Table 7.2a

Subcellular Marker	**Subcellular Compartment**
Clathrin Heavy coat (CHC-1)	Clathrin Heavy Coat
RAB-5	Endocytic vesicles and Early Endosomes
EEA-1	Early Endosomes
RAB-7	Late Endosomes
RAB-11	Recycling Endosomes
RME-1	Recycling Endosomes
GLO-1	Lysosomes
GRIP	Golgi
Cdc42	GTPase Cdc42

Table 7.2a Subcellular markers and their corresponding compartments.

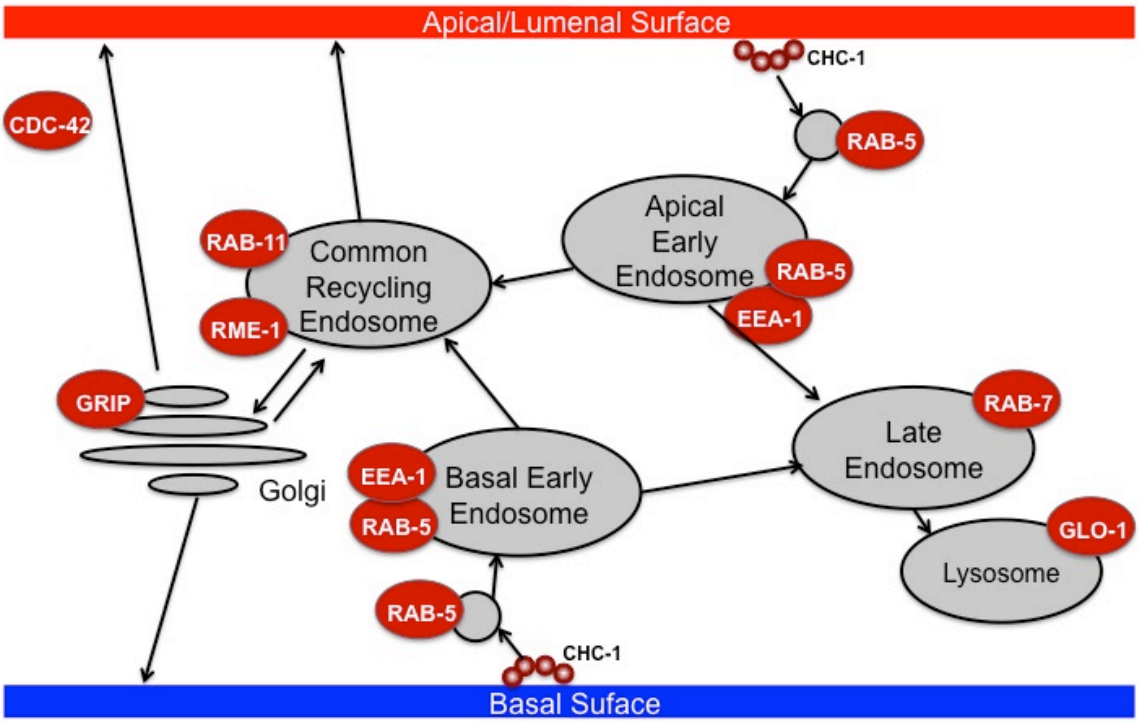

Figure 7.2a Subcellular Markers

Diagram of view inside the excretory canal with the subcellular compartments indicated in gray and their corresponding markers indicated in red.

7.3 Subcellular localization of EXC-1

To get a better idea of what EXC-1 might be doing in the cell, studies were carried out to determine the subcellular location of EXC-1. Many attempts were carried out to make a translational reporter of EXC-1, containing its native promoter and genomic sequence in-frame with fluorescent marker GFP. Unfortunately, because of the size of *exc-1* transcript, 6.6kb, it was very difficult to try and place it into a vector. So for localization of EXC-1 with in the canal I have used a construct that is under the control of a canal-specific promoter, *vha-1* (plasmid, pBK109). When injected into *exc-1 (rh26)* worms, it rescues and shows localization throughout the canal, but is richer towards the apical lumen Figure 7.3a. This enrichment near the apical surface is also found with EXC-5 and EXC-9 (Suzuki et al., 2001; Tong and Buechner, 2008).

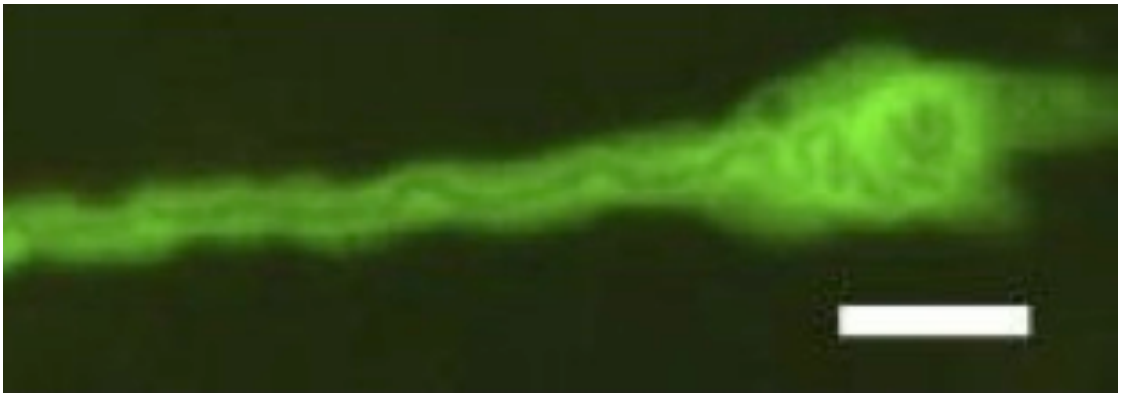

Figure 7.3a EXC-1 localization

A construct expressing EXC-1 cDNA under the control of canal-specific promoter, *vha-1*, was expressed throughout the cytoplasm of the canals with strong apical localization. Scale bar, 10μm.

7.4 Subcellular markers

When looking at these markers in wild-type worms (N2 – that have been more than 5 times outcrossed from integration) most of them showed punctate distribution, Figure 7.4a and 7.4b. CDC42 showed relatively even expression throughout the cytoplasm of the canal, Figure 7.4a.

Because of these marker strains have been integrated into the DNA, I was able to cross them into my *exc-1 (rh26)* mutant worms, relatively easy. Analyses of these subcellular markers were carried out on L4 or young adult hermaphrodites. When compared to wild-type worms, many of the markers looked very similar with their distribution, including: CHC-1, RAB-7, GLO-1, GRIP, RAB-11 and CDC42, Figure 7.4a. However, EEA-1 and RME-1 showed extreme variation in distribution when compared to wild type, Figure 7.4b and 7.4c. EEA-1 (Early Endosome Antigen 1) labels endocytic vesicles and RME-1 (Receptor-Mediated Endocytosis) labels recycling endosomes. EEA-1 shows accumulation, but only in cystic regions. Vesicles seemed to be relatively normal in regions where the canal was of normal diameter but a high amount found around the cysts. RME-1 showed the opposite effect from EEA-1. RME-1 was located normally in regions where the canal was of wild-type width but there was a loss of the RME-1 marker around the cysts. This phenotype of a build-up of EEA-1 and depletion of RME-1 around cystic regions was also found in *exc-5 (rh232)* mutants by Brendan Mattingly. This suggests that EXC-1 and EXC-5 may be working in the same region within the canal and seem to be working between trafficking of early endosomes to recycling endosomes, with EXC-1 most likely working upstream of EXC-5.

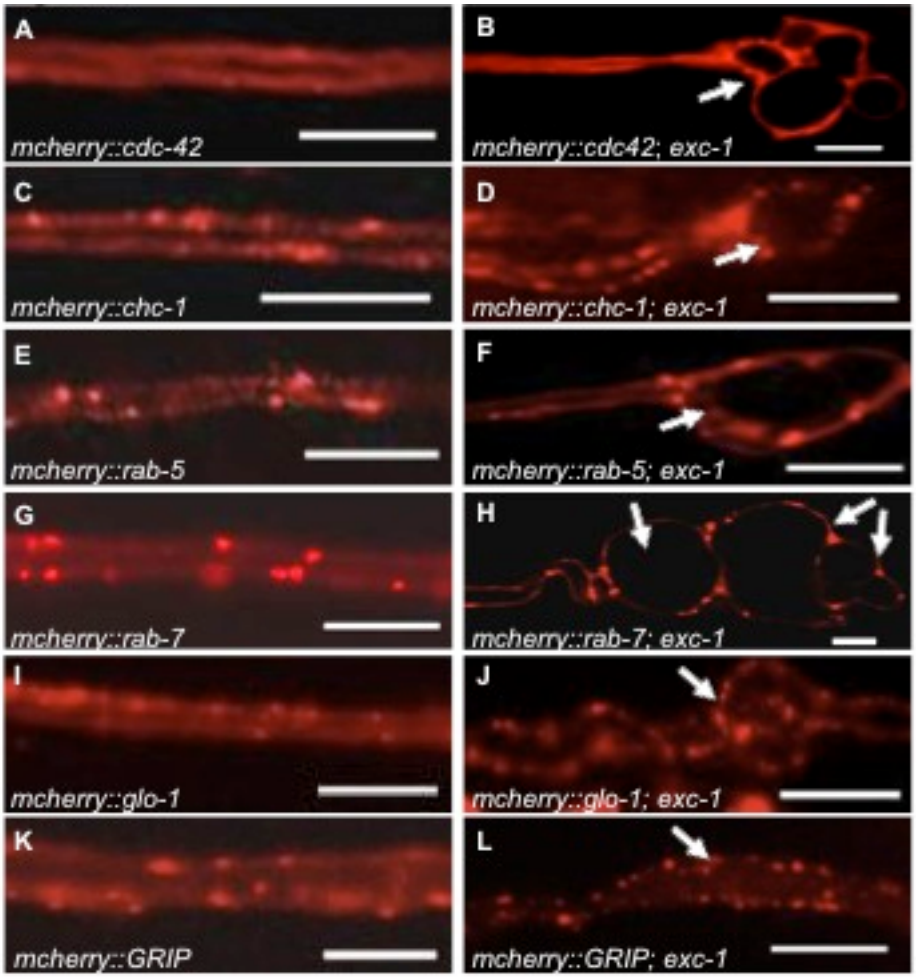

Figure 7.4a Most subcellular markers show no major effects in *exc-1* animals.

Fluorescence of animals expressing stable integrated arrays of fluorescently labeled subcellular markers within the excretory canals, driven by moderate expression marker *Pexc-9*. (A,B) *mCherry*::*cdc-42* primarily labels cytoplasm; (C,D) *mCherry*::*chc-1*, clathrin-coated pits; (E,F) *mCherry*::*rab-5*, early endosomes; (G,H) *mCherry*::*rab-7*, late endosomes; (I,J) *mCherry*::*glo-1*, lysosomes; (K,L) *mCherry*::*GRIP*, Golgi. Panels (A,C,E,G,I,K) show expression in a wild-type background; panels (B,D,F,H,J,L) show expression in *exc-1*(*rh26*) background. Arrows indicate position of large cysts in *exc-1* mutants. All bars 10 μm. Fluorescence brightened in all figures to show puncta.

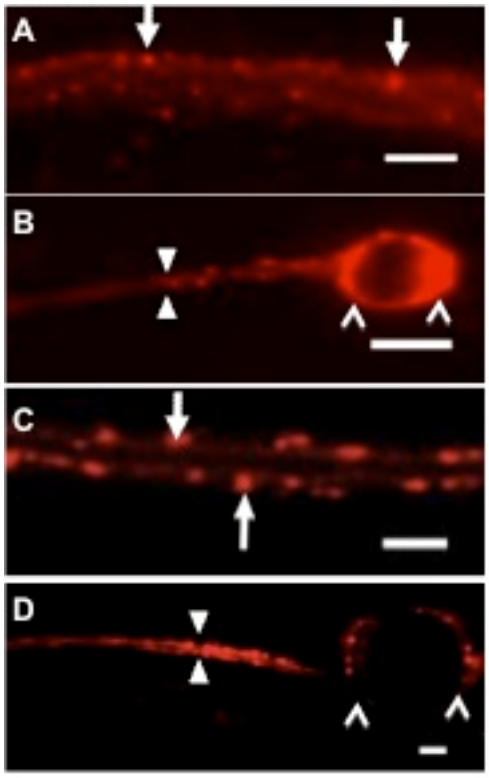

Figure 7.4b *exc-1* shows accumulation of EEA-1 and loss of RME-1 in cystic regions. Fluorescence of animals expressing stable integrated arrays of fluorescently labeled subcellular markers within the excretory canals, driven by moderate expression marker *Pexc-9*. (A,B) show distribution of EEA-1**;** (C,D) show distribution of RME-1. Puncta is evenly distributed in wild-type worms (A, C) but EEA-1 is built (B) and RME-1 is lost (D) up in cystic regions of *exc-1* mutants. Scale bar, 10μm.

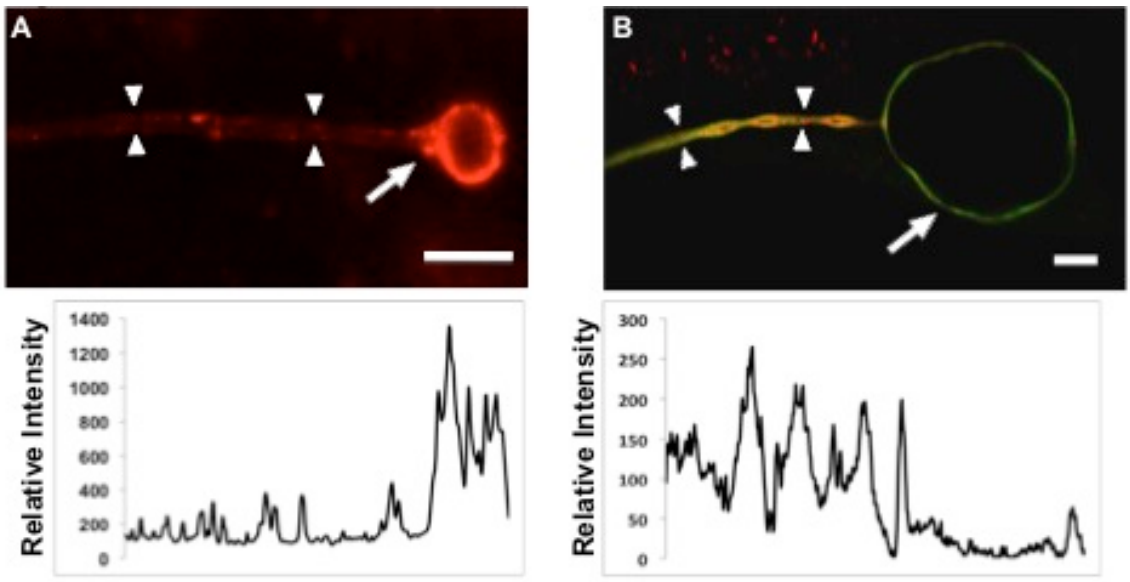

Figure 7.4c. Cysts accumulate EEA-1 while losing RME-1 expression
(A,C) Canals expressing integrated array of *Pexc-9*::*mCherry*::*eea-1* to mark early endosomes. (B,D) Canals expressing integrated array of *Pexc-9*::*mCherry*::*eea-1* to mark recycling endosomes. Animal in (B) additionally carries *Pvha-1::gfp* to label entire canal cytoplasm. (A,B) exc-1(rh26) mutants. (C,D) control expression in otherwise wild-type animals. Arrowheads in all panels show diameter of normal-width canal. Arrows in (A) and (B) indicates cyst at posterior terminus of canal. Arrows in (C) and (D) indicate typical punctate appearance of endosomes. Bars: 10 μm. All figures are brightened to show position of puncta in normal-width canals.

7.5 Electron Micrograph Images

Matthew Buechner carried out the electron micrograph imaging in Dave Hall's lab many years ago (Center for *C. elegans* Anatomy, Dept. of Neuroscience, Albert Einstein College of Medicine, Bronx, NY, 10461), Figure 7.5a, see Figure 1.5c for comparison to wild-type.

In an area of a mutant canal where cysts are forming, Figure 7.5a, canaliculi appear disordered, though the number of vesicles seems normal. Diameter of canaliculi is less uniform than in wild-type animals, and the thick electron-dense material that normally surrounds the lumen is disrupted, with cystic areas lacking the material, which appears in a disorganized manner in the cytoplasm, as previously noticed in other *exc* mutants(Fujita et al., 2003; Kolotuev et al., 2013; Suzuki et al., 2001). Finally, there are many vesicles of various sizes among and surrounding the canaliculi, which could reflect difficulties in forming the canaliculi, or an overabundance of endosomal compartments, possibly a build up of early endosomes, like we see with the subcellular markers.

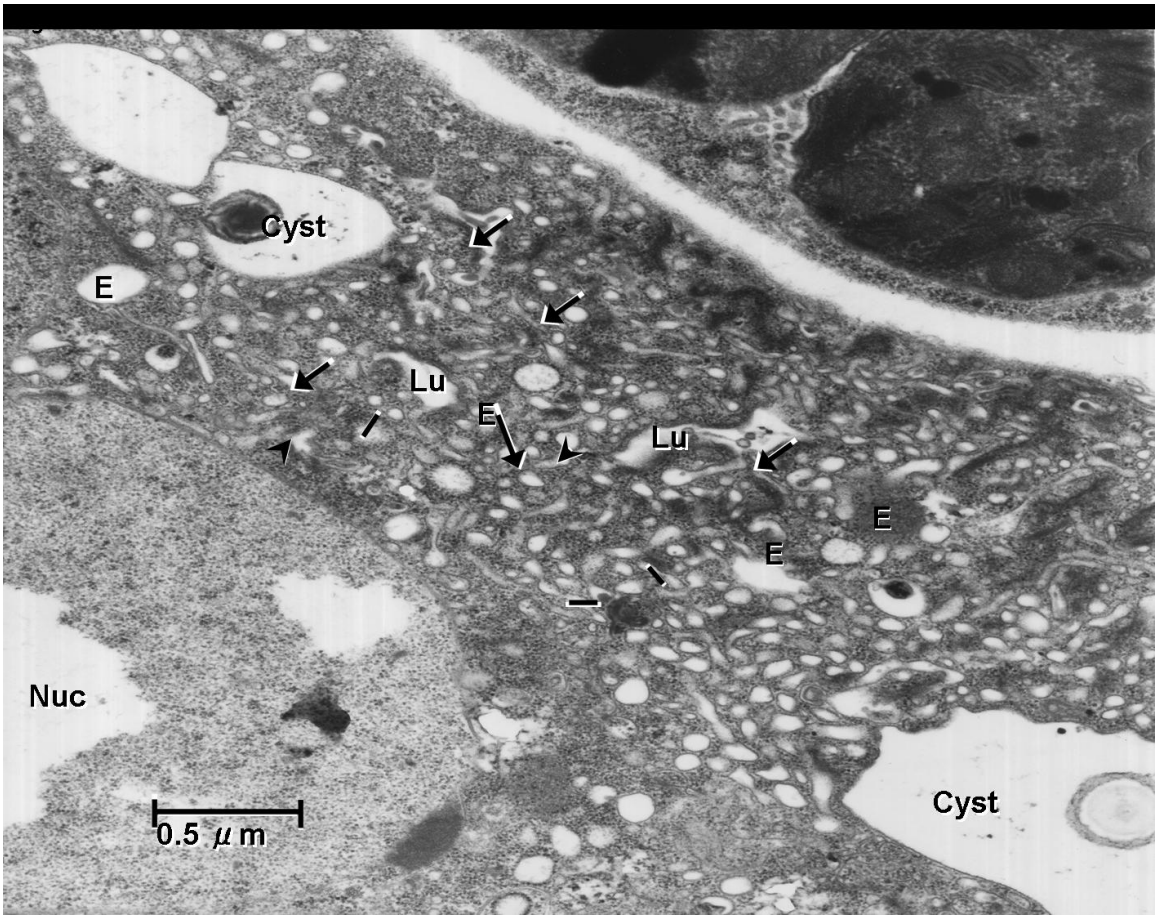

Figure 7.5a. Electron micrograph of *exc-1*(*rh26*) excretory canal.
Excretory cell body of L4 animal developing cysts. Nuc, cell nucleus. Lu, lumen of canal, surrounded by many canalicular vesicles. E, possible endosomes or abnormally large vesicles both outside and within area of canaliculi. Arrows show electron-dense terminal web-like material, both partially surrounding lumen, and disorganized material not adjacent to lumen. Arrowheads indicate regions of lumen lacking electron-dense material.

7.6 Summary

With the use of subcellular markers, it was found that *exc-1* mutant worms, around cystic regions, exhibit a build-up of early endosome marker, EEA-1 and a loss of recycling endosomes, indicated by marker RME-1. EM images suggest build up of endosomal compartments as well. These phenotypes suggest that EXC-1 is necessary for proper trafficking between these two compartments. This subcellular marker phenotype was also observed in *exc-5* worms, suggesting they may work together, with EXC-1 working upstream of EXC-5 (suggested from genetic interactions, Chapter 5).

There are many questions that arise from these results. How do EXC proteins facilitate movement of material from early to recycling endosomes? EXC proteins could facilitate pinching off of small vesicles from early endosomes, but it is also possible that EXC proteins could regulate motility of vesicles that pinch off normally. Is EXC-1 playing a similar role in membrane bending that IRGP might be playing? Previous work suggests that IRGP might be involved with molecules that bend membranes (Gregoire et al., 2011; Petkova et al., 2012), maybe EXC-1 is doing something similar within the excretory canal. These are questions that would need to be addressed with further studies.

7.7 Materials and Methods

Localization of EXC-1

The construct for localization of EXC-1 used the vector containing the promoter *vha-1* (pCV01) with the coding region of GFP. cDNA corresponding to EXC-1 was isolated the same way as described in Chapter 2. PCR amplification of this cDNA was carried out with primers 5'GTCGACTCTAGAGATGGGACACAAAA and 5'

ATAATTACCGGTCCATGAACTCCGGC that contained cut sites, XbaI and AgeI respectively, to allow for insertion into the plasmid pCV01. This construct was injected at a concentration of 25ng/µl and canals of F1 progeny of injected worms were scored in same fashion as described in chapter 2.

Subcellular Markers

All of the subcellular markers were designed, constructed, and integrated into the genome of N2 worms as previously described (Mattingly and Buechner, 2011). Strains carrying the different integrated subcellular markers were crossed to *exc-1 (rh26)* worms. F2 progeny expressing both the mutant phenotype and the fluorescent marker were isolated and maintained as a homozygous strain of both the subcellular marker and *exc-1 (rh26)*. Only two of the marker strains, EEA-1 and RME-1 required a recombination event to occurs, as they are located on the X chromosome as well.

Confocal Images

Live worms were mounted on 2% agarose pads with added 10mM muscimol or 0.5% 1-phenoxy-2-propanol as an anesthetic, as described previously (Sulston and Hodgkin, 1988). Confocal images were taken on an FV1000 Confocal microscope (Olympus) laser scanning confocal microscope, with lasers set to 488 nm excitation (GFP) or 543 nm excitation and (mCherry). Images were captured via FluoView optics, and analyzed with ImageJ software.

Subcellular Marker Measurements

NIH program ImageJ was used to analyze the brightness and locations of the subcellular markers in cystic and non-cystic areas of the excretory canals. Worms selected for analysis did not have medium or large multiple cysts grouped together, and had both a region of non-cystic, normal canal diameter and a cystic region that was usually located at the ends of the tubules. A segmented line was created along the length of the tubule with width wide enough to cover the largest cysts. A plot profile was recorded for this segmented line; from each value was subtracted the average value of a plot profile for a dark background outside the worm in that micrograph. To normalize the values a region of noncystic, normal-looking canal was assigned a brightness level of 100.

Electron Micrograph

Matthew Buechner carried out the electron micrograph imagining in Dave Hall's lab (Center for *C. elegans* Anatomy, Dept. of Neuroscience, Albert Einstein College of Medicine, Bronx, NY, 10461) For electron microscopy, L4 larvae and young adults were cut in midbody and fixed immediately in buffered (100 mM Hepes, pH 7.5) 3% glutaraldehyde, followed by post-fixation in buffered 1% OsO4 (Hall, 1995; Sulston and Hodgkin, 1988). After encasement in 1% agar, samples were dehydrated and embedded in Polybed 812 resin (Polysciences). Serial sections, ca. 70 nm, were post-stained in uranyl acetate followed by lead citrate.

Chapter 8

FRAP Assays

Chapter 8: FRAP assays
8.1 Abstract
8.2 Introduction
8.3 FRAP results
8.4 Summary
8.5 Materials and Methods

8.1 Abstract

In both *exc-1* and *exc-5* mutants there is a disruption in the recycling pathway exhibited by a build up of EEA-1 and a loss of RME-1, within the excretory canal. Confocal imaging was used to get a closer look at the trafficking within the excretory canal. This section describes the foundation work for watching vesicles move and carrying out FRAP studies, techniques that will be continued in the Buechner lab

8.2 Introduction

Within *exc-1* and *exc-5* mutants there is a disruption within the trafficking pathway within the excretory canal. Around cystic regions there is a build-up of EEA-1 and loss of RME-1. Many questions arise in regards to this phenotype: 1. Is the build-up of EEA-1 one large vesicle or is it an accumulation of many vesicles? 2. Is the build up of EEA-1, or loss of RME-1 due to the disruptions in the movement of vesicles? 3. Is vesicular trafficking faster or slower in *exc-1* and *exc-5* mutants compared to wild type? 4. Do the vesicles only move in one direction, are they only able to move in an anterorgrade direction or a posteriorgrade direction? To address these questions we wanted to investigate things closer on the subcellular level and watch the movement of vesicles within the canal.

To watch vesicles move we set out to do confocal imaging and Fluorescence Recovery After Photobleaching (FRAP) studies. FRAP assays allow for analysis of protein movement within a cell or located within the cell membrane (Axelrod et al., 1976; Goehring et al., 2010). As stated in the previous chapter, all of our subcellular markers are labeled with a mCherry flourophore 594 nm emission with a laser we are able to photobleach the mCherry marker within the canal and observe its recovery. To carry out these studies I had the assistance of Brian Ackley with use of his confocal microscope.

8.3 Results

I focused on a couple of the subcellular markers for these studies; RAB-5, RAB-7 and RME-1. I chose these markers for a couple of reasons: first, RAB-5 and RME-1 are both markers that seem to show disruption within *exc-1* mutants, an extreme phenotype for RME-1 and a milder phenotype for RAB-5. RAB-7 was chosen to serve as a control, because of similar puncta localization in both wild-type and *exc-1* mutant worms. EEA-1 was not chosen for these pilot experiments for a couple of reasons, first the marker is faintly expressed, making it very hard for analyzing the puncta, especially in non-cystic regions. Second, the EEA-1 marker tends to photobleach quickly, not allowing for enough time for accurate FRAP studies.

While observing these markers within the excretory canal, it was really interesting and exciting to see how the subcellular markers move and the timing of their movement All of the subcellular markers studied were able to move in both anterograde and posteriorgrade directions. With Image J, kymographs were made, showing the movement in both directions and giving an estimate of movement rates, Figure 8.3a.

Also identifiable with the confocal microscope was all the different shapes of endosomes (RAB-5 – Early Endosomes, RAB-7 – Late Endosomes, and RME-1 – Recycling endosomes). Fellow graduate student, Hikmat Al-Hashmi, is continuing with these FRAP studies and is developing a way for measurement of both endosome size and movement. It will be exciting to see the differences between wild-type and various *exc* mutants.

Next to carry out FRAP we wanted to be able to bleach different areas within the canal and determine its half-life and time of recovery. I was successful in being able to bleach the subcellular markers within the canal and measured fluorescence recovery caused by influx of vesicles into the area, Figure 8.3c. The half-time of recovery for early endosomes (marked with RAB-5::mCherry) in an L4 worm, was 34 seconds for a bleached area of about 8mm in length. Recovery of untethered proteins (cytoplasmic GFP) was very rapid, and we were unable to acquire any visible dimming of this marker with sustained bleaching.

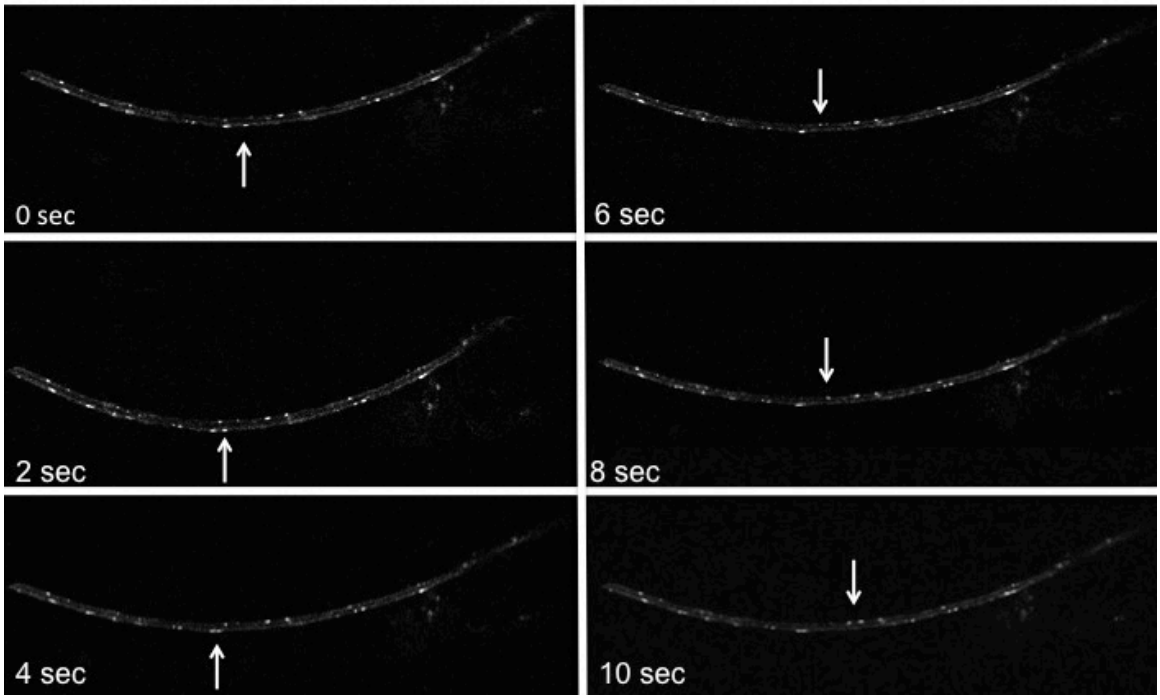

Figure 8.3a Vesicles move in both anterograde and posteriorgrade directions.
Early endosomes move in both anteriorgrade (indicated by arrows in left column) and posteriorgrade (indicated by arrows in right column) directions. Worms carry the integrated transgene, *Pexc-9::mCherry::RAB-5*.

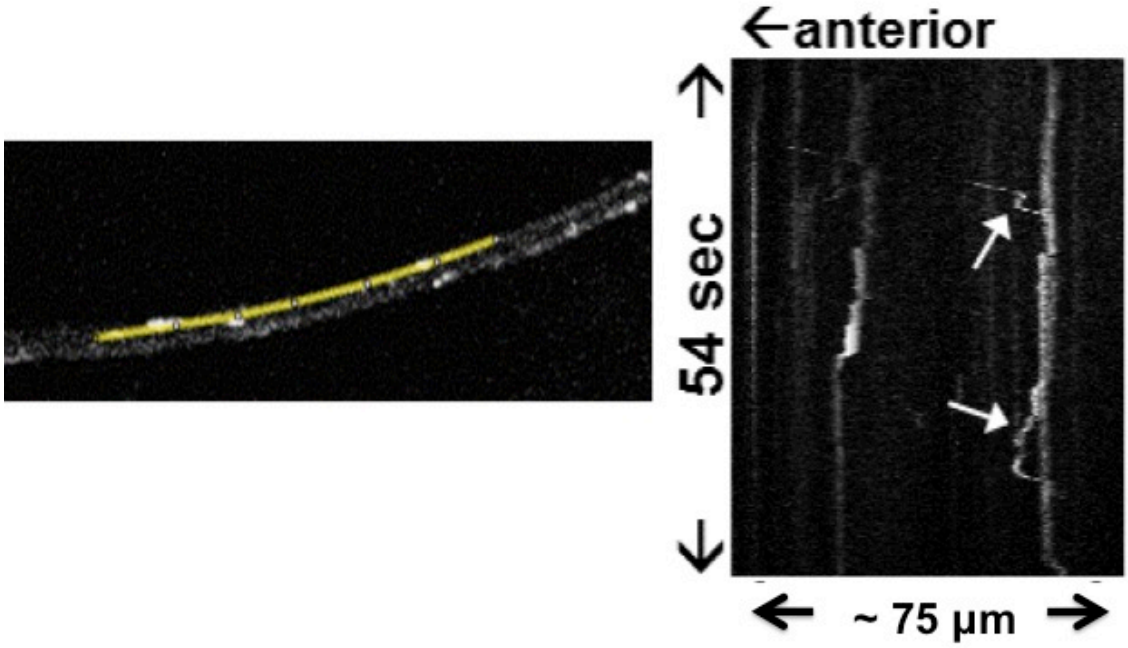

Figure 8.3b Kymograph

Yellow line in the right panel indicates area that was used for Kymograph. White areas on kymograph indicate early endosome vesicles and arrows indicate movement during the 54 seconds of imaging. Worms carry the integrated transgene, *Pexc-9::mCherry::RAB-5*.

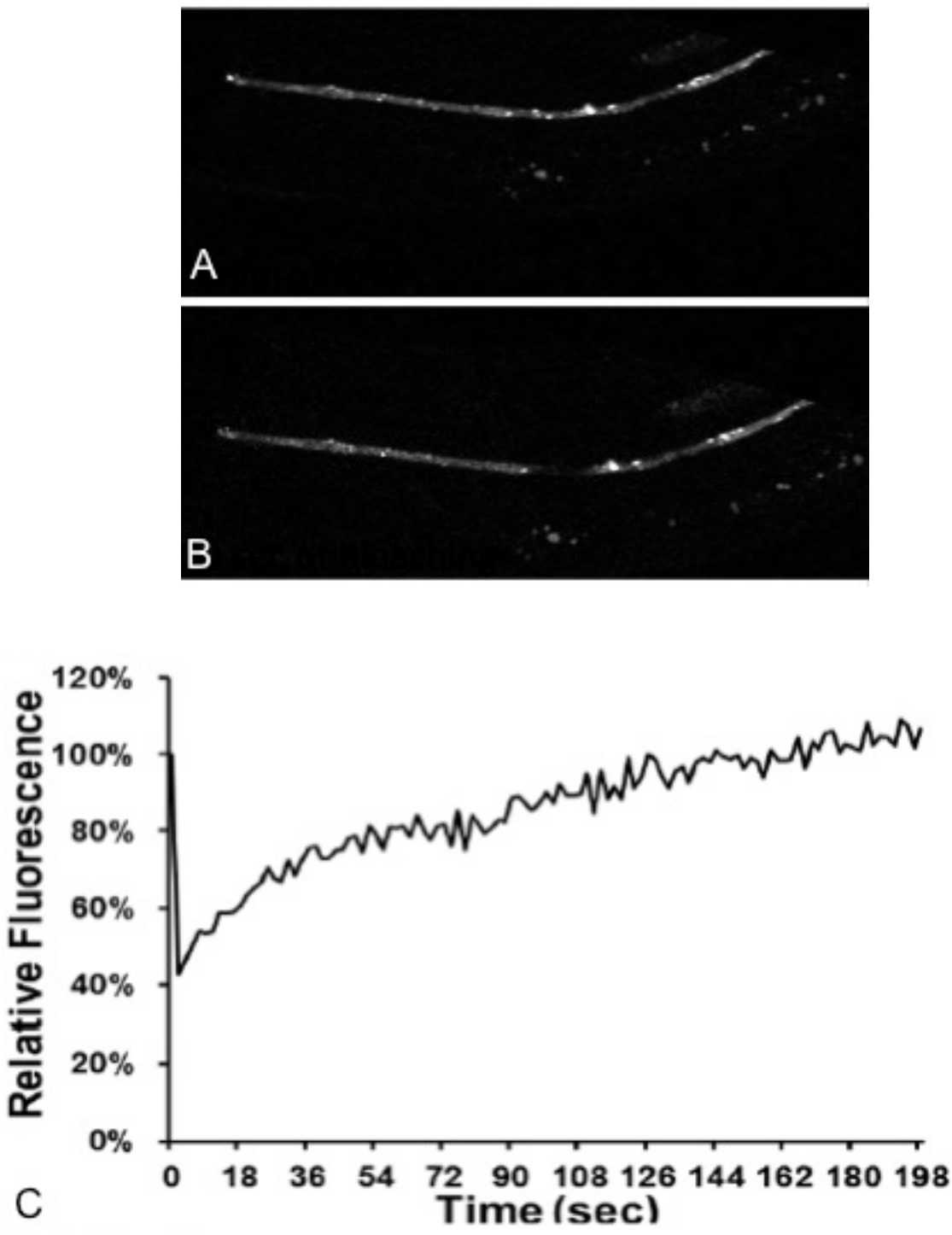
A
B
C
Relative Fluorescence
120%
100%
80%
60%
40%
20%
0%
0
18
36
54
72
90
108
126
144
162
180
198
Time (sec)

Figure 8.3c FRAP

Area that has been photobleached is able to recover. (A) Image of a left canal from a worm with integrated transgene *Pexc-9::mCherry::RAB-5* before Photobleaching. (B) Loss of puncta indicate successful bleaching of area in the canal. (C) Graph shows fluorescence before bleaching and its recovery indicated by relative fluorescence.

8.4 Summary

With the use of a laser confocal microscope, we are able to carry out FRAP studies to get a closer look at what is going on within the excretory canal. At this time studies were not carried out to observe possible differences between the cystic and non-cystic regions, but this work will be continued in the lab and we now have the understanding and tools to do it.

8.5 Materials and Methods

FRAP assays were carried out on a FV1000 Confocal microscope (Olympus) laser scanning confocal microscope, with lasers set to 488 nm excitation (GFP) or 546 nm (mCherry). Images were captured via FluoView optics, and analyzed with ImageJ software. Photobleach of subcellular markers were with a laser at 594 emission.

A plot profile was recorded for the area what was photobleached; from each value was subtracted the average value of a plot profile for a dark background outside the worm in that micrograph. 100% Fluorescence intensity was assigned to the brightness level of area that was bleached before FRAP studies were carried out.

Chapter 9

Discussion

9.1 Discussion

exc-1 mutants have a varied cystic phenotype

In *C. elegans, exc-1* mutants were identified by its severe deficiencies in maintenance of the narrow lumen of the excretory canals. *exc-1* mutants show a varied phenotype; from worms that have canals that almost look wild-type with canals extending most of the length with a small cyst, to a serve cystic phenotype with short canals containing many large cysts. Through the use of rescue assays and RNAi, I was able to map and identify the *exc-1* gene. Knockdown of the predicted gene C46E1.3 phenocopies *exc-1,* and injection of this clone into *exc-1* mutant worms rescues the cystic phenotype. We conclude that clone C46E1.3 encodes the *exc-1* gene.

exc-1 is expressed in the amphid sheath

EXC-1 is expressed in the excretory canal, and the glial amphid sheath cells. *exc-1 (rh26)* mutants exhibit occasional, abnormal formation of cyst-like structures or large vacuoles along the axon-like process. These cyst-like structures or large vacuoles do not seem to disrupt the worm's ability to form the amphid channel properly and take up dye from the outside environment. Also, *exc-1* mutants do not display any behavioral defects that may suggest that the amphid neurons aren't able to pass through the amphid sheath similar to wild-type. Though *exc-1* is not required to form and maintain the tubule-like portion of the amphid channel it may be carrying out a similar role on the cellular level as within the canal.

Interestingly, the *pros-1* (*ceh-26*) transcription factor, encoding the *C. elegans* homologue to the *prospero* homeobox gene, is also expressed primarily in the excretory canal and amphid sheath cells (Kolotuev et al., 2013). And is required for proper tubule formation as a loss of function results in a cystic phenotype as well. In this study, the amphid sheath structure was not characterized in mutants so it is unknown if *pros-1* mutants exhibit structural defects in the amphid sheath as well. A study of genes whose transcription is regulated by Prospero or CEH-26 (PROS-1) included *exc-5* but not *exc-1*, which suggests that both *exc-1* and *pros-1* transcription may be activated together by a common upstream factor.

exc-1 encodes a IRGP

EXC-1 shows strongest homology to a large family of Immunity-Related GTPase that are represented in many species. These proteins were discovered in mice, but are deleted in many mammals. Two members of the IRGP family are found in humans, IRGM and IRGC. EXC-1 shows strongest homology to IRGC, which is not inducible by interferons in any organism studied. A common feature of these proteins is an incomplete Ras-related GTP-binding domain that contains the core G1 – G4 subdomain sequences regulating binding to GTP and to activity regulators, guanine exchange factors (GEF) and guanine activating protein (GAP), but with weaker homology to the Ras G5 subdomain, though this region shows weak homology throughout the RAS superfamily. EXC-1 also shows strong structural homology to the IRGP GTP binding domain, particularly at the nucleotide binding surface. IRGC and IRGM proteins contain homodimerization motifs in the center of the RAS homology domain. This region appears to be missing in EXC-1; this

may be because EXC-1 already contains two RAS homology domains within one protein. This feature of two RAS homology domains found in EXC-1 adds to the complexity of the protein within the cell. With tandem Ras homology domains within the protein this may remove a step in binding and dimerizing for function.

Though the two Ras homology domains lack the G5 motif, EXC-1 does seem to function as a true GTPase. When EXC-1 is in its wild-type state and the genomic sequence has not been altered, it is able to rescue the *exc-1* cystic phenotype and even cause an overexpressed, convoluted canal phenotype. When EXC-1 is in a constitutively active form, it is able to rescue the cystic phenotype; however it does not induce a convoluted canal structure, suggesting that EXC-1 may require the ability to cycle between active and inactive forms to function properly. Another suggestion that the EXC-1 Ras homology domain is functional, is its variable binding partners, that depend on GTP/GDP binding.

exc-1 interacts with *exc-5* and *exc-9*

Epistasis studies carried out in the lab have identified a genetic pathway required for tubule structure, this pathway is EXC-9 → EXC-1 → EXC-5, EXC-9 acts upstream of both EXC-1 and EXC-5 and EXC-1 acts upstream of EXC-5. Yeast two-hybrid studies indicate that EXC-1 and EXC-9 bind to each other but only when EXC-1 is in its wild-type or constitutively active state, as the dominant-negative form is unable to interact with EXC-9. EXC-9 was found to bind to the region including the N-terminus, proline-rich region, and the first Ras homology domain. This may suggest that EXC-1 may

undergo a conformational change when in its inactive, GDP bound form, such that the proline rich region and 1st Ras homology domains are not exposed to interact with EXC-9. Further studies are required to verify this possibility. Other proteins that may serve as binding partners, possibly to the 2nd Ras homology domain, remain to be discovered as well. All together, these results suggest that EXC-1 binds to EXC-9 only in certain conditions and this binding is responsible for downstream activation of EXC-5 to maintain tubule shape.

Though EXC-1, EXC-9 and EXC-5 are shown to interact, it seems that this pathway requirement only occurs within the excretory canal. EXC-1, EXC-9 and EXC-5 all show separate and non-overlapping expression outside of the excretory canal. EXC-1 is expressed in the amphid sheath; EXC-9 within many neurons and is highly expressed in the uterine seam cell; the close EXC-9 homologue VALV-1 within multiple valves in the digestive and reproductive tracts (Tong and Buechner, 2008); and EXC-5 is highly expressed in the pharyngeal muscles (Suzuki et al., 2001). This also indicates that EXC-1 has different binding partners within the amphid sheath and possible function because of this.

EXC-1 and EXC-5 are needed for proper recycling

exc-1 loss-of-function mutants exhibit defects within the intracellular trafficking of the excretory canal. When EXC-1 is not present within the canal there is a build-up of the early endosome marker, EEA-1, and consequently a loss of recycling endosome marker, RME-1. This is also seen in *exc-5* loss-of-function mutants. EXC-1 and

EXC-5 seem to be required for the proper trafficking of material from the early endosome to the recycling endosome, and when this function is lost there is weakening at the apical surface, Figure 9.1a and 9.1b. The pressure from the canal pushes on these weak spots and results in a cyst formation. It is likely that future studies will show that EXC-9 is required in this pathway as well.

The excretory canal needs to maintain a proper balance of material being transported to the apical surface to maintain the lumenal shape. This is also important for the basal surface, when you have too much of EXC-1 or EXC-5 there seems to be a loss of transport of material to the basal surface, resulting in not enough material to extend out. The canal is not able to extend and stays at the cell body, though the apical surface is maintained it results in convoluting on itself. Both are disrupted suggesting that EXC-1 and EXC-5 play a role between the two and required a proper balance of material be transported from the common endosome to both the apical and basal surfaces.

Genetic results suggest that EXC-9 and EXC-1 both act upstream of the guanine exchange factor EXC-5, which mediates disappearance or movement of early endosomes and appearance of labeled recycling endosomes to prevent cyst formation. Our results did not find direct binding of EXC-1 to EXC-5, which suggests that EXC-1 activates some other protein that causes activated EXC-5 to mediate endosomal conversion to maintain narrow tubular structure.

EXC-1 as a model for IRG

The function of IRG proteins is becoming better understood. Most are stimulated through actions of the immune system. The human IRGM protein is believed to function

to regulate cell autophagy. The IRGC protein is the most widely distributed IRG protein, with a homologue in many mammalian species, and is not activated through activity of the immune system. In *C. elegans exc-1* mutants, the early and recycling endosomes are strongly affected, while only minor effects on late endosome levels were detected; these observations suggest that autophagy is not at issue here. We conclude that the EXC-1 protein, and by inference other IRGC proteins, act at a different step of endosomal trafficking than does human IRGM protein. Mice have many of these proteins, and so could regulate endosome formation at many trafficking steps.

Our yeast 2-hybrid show that activated EXC-1 binds directly to EXC-9 protein. EXC-9 is a member of the CRIP (Cysteine-Rich Intestinal Proteins) family of small cytoplasmic LIM-domain protein-binding proteins, which are expressed particularly highly in the mammalian intestine, but are found in many tissues. Our genetic results have shown that EXC-9 acts upstream of EXC-1 to maintain narrow tubular structure, and provide a possible model for investigating the function of CRIP as a possible binding partner acting upstream of mammalian IRG proteins.

The excretory canal now

From these studies we have tied in the roles of EXC-1, EXC-9 and EXC-5 as proteins all required to maintain the lumenal shape within the excretory canal, with EXC-1 and EXC-9 binding and somehow activating the function of EXC-5 to recycle material at the apical surface by trafficking material from the early endosome to the recycling endosome, see models 9.1 a, b and c.

Further studies of interactions of EXC proteins with potential partners involved in endosome movement and formation, cytoskeletal structure, and canalicular vesicle structure, should delineate the roles of these proteins in maintenance of narrow tubular structure as well as functions in other cell types in nematodes and mammals.

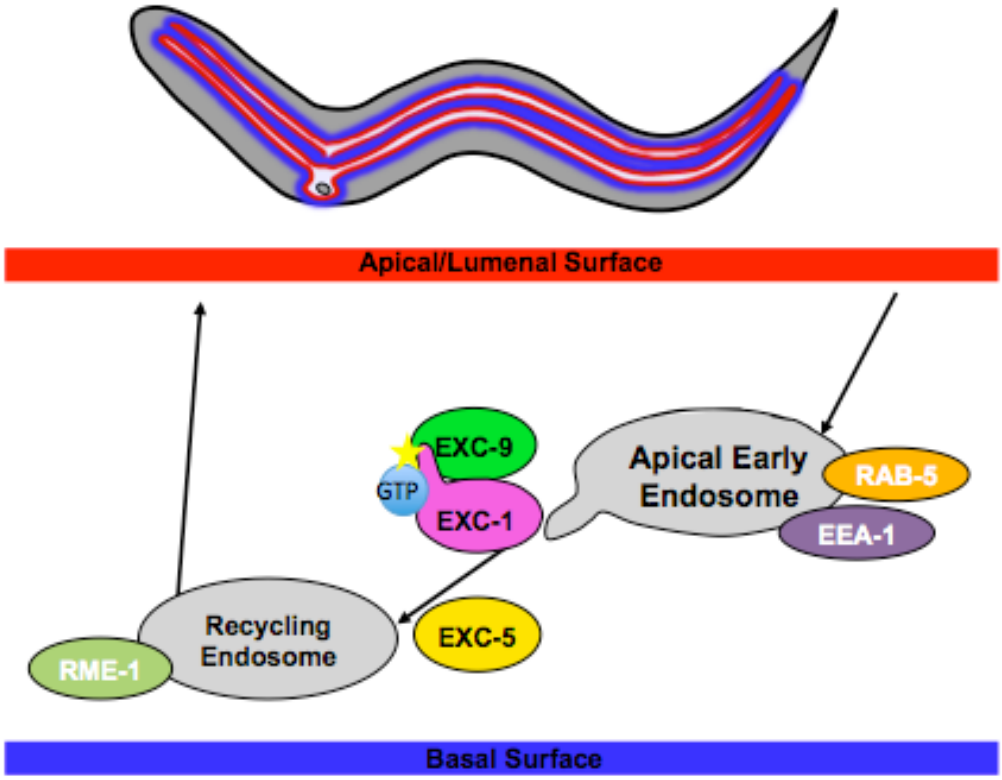

Figure 9.1a EXC-1 within the canal
EXC-1 functions in the canal by binding to EXC-9 in its wild-type or active form, which is needed for indirect, upstream activation of EXC-5. Together, EXC-1, EXC-5 and EXC-9 work together for the proper trafficking of material from the early endosome to the recycling endosome for maintenance of the apical surface.

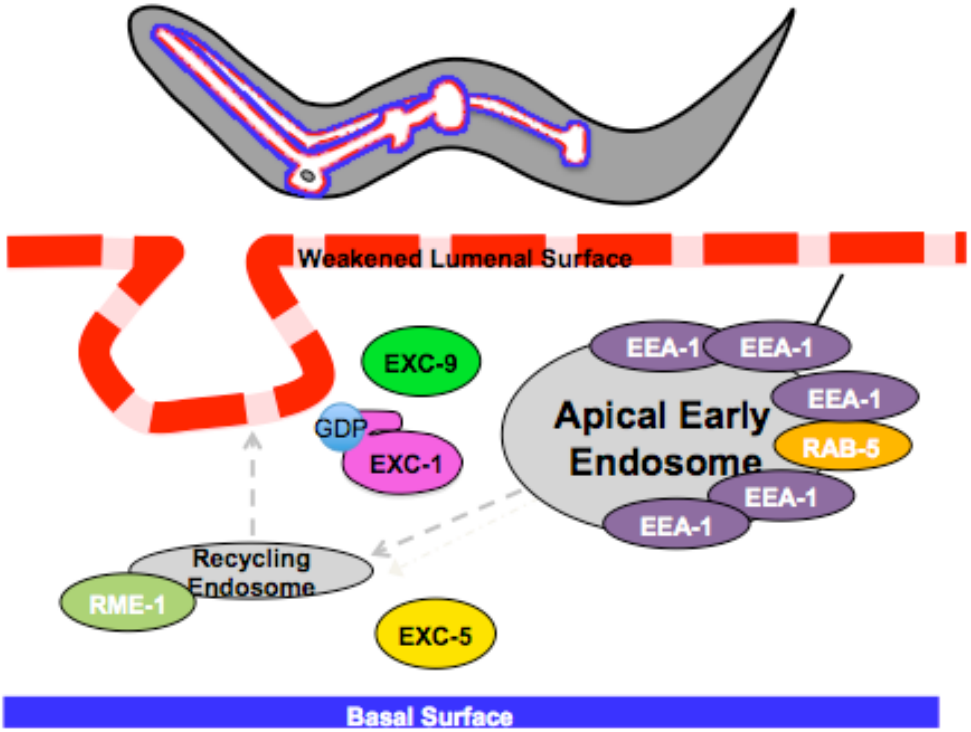

Figure 9.1b Loss of *exc-1*.

When EXC-1 is missing, or in its GDP-bound form, EXC-1 is no longer able to bind with EXC-9 resulting in a loss of downstream activation of EXC-5. Without the proper function of EXC-1 (or EXC-5 and EXC-9) material is unable to be transported from the early endosome to the recycling endosome and back to the apical/lumenal surface. This loss of material at the apical surface results in a weakened surface. The pressure within the lumen of the canal pushes on this weakened surface and results in cyst formation.

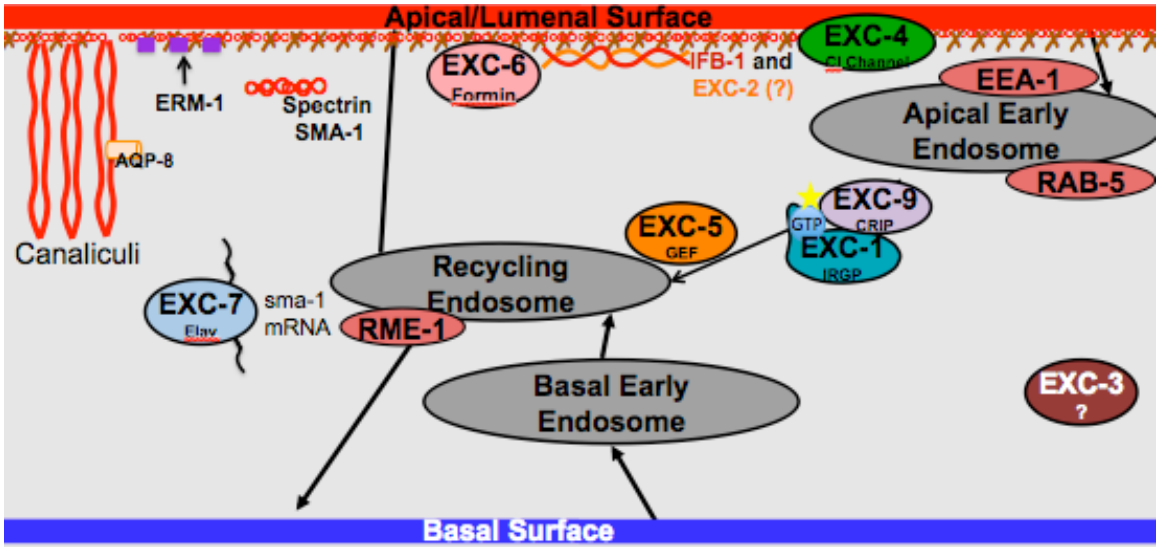

Figure 9.1c Model of canal at the end of my studies.
Since I have joined the lab, EXC-1, EXC-5 and EXC-9 have been shown to interact together for proper trafficking within the canal. Intermediate filament protein, IFB-1, has been identified for proper tubule shape as well (Kolotuev et al., 2013). EXC-2 may be another intermediate filament subunit as well, possible interacting with IFB-1 (remains to be verified). EXC-6 has been identified as a formin, which is also involved with cytoskeletal proteins. And Aquaporin 8 (AQP-8) has been identified for proper tubule formation. EXC-3 remains to be identified. Compare to model at the beginning of my studies, Figure 1.6.

References

Al-Zeer, M.A., Al-Younes, H.M., Braun, P.R., Zerrahn, J., Meyer, T.F., 2009. IFN-gamma-inducible Irga6 mediates host resistance against Chlamydia trachomatis via autophagy. PLoS One 4, e4588.

Araque, A., Parpura, V., Sanzgiri, R.P., Haydon, P.G., 1999. Tripartite synapses: glia, the unacknowledged partner. Trends in neurosciences 22, 208-215.

Axelrod, D., Koppel, D.E., Schlessinger, J., Elson, E., Webb, W.W., 1976. Mobility measurement by analysis of fluorescence photobleaching recovery kinetics. Biophysical journal 16, 1055-1069.

Bacaj, T., Lu, Y., Shaham, S., 2008a. The conserved proteins CHE-12 and DYF-11 are required for sensory cilium function in Caenorhabditis elegans. Genetics 178, 989-1002.

Bacaj, T., Tevlin, M., Lu, Y., shaham, S., 2008b. Glia Are Essential for Sensory Organ Function in C. elegans. Science 322, 744-747.

Baer, M.M., Chanut-Delalande, H., Affolter, M., 2009. Cellular and molecular mechanisms underlying the formation of biological tubes. Current topics in developmental biology 89, 137-162.

Bargmann, C.I., 2006. Chemosensation in C. elegans. WormBook : the online review of C. elegans biology, 1-29.

Bekpen, C., Hunn, J.P., Rohde, C., Parvanova, I., Guethlein, L., Dunn, D.M., Glowalla, E., Leptin, M., Howard, J.C., 2005. The interferon-inducible p47 (IRG) GTPases in vertebrates: loss of the cell autonomous resistance mechanism in the human lineage. Genome biology 6, R92.

Bekpen, C., Marques-Bonet, T., Alkan, C., Antonacci, F., Leogrande, M.B., Ventura, M., Kidd, J.M., Siswara, P., Howard, J.C., Eichler, E.E., 2009. Death and resurrection of the human IRGM gene. PLoS genetics 5, e1000403.

Bernstein-Hanley, I., Coers, J., Balsara, Z.R., Taylor, G.A., Starnbach, M.N., Dietrich, W.F., 2006. The p47 GTPases Igtp and Irgb10 map to the Chlamydia trachomatis susceptibility locus Ctrq-3 and mediate cellular resistance in mice. Proc Natl Acad Sci U S A 103, 14092-14097.

Berry, K.L., Bulow, H.E., Hall, D.H., Hobert, O., 2003. A C. elegans CLIC-like protein required for intracellular tube formation and maintenance. Science 302, 2134-2137.

Boehm, U., Guethlein, L., Klamp, T., Ozbek, K., Schaub, A., Futterer, A., Pfeffer, K., Howard, J.C., 1998. Two families of GTPases dominate the complex cellular response to IFN-gamma. Journal of immunology 161, 6715-6723.

Bourne, H.R., Sanders, D.A., McCormick, F., 1990. The GTPase superfamily: a conserved switch for diverse cell functions. Nature 348, 125-132.

Bourne, H.R., Sanders, D.A., McCormick, F., 1991. The GTPase superfamily: conserved structure and molecular mechanism. Nature 349, 117-127.

Brenner, S., 1974. The genetics of Caenorhabditis elegans. Genetics 77, 71-94.

Bucci, C., Parton, R.G., Mather, I.H., Stunnenberg, H., Simons, K., Hoflack, B., Zerial, M., 1992. The small GTPase rab5 functions as a regulatory factor in the early endocytic pathway. Cell 70, 715-728.

Buechner, M., 2002. Tubes and the single C. elegans excretory cell. Trends Cell Biol 12, 479-484.

Buechner, M., Hall, D.H., Bhatt, H., Hedgecock, E.M., 1999a. Cystic canal mutants in Caenorhabditis elegans are defective in the apical membrane domain of the renal (excretory) cell. Dev Biol 214, 227-241.

Buechner, M., Hall, D.H., Bhatt, H., Hedgecock, E.M., 1999b. Cystic Canal Mutants in *Caenorhabditis elegans* Are Defective in the Apical Membrane Domain of the Renal (Excretory) Cell. Dev Biol 214, 227-241.

Callaghan, J., Simonsen, A., Gaullier, J.M., Toh, B.H., Stenmark, H., 1999. The endosome fusion regulator early-endosomal autoantigen 1 (EEA1) is a dimer. The Biochemical journal 338 (Pt 2), 539-543.

Cassada, R.C., Russell, R.L., 1975. The dauerlarva, a post-embryonic developmental variant of the nematode Caenorhabditis elegans. Dev Biol 46, 326-342.

Consortium, C.e.D.M., 2012. large-scale screening for targeted knockouts in the Caenorhabditis elegans genome. G3 2, 1415-1425.

Consortium, *C.e*.S., 1998. Genome Sequence of the Nematode *C. elegans*: A Platform for Investigating Biology. Science 282, 2012-2018.

Del Conte-Zerial, P., Brusch, L., Rink, J.C., Collinet, C., Kalaidzidis, Y., Zerial, M., Deutsch, A., 2008. Membrane identity and GTPase cascades regulated by toggle and cut-out switches. Molecular systems biology 4, 206.

Fay, D., 2006. Genetic mapping and manipulation: chapter 1--Introduction and basics. WormBook : the online review of C. elegans biology, 1-12.

Fields, S., Song, O., 1989. A novel genetic system to detect protein-protein interactions. Nature 340, 245-246.

Fielenbach, N., Antebi, A., 2008. C. elegans dauer formation and the molecular basis of plasticity. Genes Dev 22, 2149-2165.

Fire, A., Xu, S., Montgomery, M.K., Kostas, S.A., Driver, S.E., Mello, C.C., 1998. Potent and specific genetic interference by double-stranded RNA in Caenorhabditis elegans. Nature 391, 806-811.

Flibotte, S., Edgley, M.L., Chaudhry, I., Taylor, J., Neil, S.E., Rogula, A., Zapf, R., Hirst, M., Butterfield, Y., Jones, S.J., Marra, M.A., Barstead, R.J., Moerman, D.G., 2010. Whole-genome profiling of mutagenesis in Caenorhabditis elegans. Genetics 185, 431-441.

Fujita, M., Hawkinson, D., King, K.V., Hall, D.H., Sakamoto, H., Buechner, M., 2003. The role of the ELAV homologue EXC-7 in the development of the Caenorhabditis elegans excretory canals. Dev Biol 256, 290-301.

Ghosh, A., Uthaiah, R., Howard, J., Herrmann, C., Wolf, E., 2004. Crystal structure of IIGP1: a paradigm for interferon-inducible p47 resistance GTPases. Molecular cell 15, 727-739.

Gilly, M., Wall, R., 1992. The IRG-47 gene is IFN-gamma induced in B cells and encodes a protein with GTP-binding motifs. Journal of immunology 148, 3275-3281.

Girard, L.R., Fiedler, T.J., Harris, T.W., Carvalho, F., Antoshechkin, I., Han, M., Sternberg, P.W., Stein, L.D., Chalfie, M., 2007. WormBook: the online review of Caenorhabditis elegans biology. Nucleic acids research 35, D472-475.

Gissendanner, C.R., Crossgrove, K., Kraus, K.A., Maina, C.V., Sluder, A.E., 2004. Expression and function of conserved nuclear receptor genes in Caenorhabditis elegans. Dev Biol 266, 399-416.

Gobel, V., Barrett, P.L., Hall, D.H., Fleming, J.T., 2004. Lumen morphogenesis in C. elegans requires the membrane-cytoskeleton linker erm-1. Dev Cell 6, 865-873.

Goehring, N.W., Chowdhury, D., Hyman, A.A., Grill, S.W., 2010. FRAP analysis of membrane-associated proteins: lateral diffusion and membrane-cytoplasmic exchange. Biophysical journal 99, 2443-2452.

Gorvel, J.P., Chavrier, P., Zerial, M., Gruenberg, J., 1991. rab5 controls early endosome fusion in vitro. Cell 64, 915-925.

Grant, B., Zhang, Y., Paupard, M.C., Lin, S.X., Hall, D.H., Hirsh, D., 2001. Evidence that RME-1, a conserved C. elegans EH-domain protein, functions in endocytic recycling. Nature cell biology 3, 573-579.

Grant, B.D., Caplan, S., 2008. Mechanisms of EHD/RME-1 protein function in endocytic transport. Traffic (Copenhagen, Denmark) 9, 2043-2052.

Grant, B.D., Donaldson, J.G., 2009. Pathways and mechanisms of endocytic recycling. Nat Rev Mol Cell Biol 10, 597-608.

Gregoire, I.P., Richetta, C., Meyniel-Schicklin, L., Borel, S., Pradezynski, F., Diaz, O., Deloire, A., Azocar, O., Baguet, J., Le Breton, M., Mangeot, P.E., Navratil, V., Joubert, P.E., Flacher, M., Vidalain, P.O., Andre, P., Lotteau, V., Biard-Piechaczyk, M., Rabourdin-Combe, C., Faure, M., 2011. IRGM is a common target of RNA viruses that subvert the autophagy network. PLoS pathogens 7, e1002422.

Grosshans, B.L., Ortiz, D., Novick, P., 2006. Rabs and their effectors: achieving specificity in membrane traffic. Proc Natl Acad Sci U S A 103, 11821-11827.

Gyuris, J., Golemis, E., Chertkov, H., Brent, R., 1993. Cdi1, a human G1 and S phase protein phosphatase that associates with Cdk2. Cell 75, 791-803.

Hall, D.H., 1995. Electron Microscopy and Three-Dimensional Image Reconstruction, in: Epstein, H.F., Shakes, D.C. (Eds.), *Caenorhabditis elegans*: Modern Biological Analysis of an Organism. Academic Press, San Diego, pp. 451-482.

Haydon, P.G., 2001. GLIA: listening and talking to the synapse. Nature reviews. Neuroscience 2, 185-193.

Hedgecock, E.M., Culotti, J.G., Thomson, J.N., Perkins, L.A., 1985. Axonal guidance mutants of Caenorhabditis elegans identified by filling sensory neurons with fluorescein dyes. Dev Biol 111, 158-170.

Hoekstra, D., Tyteca, D., van, I.S.C., 2004. The subapical compartment: a traffic center in membrane polarity development. J Cell Sci 117, 2183-2192.

Huett, A., McCarroll, S.A., Daly, M.J., Xavier, R.J., 2009. On the level: IRGM gene function is all about expression. Autophagy 5, 96-99.

Jean, S., Kiger, A.A., 2012. Coordination between RAB GTPase and phosphoinositide regulation and functions. Nat Rev Mol Cell Biol 13, 463-470.

Jones, S.J., Baillie, D.L., 1995. Characterization of the let-653 gene in Caenorhabditis elegans. Molecular & general genetics : MGG 248, 719-726.

Kaiser, F., Kaufmann, S.H., Zerrahn, J., 2004. IIGP, a member of the IFN inducible and microbial defense mediating 47 kDa GTPase family, interacts with the microtubule binding protein hook3. J Cell Sci 117, 1747-1756.

Khan, L.A., Zhang, H., Abraham, N., Sun, L., Fleming, J.T., Buechner, M., Hall, D.H., Gobel, V., 2013. Intracellular lumen extension requires ERM-1-dependent apical membrane expansion and AQP-8-mediated flux. Nature cell biology 15, 143-156.

Kim, U.J., Shizuya, H., de Jong, P.J., Birren, B., Simon, M.I., 1992. Stable propagation of cosmid sized human DNA inserts in an F factor based vector. Nucleic acids research 20, 1083-1085.

Kolotuev, I., Hyenne, V., Schwab, Y., Rodriguez, D., Labouesse, M., 2013. A pathway for unicellular tube extension depending on the lymphatic vessel determinant Prox1 and on osmoregulation. Nature cell biology 15, 157-168.

Kuffler, S.W., Potter, D.D., 1964. Glia in the Leech Central Nervous System: Physiological Properties and Neuron-Glia Relationship. Journal of neurophysiology 27, 290-320.

Lafuse, W.P., Brown, D., Castle, L., Zwilling, B.S., 1995. Cloning and characterization of a novel cDNA that is IFN-gamma-induced in mouse peritoneal macrophages and encodes a putative GTP-binding protein. Journal of leukocyte biology 57, 477-483.

Lazarides, E., 1980. Intermediate filaments as mechanical integrators of cellular space. Nature 283, 249-256.

Lin, S.X., Grant, B., Hirsh, D., Maxfield, F.R., 2001. Rme-1 regulates the distribution and function of the endocytic recycling compartment in mammalian cells. Nature cell biology 3, 567-572.

Lubarsky, B., Krasnow, M.A., 2003. Tube morphogenesis: making and shaping biological tubes. Cell 112, 19-28.

Macara, I.G., Lounsbury, K.M., Richards, S.A., McKiernan, C., Bar-Sagi, D., 1996. The Ras superfamily of GTPases. FASEB journal : official publication of the Federation of American Societies for Experimental Biology 10, 625-630.

MacMicking, J.D., 2004. IFN-inducible GTPases and immunity to intracellular pathogens. Trends in immunology 25, 601-609.

MacMicking, J.D., Taylor, G.A., McKinney, J.D., 2003. Immune control of tuberculosis by IFN-gamma-inducible LRG-47. Science 302, 654-659.

Martens, S., Howard, J., 2006. The interferon-inducible GTPases. Annu Rev Cell Dev Biol 22, 559-589.

Mattingly, B.C., Buechner, M., 2011. The FGD homologue EXC-5 regulates apical trafficking in C. elegans tubules. Dev Biol 359, 59-72.

Maxfield, F.R., McGraw, T.E., 2004. Endocytic recycling. Nat Rev Mol Cell Biol 5, 121-132.

McKeown, C., Praitis, V., Austin, J., 1998. *sma-1* encodes a β_H-spectrin homolog required for *Caenorhabditis elegans* morphogenesis. Development 125, 2087-2098.

Mello, C.C., Kramer, J.M., Stinchcomb, D., Ambros, V., 1991. Efficient gene transfer in C.elegans: extrachromosomal maintenance and integration of transforming sequences. Embo J 10, 3959-3970.

Meng, E.C., Pettersen, E.F., Couch, G.S., Huang, C.C., Ferrin, T.E., 2006. Tools for integrated sequence-structure analysis with UCSF Chimera. BMC bioinformatics 7, 339.

Moulder, G., Barstead, R., 1998. Reverse Genetics: Isolating Deletions in PCR Screens of Mutagenized Populations. http://snmc01.omrf.uokhsc.edu/revgen/RevGen.html.

Mu, F.T., Callaghan, J.M., Steele-Mortimer, O., Stenmark, H., Parton, R.G., Campbell, P.L., McCluskey, J., Yeo, J.P., Tock, E.P., Toh, B.H., 1995. EEA1, an early endosome-associated protein. EEA1 is a conserved alpha-helical peripheral membrane protein flanked by cysteine "fingers" and contains a calmodulin-binding IQ motif. J Biol Chem 270, 13503-13511.

Myat, M.M., Andrew, D.J., 2002. Epithelial tube morphology is determined by the polarized growth and delivery of apical membrane. Cell 111, 879-891.

Needleman, S.B., Wunsch, C.D., 1970. A general method applicable to the search for similarities in the amino acid sequence of two proteins. Journal of molecular biology 48, 443-453.

Nelson, F.K., Albert, P.S., Riddle, D.L., 1983a. Fine structure of the Caenorhabditis elegans secretory-excretory system. Journal of ultrastructure research 82, 156-171.

Nelson, F.K., Albert, P.S., Riddle, D.S., 1983b. Fine structure of the *Caenorhabditis elegans* secretory-excretory system. Journal of Ultrastructural Research 82, 156-171.

Nelson, F.K., Riddle, D.L., 1984. Functional study of the Caenorhabditis elegans secretory-excretory system using laser microsurgery. The Journal of experimental zoology 231, 45-56.

Nunes-Duby, S.E., Matsumoto, L., Landy, A., 1989. Half-att site substrates reveal the homology independence and minimal protein requirements for productive synapsis in lambda excisive recombination. Cell 59, 197-206.

Oikonomou, G., Shaham, S., 2010. The Glia of Caenorhabditis elegans. Glia.

Papic, N., Hunn, J.P., Pawlowski, N., Zerrahn, J., Howard, J.C., 2008. Inactive and active states of the interferon-inducible resistance GTPase, Irga6, in vivo. J Biol Chem 283, 32143-32151.

Parkes, M., Barrett, J.C., Prescott, N.J., Tremelling, M., Anderson, C.A., Fisher, S.A., Roberts, R.G., Nimmo, E.R., Cummings, F.R., Soars, D., Drummond, H., Lees, C.W., Khawaja, S.A., Bagnall, R., Burke, D.A., Todhunter, C.E., Ahmad, T., Onnie, C.M., McArdle, W., Strachan, D., Bethel, G., Bryan, C., Lewis, C.M., Deloukas, P., Forbes, A., Sanderson, J., Jewell, D.P., Satsangi, J., Mansfield, J.C., Wellcome Trust Case Control, C., Cardon, L., Mathew, C.G., 2007. Sequence variants in the autophagy gene IRGM and multiple other replicating loci contribute to Crohn's disease susceptibility. Nature genetics 39, 830-832.

Pearse, B.M., 1976. Clathrin: a unique protein associated with intracellular transfer of membrane by coated vesicles. Proc Natl Acad Sci U S A 73, 1255-1259.

Perens, E.A., Shaham, S., 2005. C. elegans daf-6 encodes a patched-related protein required for lumen formation. Dev Cell 8, 893-906.

Perkins, L.A., Hedgecock, E.M., Thomson, J.N., Culotti, J.G., 1986. Mutant sensory cilia in the nematode *Caenorhabditis elegans*. Dev Biol 117, 456-487.

Petkova, D.S., Viret, C., Faure, M., 2012. IRGM in autophagy and viral infections. Frontiers in immunology 3, 426.

Praitis, V., Ciccone, E., Austin, J., 2005. SMA-1 spectrin has essential roles in epithelial cell sheet morphogenesis in C. elegans. Dev Biol 283, 157-170.

Prescott, N.J., Dominy, K.M., Kubo, M., Lewis, C.M., Fisher, S.A., Redon, R., Huang, N., Stranger, B.E., Blaszczyk, K., Hudspith, B., Parkes, G., Hosono, N., Yamazaki, K., Onnie, C.M., Forbes, A., Dermitzakis, E.T., Nakamura, Y., Mansfield, J.C., Sanderson, J., Hurles, M.E., Roberts, R.G., Mathew, C.G., 2010. Independent and population-specific association of risk variants at the IRGM locus with Crohn's disease. Hum Mol Genet 19, 1828-1839.

Riddle, D.L., Albert, P.A., 1997. Genetic and Environmental Regulation of Dauer Larva Development, in: Riddle, D.L., Meyer, B.J., Priess, J.R., Blumenthal, T. (Eds.), C. elegans II. Cold Spring Harbor Press, Cold Spring Harbor, NY, pp. 739-768.

Rink, J., Ghigo, E., Kalaidzidis, Y., Zerial, M., 2005. Rab conversion as a mechanism of progression from early to late endosomes. Cell 122, 735-749.

Rodriguez-Boulan, E., Kreitzer, G., Musch, A., 2005. Organization of vesicular trafficking in epithelia. Nat Rev Mol Cell Biol 6, 233-247.

Santiago-Martinez, E., Soplop, N.H., Patel, R., Kramer, S.G., 2008. Repulsion by Slit and Roundabout prevents Shotgun/E-cadherin-mediated cell adhesion during Drosophila heart tube lumen formation. J Cell Biol 182, 241-248.

Schottenfeld-Roames, J., Ghabrial, A.S., 2013. Osmotic regulation of seamless tube growth. Nature cell biology 15, 137-139.

Shaham, S., 2006. Glia-neuron interactions in the nervous system of Caenorhabditis elegans. Current opinion in neurobiology 16, 522-528.

Simonsen, A., Lippe, R., Christoforidis, S., Gaullier, J.M., Brech, A., Callaghan, J., Toh, B.H., Murphy, C., Zerial, M., Stenmark, H., 1998. EEA1 links PI(3)K function to Rab5 regulation of endosome fusion. Nature 394, 494-498.

Singh, S.B., Davis, A.S., Taylor, G.A., Deretic, V., 2006. Human IRGM induces autophagy to eliminate intracellular mycobacteria. Science 313, 1438-1441.

Singh, S.B., Ornatowski, W., Vergne, I., Naylor, J., Delgado, M., Roberts, E., Ponpuak, M., Master, S., Pilli, M., White, E., Komatsu, M., Deretic, V., 2010. Human IRGM

regulates autophagy and cell-autonomous immunity functions through mitochondria. Nature cell biology 12, 1154-1165.

Smith, T.F., Waterman, M.S., 1981. Identification of common molecular subsequences. Journal of molecular biology 147, 195-197.

Starich, T.A., Herman, R.K., Kari, C.K., Yeh, W.H., Schackwitz, W.S., Schuyler, M.W., Collet, J., Thomas, J.H., Riddle, D.L., 1995. Mutations affecting the chemosensory neurons of Caenorhabditis elegans. Genetics 139, 171-188.

Stein, L., Sternberg, P., Durbin, R., Thierry-Mieg, J., Spieth, J., 2001. WormBase: network access to the genome and biology of Caenorhabditis elegans. Nucleic acids research 29, 82-86.

Steinman, R.M., Mellman, I.S., Muller, W.A., Cohn, Z.A., 1983. Endocytosis and the recycling of plasma membrane. J Cell Biol 96, 1-27.

Stone, C.E., Hall, D.H., Sundaram, M.V., 2009. Lipocalin signaling controls unicellular tube development in the Caenorhabditis elegans excretory system. Dev Biol.

Sulston, J.E., 1983. Neuronal Cell Lineages in the Nematode Cænorhabditis elegans. Cold Spring Harbor Symposium on Quantitative Biology 48, 443-452.

Sulston, J.E., Hodgkin, J., 1988. Methods, in: Wood, W.B. (Ed.), The Nematode *Caenorhabditis elegans*. Cold Spring Harbor Press, Cold Spring Harbor, New York, pp. 587-606.

Sulston, J.E., Horvitz, H.R., 1977. Post-embryonic Cell Lineages of the Nematode, *Cænorhabditis elegans*. Dev Biol 56, 110-156.

Suzuki, N., Buechner, M., Nishiwaki, K., Hall, D.H., Nakanishi, H., Takai, Y., Hisamoto, N., Matsumoto, K., 2001. A putative GDP-GTP exchange factor is required for development of the excretory cell in Caenorhabditis elegans. EMBO Rep 2, 530-535.

Tabara, H., Grishok, A., Mello, C.C., 1998. RNAi in C. elegans: soaking in the genome sequence. Science 282, 430-431.

Taylor, G.A., 2007. IRG proteins: key mediators of interferon-regulated host resistance to intracellular pathogens. Cellular microbiology 9, 1099-1107.

Taylor, G.A., Collazo, C.M., Yap, G.S., Nguyen, K., Gregorio, T.A., Taylor, L.S., Eagleson, B., Secrest, L., Southon, E.A., Reid, S.W., Tessarollo, L., Bray, M., McVicar, D.W., Komschlies, K.L., Young, H.A., Biron, C.A., Sher, A., Vande Woude, G.F., 2000.

Pathogen-specific loss of host resistance in mice lacking the IFN-gamma-inducible gene IGTP. Proc Natl Acad Sci U S A 97, 751-755.

Taylor, G.A., Jeffers, M., Largaespada, D.A., Jenkins, N.A., Copeland, N.G., Vande Woude, G.F., 1996. Identification of a novel GTPase, the inducibly expressed GTPase, that accumulates in response to interferon gamma. J Biol Chem 271, 20399-20405.

Timmons, L., Fire, A., 1998. Specific interference by ingested dsRNA. Nature 395, 854.

Tiwari, S., Choi, H.P., Matsuzawa, T., Pypaert, M., MacMicking, J.D., 2009. Targeting of the GTPase Irgm1 to the phagosomal membrane via PtdIns(3,4)P(2) and PtdIns(3,4,5)P(3) promotes immunity to mycobacteria. Nature immunology 10, 907-917.

Tong, X., Buechner, M., 2008. CRIP homologues maintain apical cytoskeleton to regulate tubule size in C. elegans. Dev Biol 317, 225-233.

Ullrich, O., Reinsch, S., Urbe, S., Zerial, M., Parton, R.G., 1996. Rab11 regulates recycling through the pericentriolar recycling endosome. J Cell Biol 135, 913-924.

van Deurs, B., Holm, P.K., Sandvig, K., Hansen, S.H., 1993. Are caveolae involved in clathrin-independent endocytosis? Trends Cell Biol 3, 249-251.

Wallar, B.J., Alberts, A.S., 2003. The formins: active scaffolds that remodel the cytoskeleton. Trends Cell Biol 13, 435-446.

Ward, S., Thomson, N., White, J.G., Brenner, S., 1975. Electron microscopical reconstruction of the anterior sensory anatomy of the nematode Caenorhabditis elegans.?2UU. The Journal of comparative neurology 160, 313-337.

White, J., 1987. The Anatomy, in: Wood, W.B. (Ed.), The Nematode *Caenorhabditis elegans*. Cold Spring Harbor Press, Cold Spring Harbor, NY, pp. 81-122.

Williamson, M.P., 1994. The structure and function of proline-rich regions in proteins. The Biochemical journal 297 (Pt 2), 249-260.

Wodarz, A., Hinz, U., Engelbert, M., Knust, E., 1995. Expression of crumbs confers apical character on plasma membrane domains of ectodermal epithelia of Drosophila. Cell 82, 67-76.

Wood, W.B., 1988. Introduction to *C. elegans* Biology, in: Wood, W.B. (Ed.), The Nematode Caenorhabditis elegans. Cold Spring Harbor Press, Cold Spring Harbor, NY, pp. 1-16.

Zahraoui, A., Touchot, N., Chardin, P., Tavitian, A., 1989. The human Rab genes encode a family of GTP-binding proteins related to yeast YPT1 and SEC4 products involved in secretion. J Biol Chem 264, 12394-12401.

Zerial, M., McBride, H., 2001. Rab proteins as membrane organizers. Nat Rev Mol Cell Biol 2, 107-117.

Zhang, Y., 2008. I-TASSER server for protein 3D structure prediction. BMC bioinformatics 9, 40.

Zhao, Y.O., Konen-Waisman, S., Taylor, G.A., Martens, S., Howard, J.C., 2010. Localisation and mislocalisation of the interferon-inducible immunity-related GTPase, Irgm1 (LRG-47) in mouse cells. PLoS One 5, e8648.

Zhao, Y.O., Rohde, C., Lilue, J.T., Konen-Waisman, S., Khaminets, A., Hunn, J.P., Howard, J.C., 2009. Toxoplasma gondii and the Immunity-Related GTPase (IRG) resistance system in mice: a review. Memorias do Instituto Oswaldo Cruz 104, 234-240.